

**This dissertation has been
microfilmed exactly as received**

66-14,201

DAUBEN, Dwight Lewis, 1938-
NON-NEWTONIAN FLOW THROUGH POROUS
MEDIA.

The University of Oklahoma, Ph.D., 1966
Engineering, chemical

University Microfilms, Inc., Ann Arbor, Michigan

THE UNIVERSITY OF OKLAHOMA

GRADUATE COLLEGE

NON-NEWTONIAN FLOW THROUGH POROUS MEDIA

A DISSERTATION

SUBMITTED TO THE GRADUATE FACULTY

in partial fulfillment of the requirements for the

degree of

DOCTOR OF PHILOSOPHY

BY,

DWIGHT L. DAUBEN

Norman, Oklahoma

1966

NON-NEWTONIAN FLOW THROUGH POROUS MEDIA

APPROVED BY

D. E. Menzie

Edward A. Blich

Harold V. Blunck

John G. S. Norton

Paul J. Root

DISSERTATION COMMITTEE

ABSTRACT

This research attempts to determine and analyze the physical parameters involved in the slow flow of high molecular weight polymer solutions through porous media. The polymer solutions were characterized by measurement of the non-Newtonian viscosity and normal stresses as functions of shear rate. The porous matrix consisted of a stainless steel flow cell packed with glass beads. The fluids used in this study were aqueous solutions of polyethylene oxide, with molecular weights ranging from 200,000 to over 5,000,000. Flow rates ranged from 1 to 30 ft/day.

Under certain conditions anomalously high flow resistance was observed, this being a function of flow rate, pore size, and the polymer molecular weight and concentration. A theory is advanced to explain this unusual behavior, and an empirical equation is presented which permits one to predict the non-Newtonian behavior by knowledge of the power-law constants and the permeability of the formation.

ACKNOWLEDGMENT

The author wishes to express his appreciation to the many people who helped make this work possible. Special appreciation is extended to Dr. D. E. Menzie, under whose able guidance this work was accomplished. His comments and constructive criticisms have materially enhanced this manuscript.

Appreciation is also extended to Continental Oil Company for making this research possible through their fellowship and to Pan American Petroleum Corporation for printing this dissertation.

Appreciation is extended to Newton S. Knight at the University of Oklahoma for his superb craftsmanship and conscientiousness in the design and construction of certain specialized equipment.

The assistance of fellow graduate student, Elmo Blount, in contributing a number of ideas and suggestions in this research, is gratefully acknowledged.

Finally, and most important, I wish to express appreciation to my wife, Melonnie, for her patience and understanding during the long and sometimes frustrating hours spent in this research.

TABLE OF CONTENTS

	Page
ABSTRACT	iii
ACKNOWLEDGMENT	iv
LIST OF TABLES	vii
LIST OF FIGURES.	ix
 Chapter	
I. INTRODUCTION.	1
II. LITERATURE REVIEW	3
The Use of Polymer Solutions in the Secondary Recovery of Oil	2
Physical Properties of Polymers	3
Rheology of Polymer Solutions	11
Newtonian Flow in Porous Media.	18
Non-Newtonian Flow in Porous Media.	23
III. THEORETICAL CONSIDERATIONS.	29
Statement of Problem.	29
Rheology of Polymer Solutions	34
IV. EXPERIMENTAL APPARATUS AND PROCEDURE.	41
Flow through Porous Media	41
Flow Cell	41
Physical Properties of Polymers	43
Pumping Equipment and Pressure Measurement	45
Procedure	47
Rheology of Polymer Solutions	48
Capillary Viscometer.	48
Parallel Plate Instrument	50
V. RESULTS AND ANALYSIS.	55

	Page
Viscosity of Polymer Solutions.	55
Normal Stress Measurements.	59
Flow of Polymer Solutions through	
Porous Media.	62
Presentation of Results	62
Adsorption Phenomena.	74
Factors Affecting Flow Behavior	76
Development of a Correlative Equation	89
Recommendations for Future Research	92
VI. CONCLUSIONS	94
REFERENCES	97
APPENDIX A	
NOMENCLATURE	101
APPENDIX B	
DERIVATION OF THE MOONEY-RABINOWITSCH EQUATION	104
APPENDIX C	
SIZE CALCULATIONS OF A POLYMER MOLECULE.	110
APPENDIX D	
VISCOMETRIC DATA	112
APPENDIX E	
PARALLEL PLATE DATA AND CALCULATIONS	124
APPENDIX F	
POROUS MEDIA DATA AND CALCULATIONS	129

LIST OF TABLES

Table	Page
5-1. Tabulated Data on the Polymer Solutions. . . .	56
5-2. Tabulated Normal Stress Data	62
5-3. Flow through Porous Media - Tabulated Data . .	63
5-4. Flow through Porous Media - Constants b and m.	90
D-1. Viscometric Data - 0.1% Polyox WSR-301. . . .	113
D-2. Viscometric Data - 0.585% Polyox WSR-35	114
D-3. Viscometric Data - 0.025% Polyox Coagulent. . .	115
D-4. Viscometric Data - 0.296% Polyox Coagulent. . .	116
D-5. Viscometric Data - 0.075% Polyox Coagulent. . .	117
D-6. Viscometric Data - 0.199% Polyox WSR-301. . . .	118
D-7. Viscometric Data - 0.149% Polyox Coagulent. . .	119
D-8. Viscometric Data - 0.05% Polyox WSR-301	120
D-9. Viscometric Data - 0.486% Polyox Coagulent. . .	121
D-10. Viscometric Data - 1.0% Polyox WSR-301.	122
D-11. Viscometric Data - 0.394% Polyox WSR-205. . . .	123
E-1. Basic Parallel Plate Data.	125
E-2. Parallel Plate Calculations - 1% Polyox WSR-301.	126
E-3. Parallel Plate Calculations - 0.486% Polyox Coagulent	127
E-4. Parallel Plate Calculations - 0.296% Polyox Coagulent	128

	Page
F-1. Porous Media Data and Calculations - Run 1. . .	130
F-2. Porous Media Data and Calculations - Run 2. . .	131
F-3. Porous Media Data and Calculations - Run 3. . .	132
F-4. Porous Media Data and Calculations - Run 4. . .	133
F-5. Porous Media Data and Calculations - Run 5. . .	134
F-6. Porous Media Data and Calculations - Run 6. . .	135
F-7. Porous Media Data and Calculations - Run 7. . .	136
F-8. Porous Media Data and Calculations - Run 8. . .	137
F-9. Porous Media Data and Calculations - Run 9. . .	138
F-10. Porous Media Data and Calculations - Run 10 . .	139
F-11. Porous Media Data and Calculations - Run 11 . .	140
F-12. Porous Media Data and Calculations - Run 12 . .	141
F-13. Porous Media Data and Calculations - Run 13 . .	142
F-14. Porous Media Data and Calculations - Run 14 . .	143
F-15. Porous Media Data and Calculations - Run 15 . .	144
F-16. Porous Media Data and Calculations - Run 16 . .	145
F-17. Porous Media Data and Calculations - Run 17 . .	146
F-18. Porous Media Data and Calculations - Run 18 . .	147

LIST OF FIGURES

Figure		Page
2-1.	Pictorial Representation of a "Freely Orienting" or "Random Coiling" Macromolecule in Solution.	9
2-2.	Steady Laminar Velocity Profile for a Newtonian Fluid Contained between Two Plates.	12
2-3.	Strain Distribution of a Hookean Solid.	13
2-4.	Viscosity Versus Shear Rate for Various Fluids.	15
3-1.	Shear Diagram	34
3-2.	Schematic Diagram of a Parallel Plate Instrument.	39
4-1.	Design of Flow Cell	42
4-2.	Apparatus for the Flow of Fluids through Porous Media.	46
4-3.	Diagram of Capillary Viscometer	49
4-4.	Diagram of Parallel Plate Instrument.	51
5-1a	Shear Stress Versus Shear Rate Relationships. . .	57
5-1b	Shear Stress Versus Shear Rate Relationships. . .	58
5-2.	Shear Rate Versus Tangential and Normal Shear Stress.	60
5-3a-h	Viscosity Ratio Versus Linear Velocity.	64
5-4.	Typical Shape of a Pressure Drop-Flow Rate Curve.	77
5-5.	Flow of a Viscoelastic Fluid Out of a Capillary	81

Figure		Page
5-6.	Flow of a Viscoelastic Fluid through a Pore.	83
5-7.	Entry of a Viscoelastic Fluid into a Large Opening	83

NON-NEWTONIAN FLOW THROUGH POROUS MEDIA

CHAPTER I

INTRODUCTION

The use of polymer solutions in the oil industry is of high current interest. Polymer solutions are often injected into subterranean oil bearing formations, displacing residual oil from the formation and moving it toward the producing well. The efficiency of this water-oil displacement process is governed largely by the mobility ratio, M , defined by

$$M = \frac{K_w}{\mu_w} / \frac{K_o}{\mu_o}$$

where μ is the fluid viscosity, K the permeability of the formation, and the subscripts o and w refer to oil and water respectively. The permeability of the formation to a fluid is a measure of that fluid's ability to pass through the formation under some applied pressure gradient. For a mobility ratio greater than one, the displacing water tends to finger through the less mobile oil, resulting in uneven displacement and poor oil recovery. To improve the mobility ratio, and thereby improve oil recovery, recent attempts have

been made to increase the viscosity of the injected water by the addition of certain water soluble polymers. The polymers are of very high molecular weight (a molecular weight of 3,000,000 is typical) and only a small concentration is required to significantly increase the viscosity of the solution.

The vast majority of research on non-Newtonian flow has been concerned with the so called "steady state," condition; i.e., the solution flows through a conduit of uniform cross section and flows at some constant rate. The flow behavior of many polymer solutions have been adequately described under such conditions. In porous media the fluid undergoes continuous relaxing and restressing as it flows through channels of varying diameter, and a steady state viscosity, as determined by any of the common viscometric methods, does not adequately describe the resistance to flow offered by the solution.

CHAPTER II

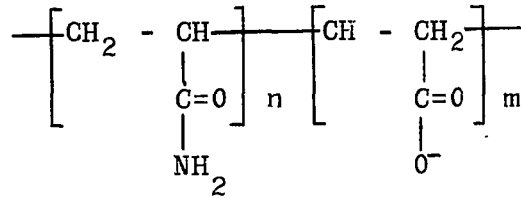
LITERATURE REVIEW

The Use of Polymer Solutions in the Secondary Recovery of Oil

The practice of adding water soluble polymer to the injected water in secondary recovery operations is not new. Investigators for years have sought for a suitable additive to increase the viscosity of the water to be injected. Most of the early attempts utilized the natural gums, such as locust bean gum, gum Karaya, and guar gum. The more recent investigations make use of the synthetic polymers, such as carboxymethylcellulose, polyvinyl alcohol, partially hydrolyzed polyacrylamide, polyacrylic acid, and polyethylene oxide.²⁷ A list of patents covering much of the work done on viscous water flooding is given by reference 33.

The commercial use of a water soluble polymer in secondary recovery operations has been very limited because of the cost of treatment and the tendency of the polymer to adsorb on the surface of the rock. Union Oil Company and Dow Chemical Company have recently patented the use of partially hydrolyzed polyacrylamide, in which it is claimed that adsorption is not a major problem.^{25,26,29} The polymer used has

the following configuration:

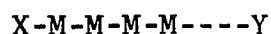


It is seen that the group containing NH_2 has been partially replaced by the carboxyl group, $\text{C} \begin{array}{l} \text{O} \\ \diagdown \\ \text{O}^- \end{array}$. The subscripts n and m indicate the relative percent of each unit ($m + n = 100\%$). The primary effect of partial hydrolyzation is to reduce the amount of adsorption of the polymer on the surfaces of the porous media. Union's original patent stipulated that the degree of hydrolyzation should be between .8 and 10%. Dow Chemical Company later patented the same process except that the degree of hydrolyzation was taken to be between 12 and 67%.²⁶ A great deal of research is currently being done on the displacement of oil by this polymer. The research that the author is familiar with indicates that higher recoveries are obtained by polymer flooding but that adsorption is still a major problem.^{4,6}

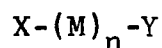
Physical Properties of Polymers

A polymer is a molecule composed of a number of repeating units. The structure of the polymer is often described in terms of its "structural unit." Structural units are groups having two or more bonding sites and are linked through covalent bonds to other molecules. The simplest

type of polymer is a linear polymer, whose chain arrangement is given by

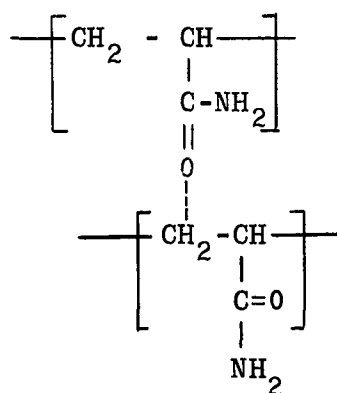


or



where M is the structural unit, n the "degree of polymerization," and X and Y are terminating monovalent molecules. If the structural unit is trivalent the polymer is "nonlinear," or "branched." In many long-chained polymers the end groups are not known and of little importance because the physical properties of the polymer solution are governed almost entirely by the structural units. Polymers containing a single repeating structural unit are referred to as "homopolymers," and those polymers containing two or more structural units are referred to as "copolymers."

In addition to the covalent bonds which hold the structural units of a polymer together, other bonding forces must be considered in order to account for some of the physical properties of a polymer. When two different areas of a polymer have unlike charges, or when the net charge on the molecule is not zero, the molecule has a permanent dipole moment. A good example of secondary valence forces is the hydrogen bonding that occurs in solutions of polyacrylamide:



Hydrogen bonding
in polyacrylamide
solutions

The molecular weight and molecular weight distribution plays an important role in the physical properties of a polymer solution. It is extremely difficult to define polymers in absolute terms, and this is particularly true in determining the molecular weight of a polymer. In any given quantity of a polymer the molecular weight varies, and one is forced to think in terms of a "number average" molecular weight or a "weight average" molecular weight. These terms are defined as

$$M_n = \frac{\sum n_i M_i}{\sum n_i}$$

$$M_w = \frac{\sum w_i M_i}{\sum w_i}$$

where M_n is the number average molecular weight and M_w the weight average molecular weight. In the first expression n_i is the number of molecules having a molecular weight M_i , and in the second expression w_i is the weight of a polymer molecule. The physical properties of a polymer solution depend upon the molecular weight distribution, and normally the more

narrow the distribution the more favorable. There are four common methods of determining the molecular weight of a polymer: osmotic pressure measurements, light scattering, ultracentrifuge, and the concept of solution intrinsic viscosity. For a more detailed description the reader is referred to reference 38. The solution viscosity of a polymer is a measure of the size of the polymer molecule and can be related empirically to its molecular weight by the expression,

$$[\eta] = CM^a \quad (2-1)$$

where $[\eta]$ is the "intrinsic viscosity," M the molecular weight, and C and a are constants depending upon a particular polymer in a particular solvent. The viscosity of the polymer solution is determined at various concentrations (all at the same shear rate), and that apparent viscosity obtained by extrapolation to zero concentration is referred to as intrinsic viscosity. The molecular weight must be determined by one of the other methods in order to calculate the constants. Once the constants are determined, however, the molecular weight of any polymer solution can be determined by calculating its intrinsic viscosity.

Determination of the molecular weight by osmotic pressure measurements represents a number average molecular weight, the light scattering and ultracentrifuge methods represent a weight average molecular weight, and the solution viscosity technique represents either a number or weight

average molecular weight depending on the type of average used to determine the constants C and a .

An important consideration in polymer solutions is the configuration which the polymer takes while in solution. In a good solvent the segments of the polymer chain have no preference for other segments over the solvent molecules. The result is that the polymer molecule either assumes a "loose" random coil type of arrangement or a rigid flexible rod type configuration (which occurs in some polyelectrolytes). In a poor solvent there is more affinity between polymer segments and a "balling" of the chains occur.³⁶ The molecule occupies less space within the solvent, and if a non-solvent is added the polymer becomes a tight ball, and if the ball is concentrated enough the polymer molecules will unite with other molecules such that flocculation occurs.

The carbon-carbon bond intersects at an angle of 69° , but the chain is free to rotate in three dimensions. The polymer molecule constantly changes its configuration, and it becomes impossible to assign a definite unchanging geometrical size to the molecule. For this reason, one must be content to talk in terms of average sizes. A number of statistical studies have been made which attempt to define the size of polymer molecules in solution. In the case of the "freely orienting" chain the junction between two adjacent bonds is perfectly free to rotate. The two bonds may assume any orientation with respect to each other. The square of

the end to end length of a freely orienting chain is given as

$$R^2 = Na^2, \quad (2-2)$$

where N is the number of bonds and a is the length of the bonds.⁴ See Figure 2-1 for a pictorial representation of the freely orienting molecule. If the chain has a certain degree of stiffness,

$$R^2 = (\text{constant}) \times Na^2 \quad (2-3)$$

where the constant varies, depending upon the model, but usually is between 1 and 10. These equations of course cannot predict the case where polymer entanglements occur.

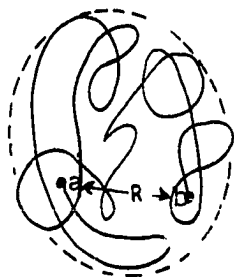


FIGURE 2-1 PICTORIAL REPRESENTATION OF A "FREELY ORIENTING" OR "RANDOM COILING" MACROMOLECULE IN SOLUTION. ENDS a AND b ARE BURIED WITHIN THE MOLECULE.

Merrill²⁰ has attempted to classify polymers based upon their configuration in a solvent. Needless to say, any attempts to classify polymers is a formidable task, when one considers the wide variety of polymers and the many physical

phenomena that they represent. Merrill classifies polymers in the following manner:

1. Random Coiling Nonelectrolytic Macromolecules in Solution. This type of macromolecule in solution is "limp," flexible, and distorted. Its size can be calculated by assuming a freely orienting chain and the use of Equations (2-2) and (2-3). Such a molecule may be represented pictorially in a manner as shown in Figure 2-1. This type of molecule has the ability to "sequester" or hold a large volume of solvent within its coils, in a manner similar to that of a sponge. The solvent inside the coil moves with the velocity of the local segment of the solvent when the fluid is in motion. Thus, the random coiling molecule may be considered to be semi-permeable. The random coil is easily deformed, and under an applied shear stress changes from its spherical orientation to elongated ellipsoids. It is very likely that the loops, particularly at low shear rates, penetrate with each other. The result is that the polymer solution consists of a large number of entangled coils, and when a coil moves it must drag along other coils. Only at very dilute concentrations, typical of intrinsic viscosity calculations, does the macromolecules exercise hydrodynamic independence. Under increasing shear rates, the coil becomes more ellipsoidal in shape and less opportunity is available for close interpenetration.

2. Random Coiling Electrolytic Macromolecules in

Solution. These types of macromolecules are soluble as a result of ionizable side groups along the chain. A very common ionic group is $-\overset{\text{O}}{\underset{\text{O}}{\text{C}}}-$. Polymer solutions of this type are very susceptible to pH changes of the solvent. As an example, if the positive ion concentration is very low in a polymer solution containing carboxyl side groups, the carboxyl segments of the polymer are repulsed from each other, and the configuration may be considered to be more stretched out than in a random coil configuration.

3. Rigid Macromolecules in Solution. Macromolecules of this type are polyelectrolytes, in which the ionic side groups cover substantially the entire length of the polymer.

Two other groups included in this classification are random coiling macromolecules in the bulk state, and aggregates of macromolecules. Because these groups are not directly applicable in this study, no further mention will be made.

Rheology of Polymer Solutions

All incompressible fluids behave according to the continuity equation and the equation of motion, stated as follows:

$$(\nabla \cdot \bar{V}) = 0 \qquad \text{Continuity equation} \qquad (2-4)$$

$$\rho \frac{D\bar{V}}{Dt} = -\nabla P - \nabla \cdot \bar{\tau} + \rho \bar{g} \qquad \text{Equation of motion} \qquad (2-5)$$

In Equations (2-4) and (2-5), \bar{V} are the velocity components,

ρ the density, P the pressure, \bar{g} the acceleration due to gravity, and $\bar{\tau}$ the stress tensor. The essential problem in rheology is to define the stress tensor in Equation (2-5). For Newtonian fluids the problem is a simple one. Consider the case of a Newtonian fluid contained between two large parallel plates of area A which are everywhere separated by a very small distance Y (see Figure 2-2). The lower plate is set in motion at a velocity of V , and at

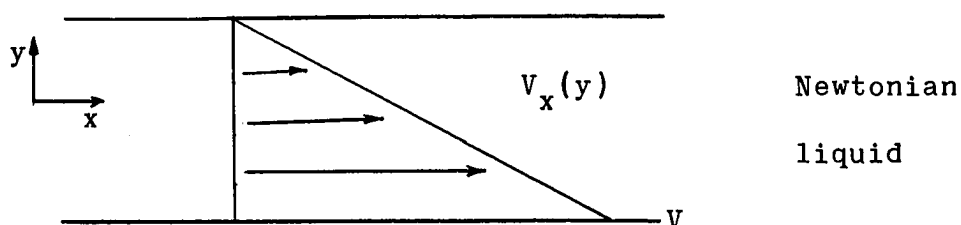


FIGURE 2-2. STEADY LAMINAR VELOCITY PROFILE FOR A NEWTONIAN FLUID CONTAINED BETWEEN TWO PLATES.

steady state conditions the velocity distribution, as shown in Figure 2-2, is reached. Providing that flow is laminar,

$$F/A = \mu V/Y ,$$

or

$$\tau_{yx} = - \mu \frac{dV_x}{dy} , \quad (2-6)$$

where τ_{yx} is the shear stress, μ the Newtonian viscosity, V_x the fluid velocity and y the plate separation. Equation (2-6) has been substituted into Equation (2-5) and the common Newtonian flow equations have been derived. At the other extreme from a Newtonian fluid is a Hookean solid. Consider the case of a solid subjected to a strain, U , at its lower

edge.

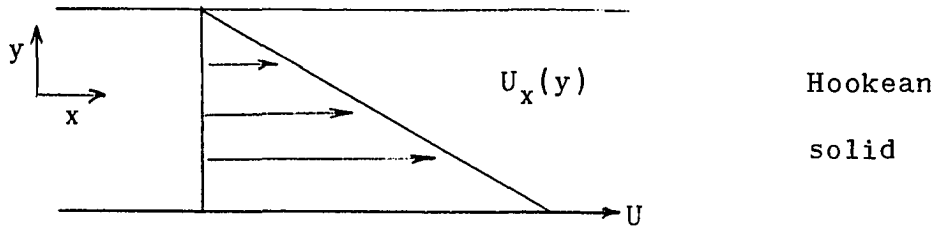


FIGURE 2-3. STRAIN DISTRIBUTION OF A HOOKEAN SOLID.

The shear stress is proportional to strain, as is now stated:

$$\tau_{yx} = - Y \frac{dU_x}{dy} . \quad (2-7)$$

In Equation (2-7) U is the amount of strain, τ_{yx} the stress applied and Y is Young's modulus.

Somewhere between the idealized cases of the Newtonian liquid and the Hookean solid lie polymers. Polymer melts and polymer solutions may be considered to be partly liquid and partly solid, and their behavior may range from one extreme to the other. Maxwell in 1860 combined Newton's law of viscosity, Equation (2-6), and Hook's law, Equation (2-7), in the following manner:

$$\tau_{yx} + t_c \frac{d \tau_{yx}}{dt} = - \eta_0 \gamma . \quad (2-8)$$

In Equation (2-8) t_c is the relaxation time, η_0 the viscosity at zero shear rate, γ the shear rate, τ_{yx} the shear stress, and $\frac{d \tau_{yx}}{dt}$ the time derivative of shear stress. Stated qualitatively, the relaxation time is the time required for the

fluid to return to its original position after a stress has been applied. For Newtonian fluids and some non-Newtonian fluids the relaxation time is very small, and the second term of Equation (2-8) may be conveniently dropped, leaving Equation (2-6). Equation (2-8) may be represented by a spring and dashpot, and such mathematical treatment is known as "linear viscoelastic behavior." Equation (2-8) may be expanded in a generalized manner to include all components of the stress tensor.

The relationship of shear stress and shear rate of a fluid comprise the field of conventional viscometry. The viscosity of a fluid, η , may be defined as

$$\tau = - \eta \dot{\gamma} . \quad (2-9)$$

In the Newtonian case η is constant (referred to as μ) and in the non-Newtonian case η varies as a function of shear rate. Non-Newtonian fluids exhibit various properties, and many descriptive terms have been used in an attempt to classify the fluids. The term "pseudoplastic" is given to fluids which exhibit a decreasing viscosity with increasing shear rate. Most low concentration polymer solutions and polymer melts exhibit this property. A "dilatant" fluid exhibits an increasing viscosity with increasing shear rates. Some pseudo-plastic fluids approach Newtonian behavior both at low shear rates and at high shear rates,

the interconnecting region being non-Newtonian. The term "first Newtonian" and "second Newtonian" have been applied respectively to these regions. These descriptive terms are illustrated in Figure 2-4.

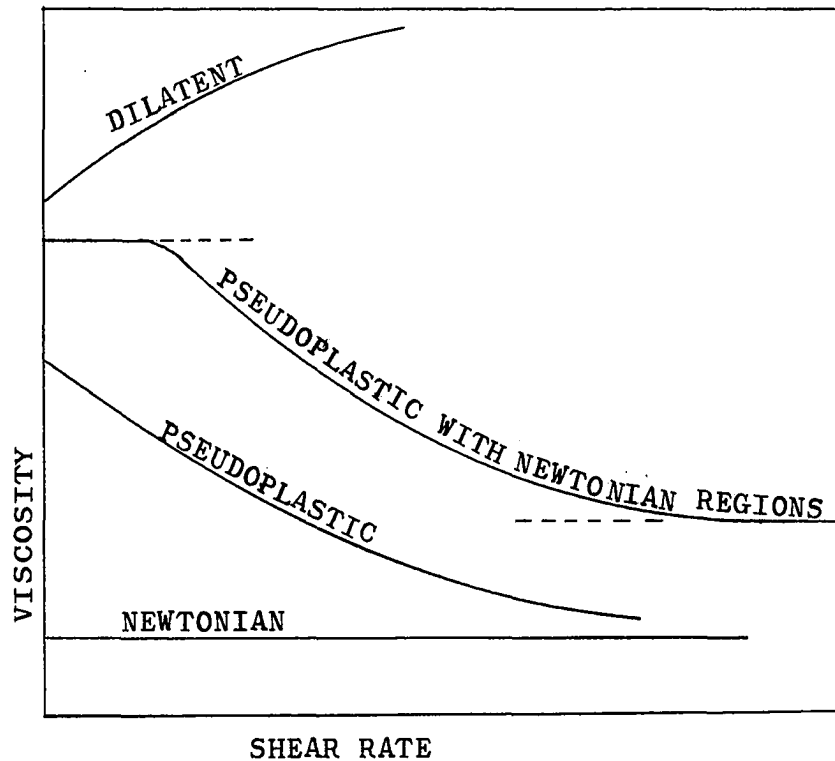


FIGURE 2-4. VISCOSITY VERSUS SHEAR RATE FOR VARIOUS FLUIDS.

A number of empirical mathematical models have been developed to express quantitatively the relationship between shear rate and shear stress. The "power law" equation is adequate to describe pseudoplastic and dilatent fluids which do not have Newtonian regions. The power law is given by

$$\tau = - C \dot{\gamma}^n , \quad (2-10)$$

where τ is the shear stress, $\dot{\gamma}$, the shear rate, and C and n are constants to be determined experimentally. A three parameter Ellis model is useful to predict behavior of pseudo-plastic fluids exhibiting a first Newtonian. The Ellis model is given by

$$- \dot{\gamma} = \phi_0 \tau + \phi_1 \tau^m , \quad (2-11)$$

where ϕ_0 , ϕ_1 , and m are constants to be determined experimentally. The Bingham model assumes Newtonian behavior and a "yield value:"

$$\tau - \psi = \eta(-\dot{\gamma}) . \quad (2-12)$$

In Equation (2-12), ψ is the yield value, and may be defined qualitatively as that stress required for initial flow.

The measurement of viscosity may be carried out in a number of ways. A complete summary of laboratory viscometric methods is given by Van Wazer.⁴³ The most common devices are the rotational devices, such as the Fann V-G Meter and the Brookfield viscometer, and the capillary viscometers, such as the Ostwald and the Ubbelohde. A great number of special purpose viscometers have been developed. The theory related to capillary flow will be presented in Chapter III.

An important class of non-Newtonian fluids are those which exhibit viscoelasticity. For a complete review of

viscoelastic properties of polymer solutions, the reader is referred to Frederickson,^{12,13} or Ferry.¹⁰ Viscoelastic fluids exhibit a great variety of rheological phenomena. Some of these phenomena are given as follows:

1. Non-Newtonian Viscosity. As was previously indicated, a fluid is non-Newtonian if the relationship between shear rate and shear stress is non-linear.

2. Weissenberg or Normal Stress Effect. Fluids which exhibit this effect will climb the bob in a rotational viscometer, or in a capillary tube, swell as the fluid exits. Such phenomena illustrate that stresses normal to the direction of fluid motion are generated. The initial work of Merrington²¹ provided the stimulus for considerable research in the investigation of this effect.

3. Thixotropy and rheopexy. Many viscoelastic fluids exhibit time dependent effects, either spontaneously reversible or irreversible. For reversible behavior, certain materials become more fluid with increasing time under steady state conditions. Such fluids are called "thixotropic." The opposite effect, in which materials exhibit more flow resistance with time when subjected to steady state flow is "rheoplectic."

Characterization of viscoelastic flow behavior has not advanced to the state that other non-Newtonian fluids have, although considerable progress has been made in viscoelastic phenomena and its measurement. For molten polymers

and polymer solutions in which flow occurs as a small stress is applied, two types of viscoelastic measurements are taken. These are oscillatory measurements and steady state measurements. Oscillatory viscoelastometers are used to measure the transient behavior of polymers; one parameter which can be determined from such a device is the relaxation time. Several instruments have been designed to measure normal stresses under steady state flow conditions. The Weissenberg rheogonometer is the only commercially built device for the express purpose of normal stress measurement. The rheogonometer, described by reference 43, consists essentially of a cone and plate viscometer with pressure taps to measure normal forces and determine their distribution as a function of radial distance and shear rate. Philippoff²⁸ and Metzner, Houghton, Sailor, and White,²² developed a method of normal stress determinations by an analysis of the jet from the end of a capillary. The magnitude of the normal stress was shown to be a function of the ratio, D_j/D , where D_j is the diameter of the enlarged jet, and D the diameter of the capillary. A parallel plate instrument is also used to measure normal stresses.^{16,17,18,39,44} A detailed description of this device is given in Chapter IV.

Newtonian Flow in Porous Media

The theory of laminar flow in porous media is based on a classical experiment performed by Darcy in 1856. He

deduced the following relationship for flow through a horizontal packed bed:

$$q = \frac{\chi A \Delta P}{L} \quad (2-13)$$

In Equation (2-13), q is the volumetric flow rate, A the cross sectional flow area, ΔP the pressure drop across a bed of length L . χ is a constant depending upon the properties of the fluid and of the porous media. Various investigators have subsequently modified Equation (2-13) by the assumption that χ can be replaced by the following expression:

$$\chi = K/\mu \quad (2-14)$$

In Equation (2-14) K is a constant for a particular porous bed, and μ the viscosity of the fluid. Using this assumption one arrives at the more familiar form of the Darcy equation:

$$q = \frac{KA\Delta P}{\mu L} \quad (2-15)$$

The Darcy equation can be expressed in two differential forms.³⁴ If L becomes infinitesimal,

$$\bar{q} = \frac{K}{\mu} (\text{grad } P - \rho \bar{g}) \quad (2-16)$$

In Equation (2-16) \bar{q} is a vector quantity. The term $\rho \bar{g}$ is added for the case where the bed is not horizontal. Equation (2-16) is equivalent to a force potential, θ , defined by

$$\theta = gz + \int_{P_0}^P \frac{dP}{\rho(P)} \quad (2-17)$$

$$\bar{q} = \frac{K\rho}{\mu} \text{grad } \theta$$

where z is a vertical co-ordinate. The second differential forms considers the permeability and viscosity to be variables. Thus

$$\bar{q} = \text{grad} \left(\frac{KP}{\mu} \right) + \frac{K\rho g}{\mu} . \quad (2-18)$$

A velocity potential, ψ , can be introduced as follows:

$$\psi = \frac{KP}{\mu} + \int_{z_0}^z \frac{K\rho g}{\mu} dz \quad (2-19)$$

$$\bar{q} = \text{grad} \psi .$$

Equations (2-17) and (2-19) are both theoretically possible, but it is not possible to distinguish between the two forms where experiments are run with constant viscosity fluids and porous media of homogeneous permeability. Equation (2-17) is the commonly used expression because it can be handled more easily and can be extended to immiscible multiphase flow (relative permeability concept).

A number of attempts have been made to find an analytical expression for the permeability constant to be used in the Darcy equation. The theories developed can be generally classified into three groups:

1) Hydraulic Radius Theory. The assumption is made that the porous media is equivalent to a series of channels. These theories all make use of the observation that the units of permeability have the dimension of area or a length

squared. Therefore, the hydraulic radius theories assume the following expression for permeability:

$$K = C \frac{R_h^2}{f(\phi)} \quad (2-20)$$

In Equation (2-20) C is a constant, R_h the hydraulic radius, $f(\phi)$ some function of porosity.

2) Drag Theory. This theory considers the particles to be obstacles to an otherwise straight flow of the fluid. The drag on each particle is calculated from the Navier-Stokes equations and the sum of the resistance of all the particles is thought to equal the total resistance of the bed to the flow of the fluid.

3) Statistical Theory. This theory suggests that the porous media is intrinsically disordered. This is the opposite view of the other methods which consider the porous media to be intrinsically ordered. The Navier-Stokes equation may not be used for such disordered media.

The Kozeny equation is commonly used for the flow of fluids through a packed bed. The equation makes use of the hydraulic radius theory, and relates the permeability to the porosity of the bed and the size of the spheres comprising the porous matrix.

$$K = \frac{D_p^2 \phi^3}{C(1-\phi^2)} \quad (2-21)$$

D_p is the diameter of the spheres, and C is a constant and

values ranging from 150 to over 200 have been reported in the literature. In Equation (2-21) K is given in cm^2 , and D_p in cm . The permeability calculated from this equation can then be used in Equation (2-15). The Kozeny equation has been used with moderate success for flow in packed beds.

The Darcy equation is generally restricted to low flow velocity. At higher velocities it is customary to introduce a Reynolds number for porous media, defined as follows:

$$R_e = \frac{q\rho\delta}{\mu} \quad (2-22)$$

In this equation R_e is the Reynolds number, q the flow rate, ρ the fluid density, μ the viscosity, and δ a diameter associated with the porous media. The resistance to flow, f , is represented by

$$f = 2 \delta \text{ grad } P / q^2 \rho \quad (2-23)$$

In this representation, Darcy's equation can be written as

$$\lambda = C / R_e \quad (2-24)$$

where C is a constant.

Other forms of high velocity flow equation have been developed. One form suggests that Darcy's equation can be modified by including a second-order term in the velocity.³⁴

$$\frac{\Delta P}{\Delta x} = aq + bq^2 \quad (2-25)$$

Constants a and b have been related to the porosity of the bed particle diameter.¹

Another equation sometimes used is:³⁴

$$\frac{\Delta P}{\Delta x} = a q^m \quad (2-26)$$

where a and m are constants to be determined experimentally.

Non-Newtonian Flow in Porous Media

Only a few published papers are available on the subject of non-Newtonian flow in porous media. The first published work is by T. J. Sadowski at the University of Wisconsin.^{31,32} The experimental part of his research consisted in flowing various concentrations of polymer solutions through a packed bed. The polymers used in his research were polyethylene glycol (molecular weight 6,000 - 20,000), polyvinyl alcohol (MW 150,000), and hydroxethylcellulose (MW 163,000 and 346,000). The experimental procedure consisted of both constant rate and constant pressure runs. The porous matrix on the constant rate runs consisted of lead shot ranging from 0.1124 cm to 0.2327 cm in diameter and glass beads 0.2807 cm in diameter. Rheological studies showed that the polyethylene glycol solutions were essentially Newtonian, polyvinyl alcohol solutions and lower molecular weight hydroxethylcellulose were non-Newtonian and exhibited both a lower and upper shear rate range in which Newtonian behavior was observed. The higher molecular weight hydroxethylcellulose exhibited an upper Newtonian range but appeared to have no lower Newtonian range. This polymer also appeared to be

viscoelastic. Sadowski attempted to define mathematically non-Newtonian flow in porous media by relating the Ellis model flow equation for capillaries to flow in porous media by use of the hydraulic radius concept and the Kozeny equation. The experimental data also were presented in the form of a friction factor vs Reynolds number for porous media. By the use of the mathematical equation or the friction factor chart and shear rate - shear stress information it then becomes possible to describe the flow behavior of any given polymer solution in porous media. The constant rate runs were all quantitatively consistent with the exception of the higher molecular weight hydroxethylcellulose. At a certain critical flow rate, this fluid exhibited more friction than predicted. The author concluded that this was a viscoelastic effect, and introduced an additional parameter (relaxation time) to account for the behavior.

In the constant pressure runs Sadowski was unable to maintain an equilibrium flow condition. The flow rate continuously dropped. This phenomena led the author to the conclusion that a gel structure was being formed within the porous media, and added resistance to flow. Sadowski suggested that in porous media, that a dynamic equilibrium condition exists between the tendency of the polymer molecules to adsorb on the surface of the spheres and the tendency of the fluid movement to remove adsorbed polymer. In the very small pores where little fluid travels, the velocity

field has a value only slightly greater than zero. The tendency of the adsorbed layer to be swept away is markedly lowered. Thus the tendency for adsorption is favored. The adsorbed polymer molecules extending into the bulk fluid, may serve as attachment sites for other molecules from the immediately adjacent particle surface and from the bulk field. In this way, a gel structure may be forced to form within the various parts of the bed. Thus the gel structure may plug minute pores or fill in the tighter regions. The tendency for gel formation is enhanced by an increase in the molecular weight, decrease in the size of the particles, by a decrease in the bulk flow rate of the fluid, and by an increase in the time during which the fluid flows through the bed.

Christopher and Middleman⁵ also studied the flow of non-Newtonian fluids through porous media. Their mathematical development was very similar to that of Sadowski--the primary difference being that a power law model was used instead of an Ellis model. Their treatment will be summarized here instead of Sadowski's because of the simpler expressions resulting from power law treatment.

The laminar flow of Newtonian fluids through porous media can be described by use of the Blake-Kozeny equation:

$$v = \frac{\Delta P D^2 \phi^3}{150 L \mu (1-\phi)^2} \quad (2-27)$$

This equation makes use of the Darcy equation, and the

permeability relationship,

$$K = \frac{D_p^2 \phi^3}{150 (1-\phi)^2} \quad (2-28)$$

Here K has the units cm^2 . The equation describing the flow of a power law fluid in a capillary is given by

$$\langle v \rangle = \frac{n}{3n+1} D^{1+1/n} \left(\frac{\Delta P}{2CL} \right)^{1/n} \quad (2-29)$$

where n and C are power law constants, D the tube diameter, ΔP the pressure drop, L the length, and $\langle v \rangle$ the average flow velocity. For flow in a capillary,

$$\tau_w = C \gamma_w^n \quad (2-30)$$

The hydraulic radius, R_h , is defined as follows:

$$R_h = \frac{D_p}{6} \frac{\phi}{1-\phi} \quad (2-31)$$

$$D = 4 R_h \quad .$$

By introducing Equation (2-31) into (2-29) and replacing L by $25/12L$ (tortuosity factor) the following equation is derived:

$$v = \left(\frac{K \Delta P}{HL} \right)^{1/n} \quad (2-32)$$

$$H = \frac{C}{12} \left(9 + \frac{3}{n} \right)^n (150 K \phi)^{(1-n)/2} \quad .$$

Thus, by knowing the power law constants, C and n, and the permeability, K, Equation can be used to describe flow in

porous media.

Their results were also presented in the form of a friction factor versus Reynolds number relationship. The friction factor was defined as

$$f = \frac{\Delta P D_p \phi^3 \rho}{LG^2 (1-\phi)} , \quad (2-33)$$

and Reynolds number by

$$R_e = \frac{D_p G^{2-n} \rho^{n-1}}{150 H(1-\phi)} , \quad (2-34)$$

where

$$f = 1/R_e . \quad (2-35)$$

In Equation (2-33) G is the mass flow rate, defined by

$$G = \rho V . \quad (2-36)$$

The non-Newtonian fluids investigated in their research were aqueous solutions of carboxymethylcellulose (CMC Type 70 high molecular weight, Hercules Powder Co.) and a toluene solution of polyisobutylene (PIB L 100, Enjay Co.).

McKinley, Jahns, Harris, and Greenhorn¹⁹ studied the linear flow of a non-Newtonian fluid (aqueous solution of Dextran--a polysaccharide) in porous media. A modification of Darcy's law, which uses capillary rheology data, is developed to describe non-Newtonian flow in underground reservoirs. The generalization, in effect, replaces the porous media with a capillary of equivalent radius proportional to the square root of the ratio of permeability to porosity.

The constant of proportionality should be independent of permeability and porosity for a given type of rock. This has been partially confirmed experimentally. In principle, a capillary rheogram and a single core test permit evaluation of the constant. The non-Newtonian flow can be predicted in this type of rock regardless of porosity, permeability, or flow rate.

Pye²⁹ was concerned with the secondary recovery of oil by the use of polymer solutions, but encountered a very unusual and somewhat unexpected phenomena in flowing aqueous solutions of partially hydrolyzed polyacrylamide through a rock. His research indicated that the apparent viscosity in porous media, as calculated from Darcy's equation,

$$\mu = \frac{KA\Delta P}{qL} \quad (2-13)$$

was considerably higher than the viscosity determined from the common viscometric methods. The permeability, K, was determined by flowing water through the porous media, and was assumed to not change during polymer flow. There is evidence⁶ to indicate that some of the polymer will adsorb to the rock surfaces and decrease the permeability. Under such circumstances, a reduced permeability is indistinguishable from an anomalously high viscosity. The author indicated that the effect was primarily a high apparent viscosity.

CHAPTER III

THEORETICAL CONSIDERATIONS

Statement of Problem

The basic equation describing the linear flow of an incompressible fluid through porous media is

$$q = \frac{KA\Delta P}{\mu L} \quad (2-15)$$

As was indicated in Chapter II the assumption was made in the derivation of the Darcy equation that the viscosity of the fluid is a property independent of the physical properties of the porous media. In the case of Newtonian fluids this assumption is valid, as the viscosity remains constant for all shear rates. For a non-Newtonian fluid the viscosity changes with shear rate and the assumption no longer is valid. The shear rate for a capillary may be approximated by

$$\gamma_w = \frac{4 V_{avg}}{R} \quad (3-1)$$

where γ_w is the shear rate at the radius R , and V_{avg} is the average velocity of flow. If Equation (3-1) can be applied to flow in porous media, R represents some average size of

flow path, and V_{avg} an average velocity of fluid movement. The cross sectional area of the individual flow channels vary considerably as the fluid travels through constriction into larger openings back into constrictions, etc. Consequently, the velocity in each flow channel varies widely, in the larger openings traveling at a slower velocity than the average, and in the tighter places, traveling at a faster velocity than the average. The "filter velocity," V , is defined as

$$V = q/A \quad (3-2)$$

where q is the volumetric flow rate and A the cross sectional area. A "pore velocity," $\langle V \rangle$, defines an average velocity of fluid movement, and is given as

$$\langle V \rangle = \frac{V}{\phi} \quad (3-3)$$

where ϕ is the porosity of the porous media. Equation (3-3) is known as the Dupuit-Forchheimer assumption.³⁴

Equation (2-15) cannot be used to describe the flow of non-Newtonian fluids in porous media. In the case of pseudo-plastic fluids such as used in this research, one could reason that the apparent viscosity in porous media would decrease as the flow rate, q , is increased; i.e., the viscosity decreases as the shear rate increases. The results of Sadowski³¹ and Christopher⁵ showed this to be the case. The flow rates used in their studies varied over

a wide range, and were generally at much higher rates than could be expected in secondary recovery operations. The question which naturally arises at this point is "Can one expect non-Newtonian flow behavior in porous media at the low flow rates and narrow range of rates commonly occurring in secondary recovery operations?" By assuming some typical pore radius and range of pore velocities one can quickly see that the shear rates encountered are very low and do not vary over a wide range. By this reasoning, one can assume that very little non-Newtonian behavior can be expected. The very surprising result, however, is that under certain conditions, non-Newtonian behavior is very pronounced at these low rates, as this research will show.

The specific objectives of this research and the variables to be considered will now be presented. This investigation attempts to define the effect of the physical properties of the porous media on the flow behavior of non-Newtonian fluids. The research consists of two main parts:

A. Rheological Description of Fluids. The viscosity of each polymer solution is measured by means of a capillary viscometer. Data are taken in the low shear rate range. The normal stresses of the polymer solutions are also measured by means of a specially built parallel plate instrument.

B. Flow of Polymer Solutions Through Porous Media.

1. Flow Rate. The relationship of pressure drop and flow rate is studied. For non-Newtonian flow behavior

the relationship should be non-linear. It can be seen from Darcy's equation, Equation (2-15), that for Newtonian fluids a linear relationship exists between pressure drop and flow rate.

2. Molecular Weight. It is known that the non-Newtonian viscosity and degree of elasticity are functions of molecular weight. Polymers ranging from a molecular weight of 200,000 to over 5,000,000 are used in this research.

3. Pore Size. The pore size is varied by using different sizes of glass beads, the smaller the beads the smaller the pores through which the polymer solution must travel. The beads used in this study vary from a diameter of 53 microns to a diameter of 250 microns. In a bed packed with spheres the pore size is some fraction of the size of the sphere. It appears possible that the size of a macromolecule (particularly the higher molecular weight polymers) may be large enough with respect to the size of the flow path that some interaction between the macromolecule and the sides of the flow path may occur. Merrill¹⁹ indicates that in a capillary viscometer if the capillary diameter is less than 20 times the diameter of the largest particle that particle-wall interactions can occur, resulting in an additional pressure drop. An example was cited in which an investigator was measuring the viscosity of blood by using capillaries of different diameters. The investigator found the viscosity to decrease profoundly, and then to increase to infinity as the

capillary diameter was decreased to about five times the diameter of the red cells. In the case of polymer solutions many entanglements of the coils occur, and the effective diameter of the coils may be many times greater than that for a single coil.

4. Concentration. A polymer solution generally becomes more non-Newtonian and more viscoelastic as the concentration is increased.

The object of this research is two-fold: to understand more clearly the physical parameters involved in flowing long chained polymers through porous media, and to mathematically correlate the flow behavior in porous media to its flow behavior in a capillary viscometer.

Polyethylene oxide was used in this study. This polymer is manufactured by Union Carbide under the trade name of "Polyox," and different molecular weights are available. It was decided to work exclusively with this polymer so that the above mentioned variables could be studied more clearly. In most ways polyethylene oxide is a typical polymer, but does have some unique properties. Polyethylene oxide solutions are known to be among the most highly elastic of polymer solutions. Even at very small concentrations the elastic effects are noticeable. These polymers have a very high affinity for water, and are known to have a highly developed network structure. The molecules form tightly into many entanglements and associations.⁴⁶

Rheology of Polymer Solutions

Consider the case of an incompressible liquid being sheared between two parallel plates, as shown in Figure 3-1.

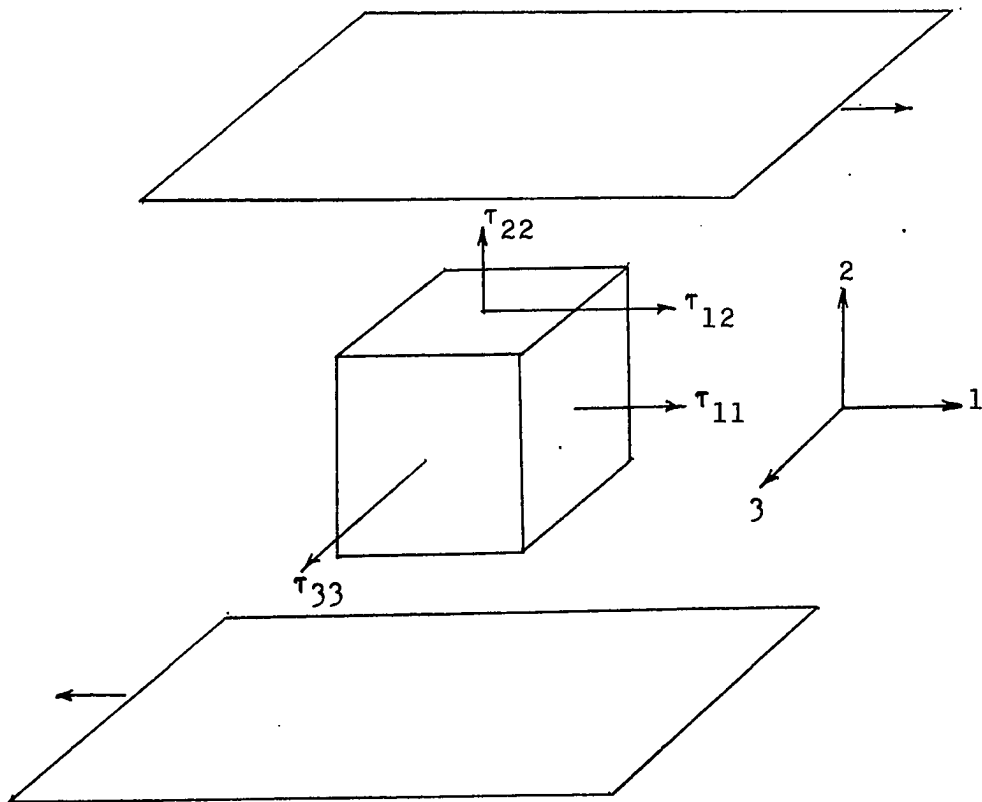


FIGURE 3-1. SHEAR DIAGRAM

The notation used in Figure 3-1 will be used in this development. For a Newtonian liquid the viscosity is constant, and may be related simply to one stress component, as follows:

$$\tau_{12} = \mu \gamma .$$

Written in terms of the tensor components a Newtonian liquid

may be represented as ⁴⁴

$$\begin{vmatrix} \tau_{11} & \tau_{12} & \tau_{13} \\ \tau_{12} & \tau_{22} & \tau_{23} \\ \tau_{13} & \tau_{23} & \tau_{33} \end{vmatrix} = - \begin{vmatrix} P & 0 & 0 \\ 0 & P & 0 \\ 0 & 0 & P \end{vmatrix} + \begin{vmatrix} 0 & \tau_{12} & 0 \\ \tau_{12} & 0 & 0 \\ 0 & 0 & 0 \end{vmatrix} \quad (3-4)$$

Weissenberg^{30,44} proposed the following relationship for an incompressible viscoelastic fluid:

$$\begin{vmatrix} \tau_{11} & \tau_{12} & \tau_{13} \\ \tau_{12} & \tau_{22} & \tau_{23} \\ \tau_{13} & \tau_{23} & \tau_{33} \end{vmatrix} = - \begin{vmatrix} P & 0 & 0 \\ 0 & P & 0 \\ 0 & 0 & P \end{vmatrix} + \begin{vmatrix} P_{11} & \tau_{12} & 0 \\ \tau_{12} & P_{22} & 0 \\ 0 & 0 & P_{33} \end{vmatrix} \quad (3-5)$$

The pressure P in a viscoelastic fluid is usually defined as

$$P = -1/3 \tau = -1/3 (\tau_{11} + \tau_{22} + \tau_{33}) . \quad (3-6)$$

This pressure is known as the isotropic pressure. By (3-5) and the definition in Equation (3-6), one can deduce that

$$P_{11} + P_{22} + P_{33} = 0 \quad (3-7)$$

Weissenberg hypothesized that P_{22} and P_{33} are equal and less than P_{11} .⁴⁴ A great deal of controversy still exists over this assumption and some experimental evidence indicates that it is not a valid assumption. The majority of evidence accumulated so far, however, indicates that the assumption is reasonably accurate. If this assumption can be made, measurements of $(P_{11} - P_{22})$ and τ_{12} as functions of shear

rate will completely define the rheological behavior of the liquid. In this research τ_{12} versus shear rate was found by flow in a capillary, and $(P_{11} - P_{22})$ versus shear rate found by a parallel plate instrument. In this paper, as is common elsewhere, if no subscript is associated with the stress component, the component τ_{12} is implied.

The steady flow of liquids through a capillary will now be considered. Starting from the equation of motion, the Mooney-Rabinowitsch equation can be developed (See Appendix B):

$$-\dot{\gamma}_w = \left(\frac{-dV}{dr} \right)_w = \left(\frac{3+b}{4} \right) \left(\frac{4Q}{\pi R^3} \right) \quad (3-8)$$

$$b = \frac{d \log (4Q / \pi R^3)}{d \log (\Delta P R / 2L)} .$$

The shear stress is given by

$$\tau_w = \frac{\Delta P R}{2L} . \quad (3-9)$$

In Equations (3-8) and (3-9) $\dot{\gamma}_w$ is the shear rate at the wall, τ_w the shear stress at the wall, q the flow rate, R the radius of the capillary, L the length of the capillary, and ΔP the pressure drop across the capillary. The Newtonian expression for shear rate is

$$(-\dot{\gamma}_w) = \frac{4Q}{\pi R^3} . \quad (3-10)$$

Thus the term $(3+b)/4$ in Equation (3-8) is a term to correct for non-Newtonian behavior. The viscosity is a function of shear rate, and is defined as

$$\eta(\dot{\gamma}_w) = \frac{\tau_w}{(-\dot{\gamma}_w)} . \quad (3-11)$$

A curve of shear stress versus shear rate will normally plot as a straight line on log paper. The slope of the line is the factor b in Equation (3-8). The factor b will normally range from one (Newtonian case) and up. In this research, it was found that all polymer solutions fit the power-law model quite well, and the constants C and n were determined for each polymer solution. The power law model was given in Chapter II but again will be stated:

$$\tau_w = C \dot{\gamma}_w^n . \quad (3-12)$$

The expression for volumetric flow rate through a capillary is found by substituting Equation (3-12) into the general form of Equation (3-9), integrating using the boundary condition that $V = 0$ at $r = R$, and using the relationship $dQ = VdA$.

$$q = \pi \left(\frac{\Delta P}{2CL} \right)^{1/n} \left[\frac{n}{3n+1} \right] R^{\frac{3n+1}{n}} . \quad (3-13)$$

The average velocity, V_{avg} , is found by substituting $V_{avg} = q/A$ into Equation (3-13):

$$V_{avg} = \left(\frac{\Delta P}{2CL} \right)^{1/n} \left(\frac{n}{3n+1} \right) R^{\frac{n+1}{n}} . \quad (3-14)$$

A parallel plate instrument was designed and built for the purpose of measuring the normal stresses of polymer solutions. A pictorial sketch is shown in Figure 3-2. The outer cup rotates, and the fluid is sheared between the parallel surfaces of the disc and cup. The fluid rises in the capillary tubes in a manner as shown in the figure. Only viscoelastic fluids exhibit this property.

To be consistent with the nomenclature adopted in Figure 3-1, the tangential direction ϕ is denoted 1, the axial direction z is denoted 2, and the radial direction 3. The derivation of the parallel plate equation will follow that of Metzner.⁴⁴ The following assumptions are made:

1. There is symmetry with respect to the circumferential direction ϕ , so that all derivatives with respect to it are zero.

$$2. \quad V_{\phi} = V_{\phi}(r, z)$$

$$3. \quad \tau_{r\phi} = \tau_{zr} = 0$$

$$4. \quad V_r = V_z = 0$$

The Navier-Stokes equations (See Appendix B) reduce to

$$\frac{-\rho V_1^2}{r} = \frac{dP}{dr} + \frac{dP_{33}}{dr} + \frac{P_{33} - P_{11}}{r} \quad (3-15)$$

$$0 = \frac{dP}{dz} + \frac{dP_{22}}{dz} \quad (3-16)$$

$$0 = \frac{d\tau_{12}}{dz} \quad (3-17)$$

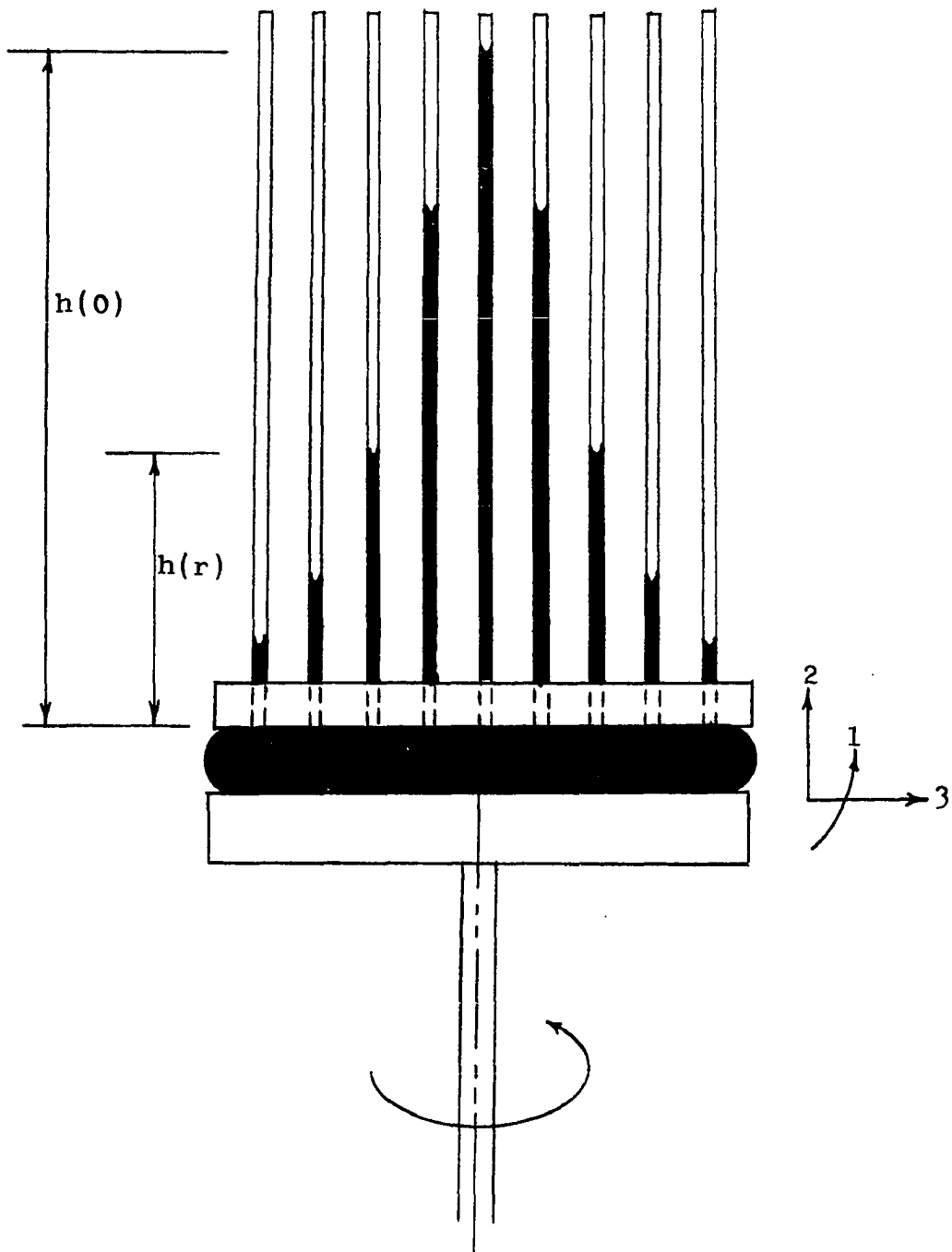


FIGURE 3-2. SCHEMATIC DIAGRAM OF PARALLEL PLATE INSTRUMENT

The capillary rise is related to the normal stresses by

$$\rho gh = -\tau_{22} = P - P_{22} \quad . \quad (3-18)$$

By combining Equation (3-18) and (3-15), making the assumption that $P_{22} = P_{33}$ and neglecting centrifugal forces, one arrives at the parallel plate equation:

$$-\rho g \frac{dh}{d_{1nr}} = P_{11} - P_{22} \quad . \quad (3-19)$$

The recoverable shear may be defined as

$$S = \frac{P_{11} - P_{22}}{\tau_{12}} \quad . \quad (3-20)$$

An "apparent relaxation time" was defined by Kotaka¹⁶ to be

$$t_c = \frac{S}{\dot{\gamma}} \quad . \quad (3-21)$$

This cannot be considered a true relaxation time, since no direct measurements of this quantity was made. Even direct measurement is subject to question, since the measured value often depends upon the type of experiment used in its determination. Equation (3-21) can be used, therefore, to give only an order of magnitude estimate.

CHAPTER IV

EXPERIMENTAL APPARATUS AND PROCEDURE

Flow through Porous Media

Flow Cell

The flow cell was constructed of stainless steel with an internal diameter of 1.757" and a length of 12". The volume of the cell, as determined by measuring the volume of water required to fill the cell is 474 cc. One end plate was permanently attached to the cell by silver soldering. The other end plate was removable, and held in position by tie rods connecting the two end plates. The inlet and exit ports are $\frac{1}{4}$ " threaded holes. On the inlet and exit ports 1/8" pipe thread to 1/4" compression thread male connectors were used. The connectors had a fine mesh screen soldered on one end to prevent any beads from leaving the cell.

The various glass beads used in this research were made from high grade optical crown glass, soda lime type, and has a silica content of not less than sixty eight percent. The beads are available from Cataphote Corporation. The beads are very hard and have a very high resistance to wear and fracture. The manufacturers claim that at least 95% of

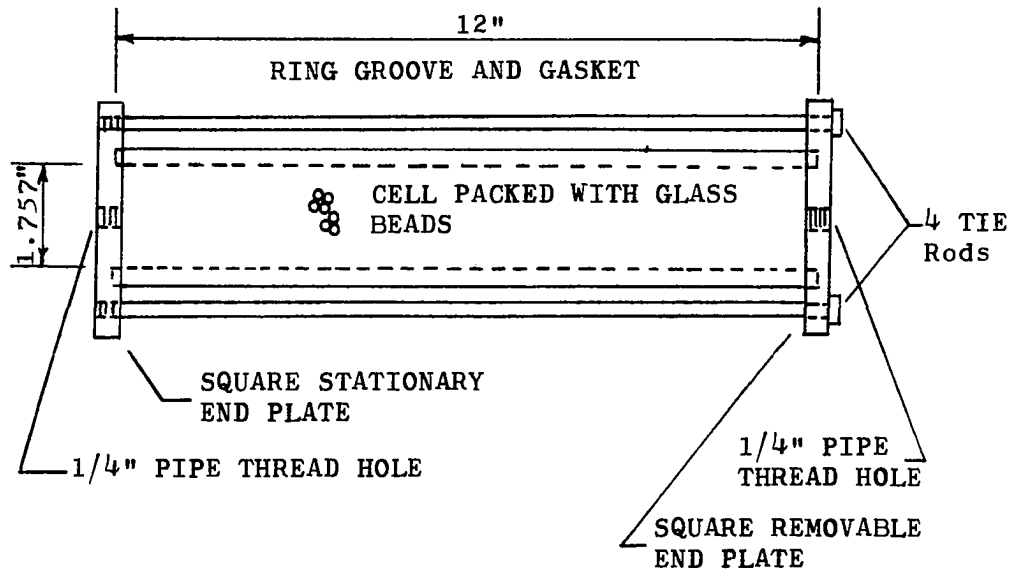


FIGURE 4-1. DESIGN OF FLOW CELL

the beads are true spheres, and that the beads are essentially free of surface scoring and foreign matter. Ninety percent of the beads are also guaranteed to be within the size range specified. The following bead sizes were used: 50-70 mesh, 70-100 mesh, 140-200 mesh, and 200-270 mesh. The diameter of the spheres in microns are, respectively, 300-270, 210-149, 105-74, 74-53.

The beads were packed into the cell by use of a vacuum pump connected to one end and an automatic sander, used as a vibrator. With a vacuum on one end, the cell was held in a vertical position and dry beads were poured slowly through the top; simultaneously, the cell was held tightly against the vibrator. The flow cell was weighed before and after

packing, and the porosity was calculated based upon the weight of the beads and their specific gravity. This is a common and simple type of calculation, and the reader is referred to any text on reservoir engineering for the procedure. The specific gravity of the beads was calculated by placing a known weight of beads into a graduated cylinder containing water and measuring the volume of water displaced by the beads. The porosity was also calculated based upon the weight of the liquid in the cell after a run had been completed. The percent deviation of the two calculated porosities was always less than 2 % of pore volume. The porosity based from the knowledge of liquid weight in the cell was considered to be more accurate, and it was this value that was used in the calculations.

Physical Properties of Polymers

The polymer used in this study is polyethylene oxide, available from Union Carbide. The following polymers were used in this study:

Polyox WSR-35	MW	200,000
Polyox WSR-205	MW	600,000
Polyox WSR-301	MW	4,000,000
Polyox Coagulent	MW	> 5,000,000

It is not known what method was used to determine the molecular weight, and for this reason, it is not known whether these molecular weights represent a number average or a weight average. In addition, it should be emphasized that it is very difficult to specify with precision the molecular weight

of molecules of this size. Thus, the reported molecular weights of these polymers can be expected to be only an approximation.

Polyox in the bulk state is in the form of white granules, and range in size from a fine powder (WSR-35) up to course granules (Coagulent). The ability of Polyox to thicken water is primarily a function of molecular weight; thus, the most viscous solutions are formed with Coagulent and the least with WSR-35.

The mixing of polymer solutions requires special consideration. Long chained polymers such as those used in this study, lose some of its viscosity and elasticity under the influence of shearing. For this reason, one should avoid using a high speed blender or any other high shearing action. One requirement for the mixing of polymer solutions is that the polymer granules must be initially wetted by the solvent. If the granules are not well dispersed in the solvent, they tend to accumulate in "lumps" and excessive times are required for them to completely dissolve. In this research, the polymer solutions were mixed by hand agitation, and allowed to set for at least two days before use.

Polyox solutions have a tendency for auto-oxidation over a long period of time with a consequent loss of viscosity. Isopropanol effectively inhibits auto-oxidation. Optimum stabilization of dilute solutions of Polyox resins

appears to result when the ratio of isopropanol to Polyox resin is at least five to one, but good stabilization can be achieved at much lower concentrations of isopropanol.⁴⁰ In this research, the amount of isopropanol added in each case was about five times the weight of the resin.

Polyox solutions appear slightly hazy to moderately opaque. Haziness is caused by the presence of small amounts of inorganic salts remaining from the polymerization reaction, and does not indicate incomplete solution of the resin.⁴⁰ Where clarity is required the pH of the solution may be lowered to 5-6 by acetic acid. Acidification affects viscosity during long periods of storage, and for this reason, acidification should be delayed until it is ready for use.

Pumping Equipment and Pressure Measurement

A diagram of the pumping equipment and manometer is shown in Figure 4-2. The rate at which a fluid can be pumped is controlled by both the Zero-Max gear reducer and the Graham transmission. The Zenith pump is capable of pumping fluids at a constant rate over a wide range of flow rates; and more important, the pump can operate at extremely low rates, such as one cc/hr. The Zenith pump operates much better if a viscous liquid is used. For this reason, as well as to avoid possible contamination of the polymer solution, a viscous oil was pumped into the top of a reservoir, displacing polymer solution out the bottom and into the flow

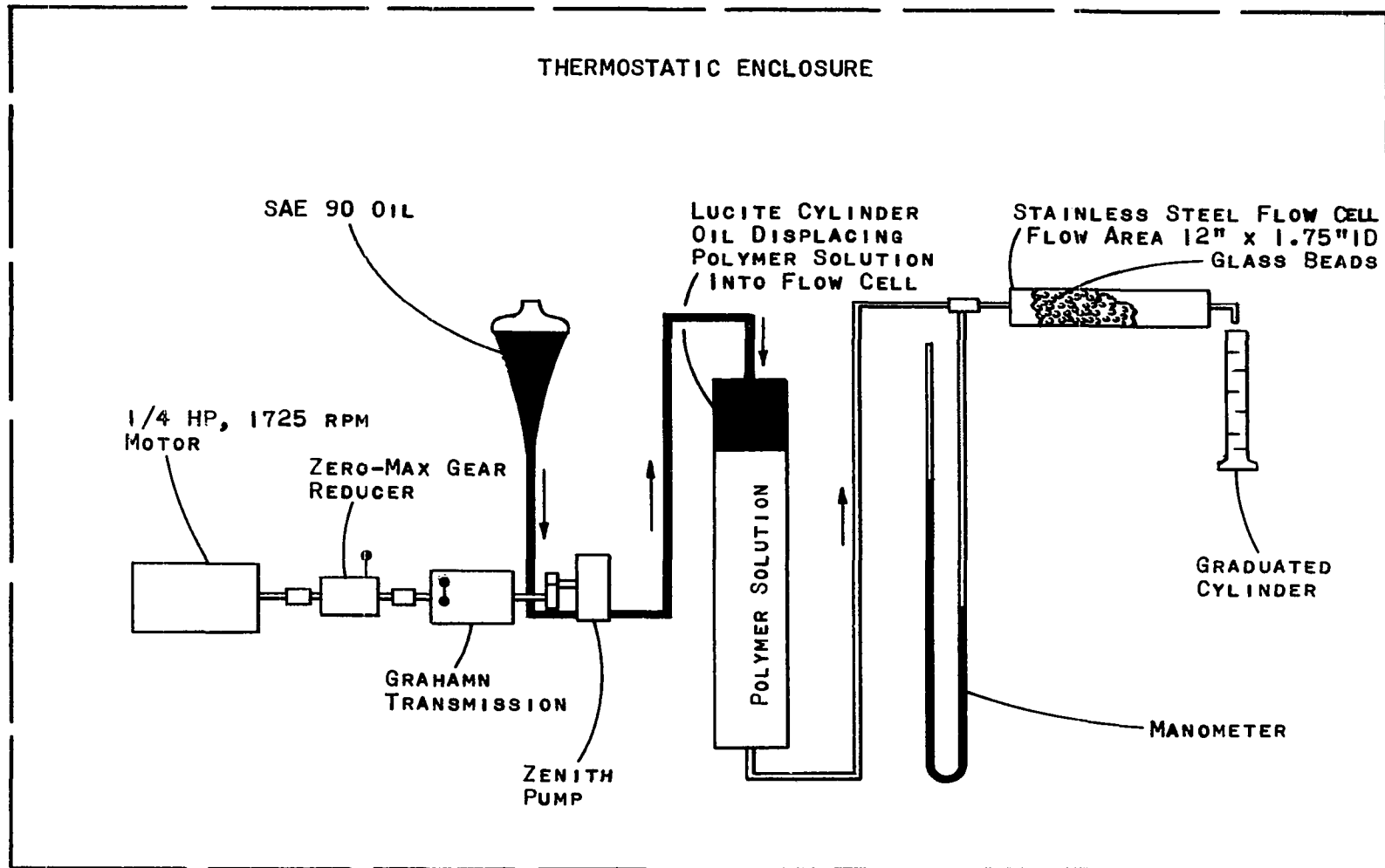


FIGURE 4-2. APPARATUS FOR THE FLOW OF FLUIDS THROUGH POROUS MEDIA

cell. The viscous oil was Phillips All Purpose Gear Oil, SAE 90. The pressure drop was measured by a manometer connected in the line just before entering the flow cell; the pressure drop recorded represents the entire pressure drop across the cell, and thus includes any entrance or exit effects that may exist. The manometer was filled with mercury, and was capable of pressure drops up to 45 psi. For higher pressure runs, a pressure gauge was used. The gauge was calibrated against a dead weight tester.

Procedure

The flow cell was first weighed dry, packed with glass beads in a manner previously described, and weighed again. The weight of the beads was determined and recorded. The cell was then saturated with distilled water, by evacuating the cell, and then allowing the beads to imbibe water. The permeability of the bead pack was then determined by pumping distilled water through the bead pack, measuring the flow rate and corresponding pressure drop. Several flow rates were made. The permeability of the bead pack is calculated from Darcy's equation,

$$K = \frac{Q\mu L}{A\Delta P} .$$

The quantities in this equation have been previously defined, and are listed in Appendix A. The polymer solution was then injected into the flow cell, displacing the water. Samples

of the efflux were periodically taken for the purpose of determining the concentration of the polymer. To test the concentration of polymer in the solution, a ten cc sample was taken, placed in an Ostwald viscometer, and the efflux time recorded. If the efflux time is the same as that for a polymer solution of full concentration, it was presumed that the polymer was at full strength throughout the flow cell. The pressure drop on the manometer was checked periodically, and when complete stabilization had occurred, the pressure drop, flow rate, and cumulative volume injected, were recorded. The flow rate was determined by measuring the time required for a measured volume of liquid to be discharged. After the data were recorded, the flow rate was changed, and the system allowed to come to equilibrium. After all the recordings have been made, the saturated cell is weighed, for the purpose of determining the weight of the liquid (for porosity determination). The cell and reservoir were then cleaned in preparation for a new run.

Rheology of Polymer Solutions

Capillary Viscometer

The viscometer consisted of a capillary tube and a reservoir of fluid connected to one end of the capillary by means of a flexible hose. The arrangement is shown in Figure 4-3. The information required to calculate the viscosity are the flow rate, pressure drop, radius of capillary,

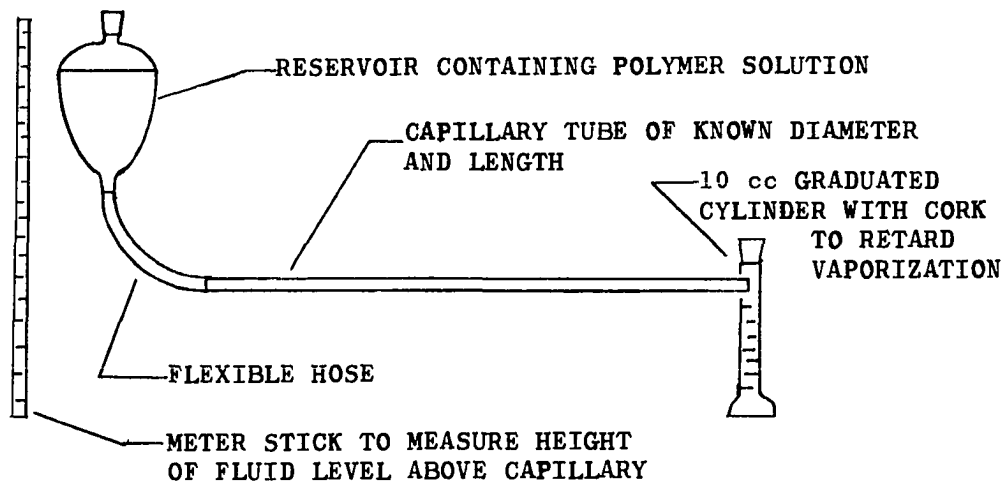


FIGURE 4-3. DIAGRAM OF CAPILLARY VISCOMETER

and length of capillary. The shear rate and shear stress are then calculated by means of Equations (3-8) and (3-9), and the viscosity by Equation (3-11). The reservoir containing the polymer solution was arranged so that it could be moved up or down. The pressure drop, ΔP , across the capillary is

$$P = h\rho g$$

where h is the height of the fluid level above the capillary, ρ the fluid density, and g the acceleration due to gravity. During a test, the height of the fluid level remains essentially constant. In this research low shear rate data were desired. As can be seen from Equation (3-8) low shear rate data can best be accomplished by having a relatively large radius. Practically, however, the radius should be small enough to exert some retarding force on the flow so that the

sample can be collected at convenient time intervals, and to avoid kinetic energy effects caused by the rapid flow out of a capillary. Shear rate data were taken from approximately 3 sec^{-1} to around 1000 sec^{-1} . The radius of the tube was determined by injecting a quantity of mercury in the capillary, measuring its length, and weighing the mercury. The radius can then be calculated. Viscosity measurements were taken at $25^{\circ}\text{C} \pm \frac{1}{2}^{\circ}\text{C}$. The density of the polymer solutions was determined from an analytical balance, and all of the solutions had a density the same as distilled water (0.997 gm/cc at 25°C).

Parallel Plate Instrument

This instrument is used to determine the normal stress as a function of shear rate. See Figure 4-4. The instrument was designed similar to that of Tamura.³⁹ The instrument consists essentially of a rotating cup and disc. The disc sets down into the cup containing polymer solution, and as the cup rotates the fluid is sheared between the two surfaces. The shear rate is given by

$$\dot{\gamma} = \frac{\Omega r}{l}$$

where Ω is the rotational speed in radians per second, r the distance from the center, and l the spacing between the two surfaces.

The spacing between the two parallel surfaces was set

by means of specially prepared spacers, and ranged from 0.0378" to 0.0708". The cup can be rotated at various speeds, permitting a wide range of shear rate data to be taken. The height of the fluid rise in each capillary is measured by means of a traveling microscope adjustment, and recorded as functions of the rotational speed, radius and spacing. From these data and the theory developed in Chapter III, one can calculate the normal stress as a function of shear rate. Tamura³⁹ indicated that in order to avoid centrifugal effects a cup of these dimensions should not be rotated in excess of around 75 rpm.

Both the cup and disc are made of stainless steel, and the surfaces are machined to within 0.001" accuracy. The cup must rotate with no wobble and the spacing between the two surfaces must be at all points equidistant, or the fluid rise in the tubes will be remarkably disymmetrical. The tubes are tapped symmetrically about the center, and at a particular radius the height of the fluid rise is recorded and an average of the two are taken. Because of the precision construction of the instrument the values were found to be fairly close. The tubes used in the instrument had an outside diameter of $\frac{1}{4}$ " and an inside diameter of 0.039" \pm 0.0004". One quarter holes were tapped into the disk to within approximately 1/8" of the other side. Holes of 0.0395" diameter were then tapped through to the other side. By exposing only a very small hole to the surface being

sheared, any fluid disturbances due to the openings will be minimized. The fluids rise in the capillaries to a certain height due to capillary pressure. In calculating the normal stress only the relative differences in fluid height are used; thus the height to which the fluid rises under static conditions is not important, provided that the height is the same in each capillary. No temperature control is made except for the thermostatically controlled atmosphere. Temperature measurements of the polymer solution indicated no detectable rise in temperature due to viscous heating.

The following procedure is carried out in the collection of data and the calculation of normal stresses:

1. Put the polymer solution in the cup, lower the disc into approximate position. The spacing between the two surfaces is set, and the disc centered within the cup.
2. Rotate the cup at the desired speed. Allow plenty of time for the fluid in the capillaries to reach an equilibrium position. For thick solutions several hours are required, but for thinner solutions only a few minutes are required. Record the rotational speed, spacing, and the height of the fluid rise as a function of radius. The height of the fluid with respect to any arbitrary point is acceptable.
3. The rotational speed can be changed to provide more data, and Step 2 repeated.
4. To calculate the normal stress as a function of shear rate a plot of $(h_z(0) - h_z(r))$ versus the log of the

radius, $\log_{10}r$, is made. For a given rotational speed and spacing the shear rate is calculated at each value of r selected. The slope $d(h_z(0) - h_z(r))/d\log_{10}r$ is calculated at each value of r and the pressure gradient is found by

$$\frac{dP_{22}}{d\ln r} = \frac{\rho g}{2.303} \frac{d(h_z(0) - h_z(r))}{d\log r}$$

Since

$$\frac{dP_{22}}{d\ln r} = P_{11} - P_{22} \quad (3-15)$$

a plot of $(P_{11} - P_{22})$ versus γ can be made. The recoverable shear, S , can be found by

$$S = \frac{P_{11} - P_{22}}{\tau_{12}} \quad (3-16)$$

where τ_{12} is found from capillary data.

CHAPTER V

RESULTS AND ANALYSIS

Viscosity of Polymer Solutions

The viscosity of the different polymer solutions was measured by means of a capillary viscometer, previously described. The results are shown in Figure 5-1. The data appeared to fit the power law model quite well, and the constants C and n were found for each polymer solution. The power law is again stated, for purposes of convenience.

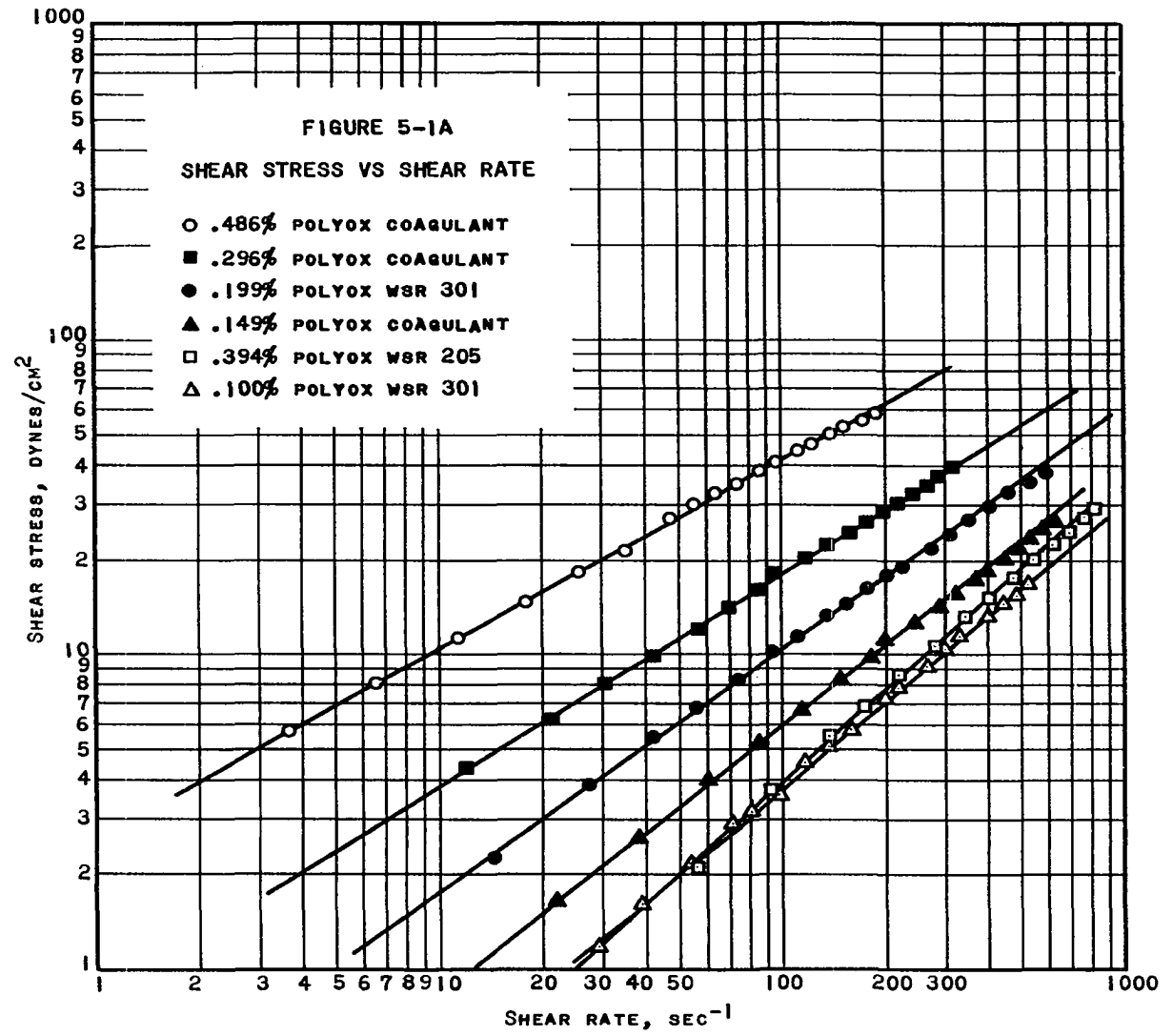
$$\tau_w = C \gamma_w^n$$

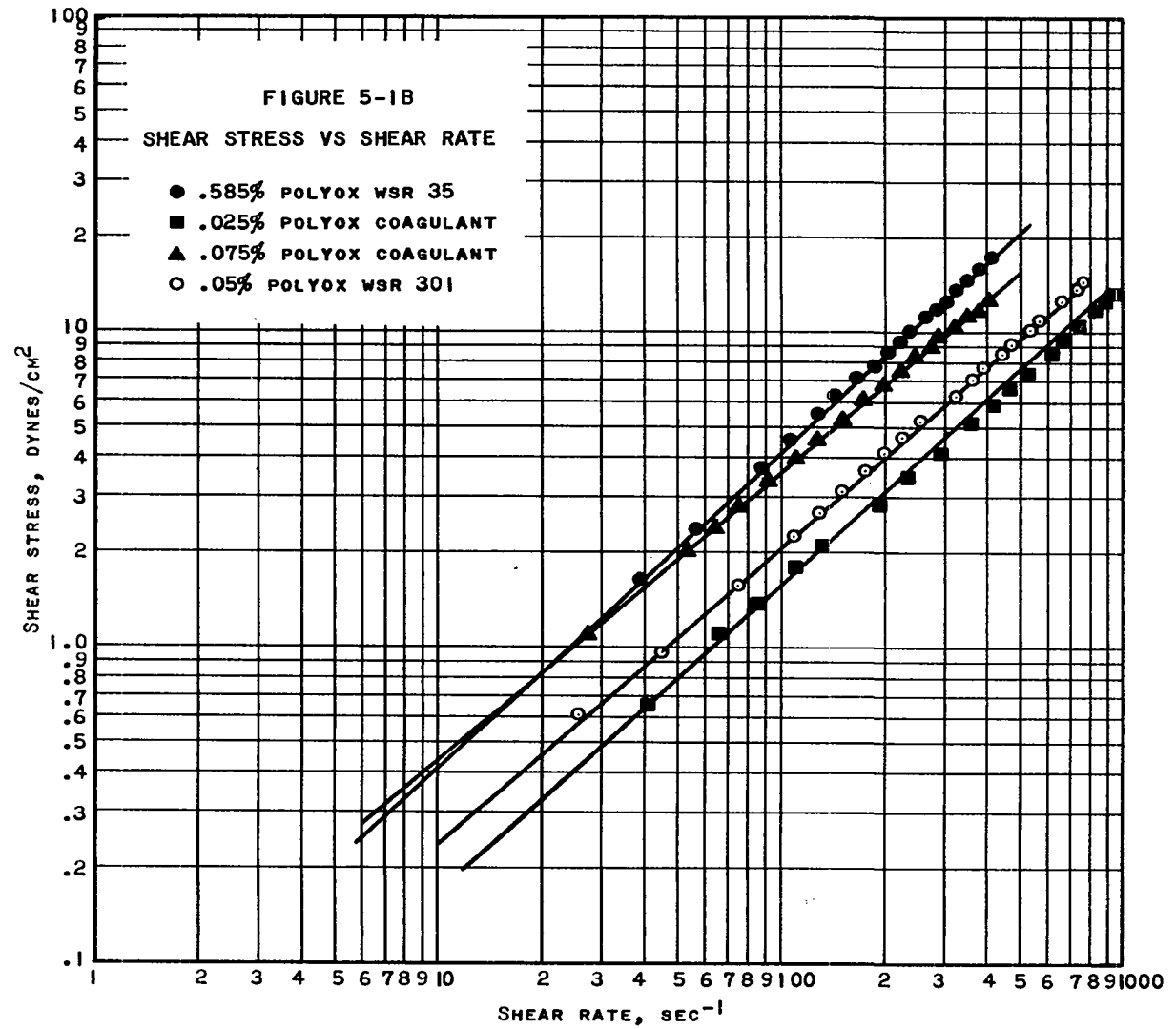
The data on the polymer solutions are tabulated in Table 5.1. In the case of Newtonian fluids the constant n in the power law model is one. The 0.585% solution of WSR-35 and the 0.025% solution of Coagulant appeared to be essentially Newtonian while flowing through a capillary. Non-Newtonian behavior increases as the value of the constant n decreases. Everything else held constant the solution becomes more non-Newtonian as the concentration is increased. Analysis of Table 5-1 also shows that the more viscous solutions are formed by the higher molecular weight polymers.

TABLE 5-1

TABULATED DATA ON THE POLYMER SOLUTIONS

Molecular Weight	Polymer	Concentration Weight Percent	C $\frac{\text{dynes-sec}^n}{\text{cm}^2}$	n
4,000,000	WSR-301	0.050	0.022	0.980
4,000,000	WSR-301	0.100	0.055	0.920
4,000,000	WSR-301	0.199	0.328	0.750
4,000,000	WSR-301	1,000	25.300	0.459
200,000	WSR-35	0.585	0.042	1.000
600,000	WSR-205	0.394	0.045	0.972
5,000,000	Coagulent	0.025	0.016	1.000
5,000,000	Coagulent	0.075	0.053	0.919
5,000,000	Coagulent	0.149	0.121	0.849
5,000,000	Coagulent	0.296	0.792	0.682
5,000,000	Coagulent	0.486	2.602	0.604

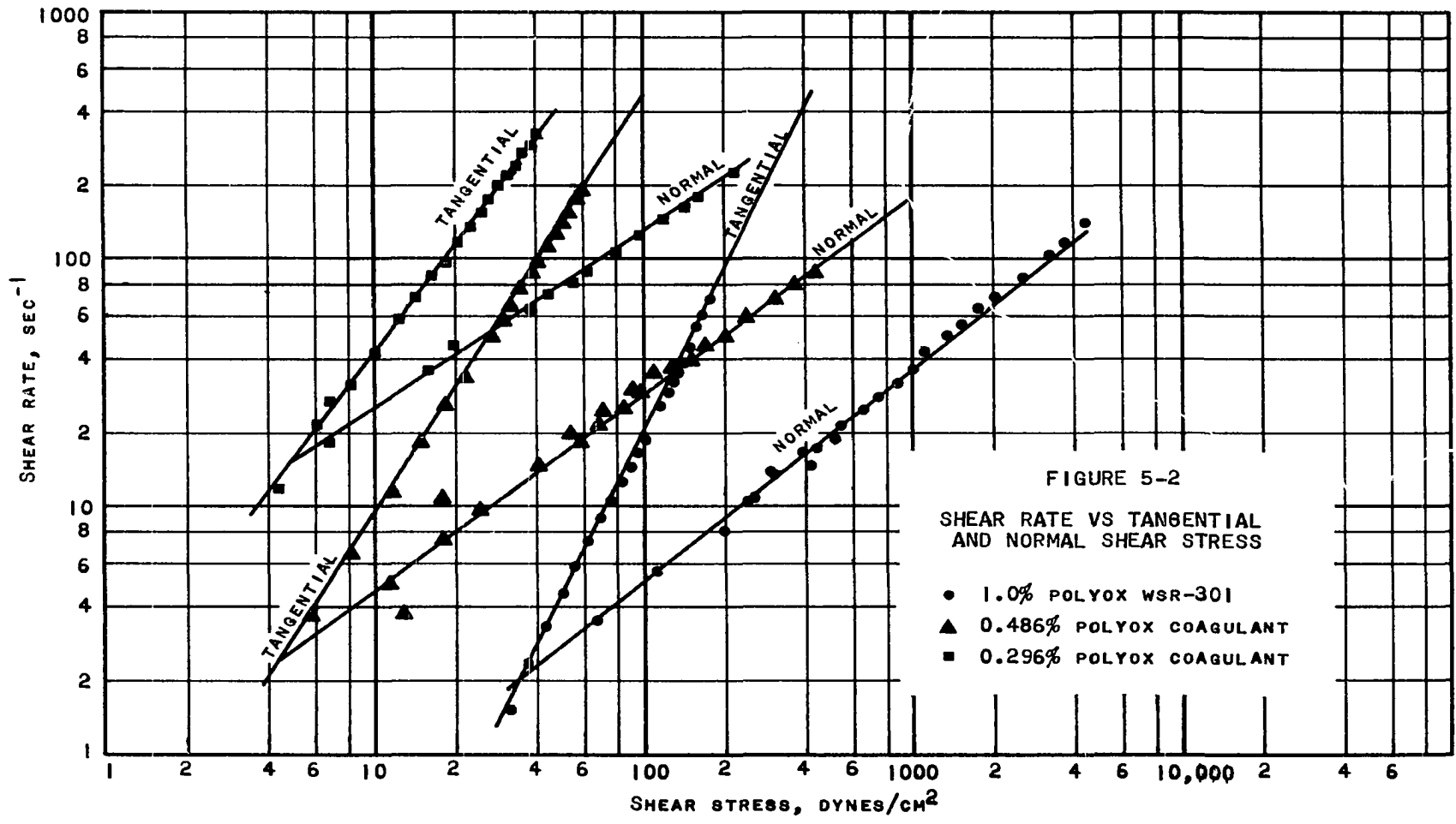




Objections can be made to representing shear rate-shear stress data by the power law model. The power law predicts an infinite viscosity in the limit of vanishing shear rate, and a zero viscosity in the limit of infinite shear rate. Some real polymer solutions exhibit Newtonian behavior at low shear, and the power law model cannot predict this behavior. This is a fundamental failure of the power law model and provides for a valid objection to its generalized application. The data taken in this research, however, fit the power law model quite well. In cases where some slight deviation of power law behavior was observed, the model was adapted to fit the lower shear rate data, which is of more importance in this study.

Normal Stress Measurements

The normal stresses of several polymer solutions were measured in a parallel plate instrument, and the results are shown in Figure 5-2. Normal stress measurements were made only on 0.296% Polyox Coagulant solution, and a 1% solution of WSR-301. Below a concentration of 0.3%, the normal stress could not be measured on the parallel plate instrument. Normal stresses exist below this concentration but the height of the fluid rise in the capillaries was too small to measure accurately. If for example, one assumes that $(P_{11} - P_{22})$ is equal to τ_{12} , $dh/dl \ln r$ as calculated from Equation (3-19) is extremely small for concentrations less than 0.3%.



Measurement of the normal stresses in dilute solutions is a difficult instrumentation problem and some method other than the parallel plate instrument must be used. Because normal stress data are not available for the dilute concentrations used in this research, an elastic parameter was not included in the correlative equation. Nevertheless, the normal stress data taken yielded some valuable information concerning the relative magnitudes of the normal and tangential stress components, and provided information on the relaxation time of these polymer solutions.

It was found that normal stress data plotted fairly well on a log plot. This suggests that the normal stress data can be represented by an expression similar to the power law equation. The equation

$$P_{11} - P_{22} = - C' \gamma^{n'} \quad (5-1)$$

was used, where $P_{11} - P_{22}$ is the normal stress difference, C' and n' the experimentally determined constants. Accordingly, the recoverable shear may be represented by

$$S = \frac{P_{11} - P_{22}}{\tau_{12}} = \left(\frac{C'}{C} \right) \gamma^{n'-n} , \quad (5-2)$$

and the relaxation time by

$$t_c = \left(\frac{C'}{C} \right) \gamma^{n'-n-1} . \quad (5-3)$$

Examination of Figure 5-2 shows increased scatter of data in

the low shear rate range. This is caused by the relatively small differences of h near the center of the tubes. Any small error made in the measurement becomes magnified in the process of the calculations.

TABLE 5-2

TABULATED NORMAL STRESS DATA

Polymer	Stress Component	C or C' $\frac{\text{dynes-sec}^n}{\text{cm}^2}$	n or n'
1.00% Polyox WSR-301	Tangential	25.3	0.459
	Normal	16.0	1.140
0.486% Polyox Coagulent	Tangential	2.602	0.604
	Normal	1.563	1.236
0.296% Polyox Coagulent	Tangential	0.792	0.682
	Normal	0.0833	1.479

Flow of Polymer Solutions through Porous Media

Presentation of Results

Table 5-3 summarizes some of the basic data of each flow test, and Figures 5-3 a, b, c, etc. are graphical presentations of the results of flowing polymer solutions through porous media.

Figure 5-3 shows the viscosity ratio in porous media as a function of the linear flow velocity. The viscosity ratio is defined as follows:

TABLE 5-3

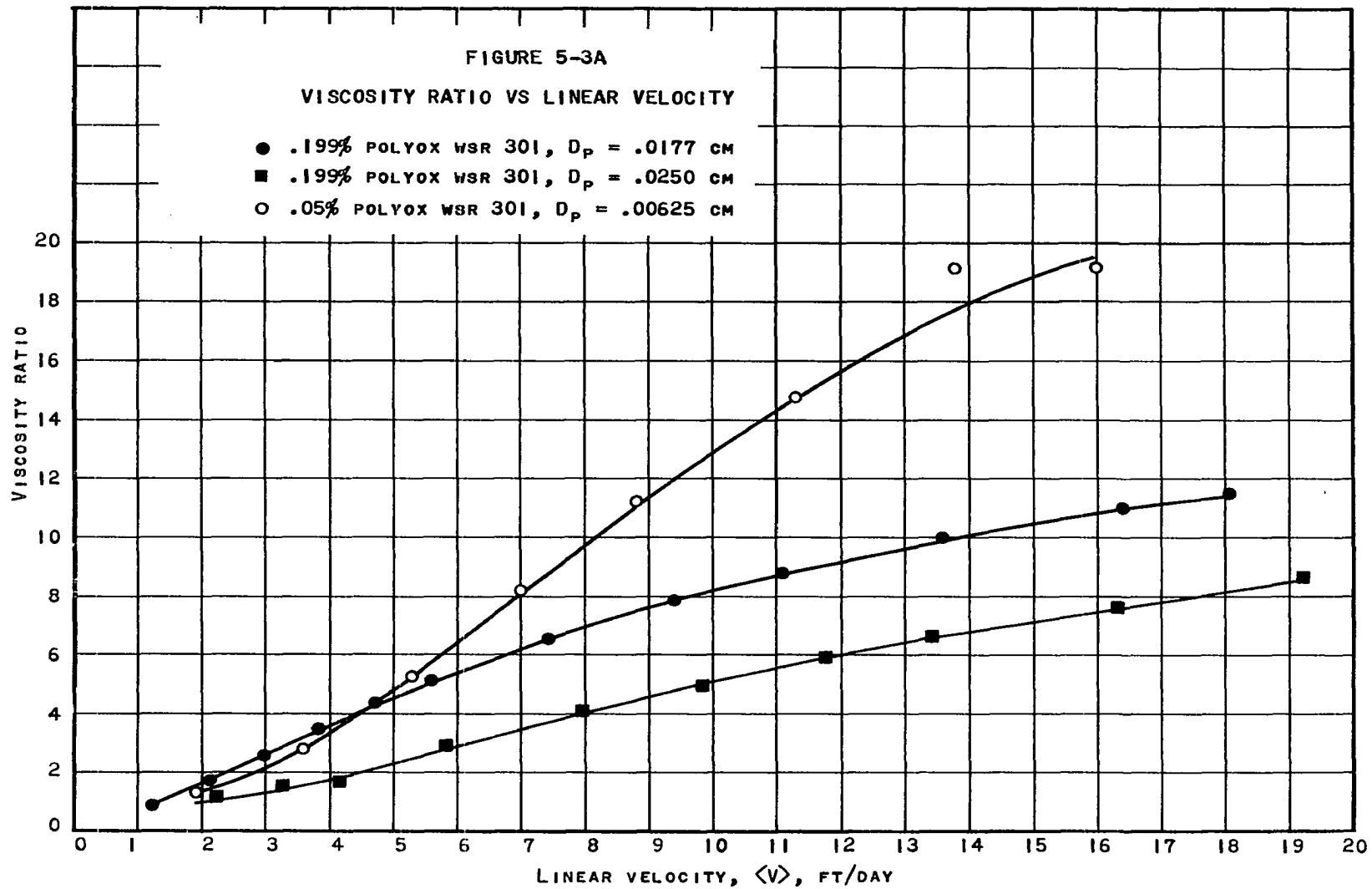
FLOW THROUGH POROUS MEDIA - TABULATED DATA

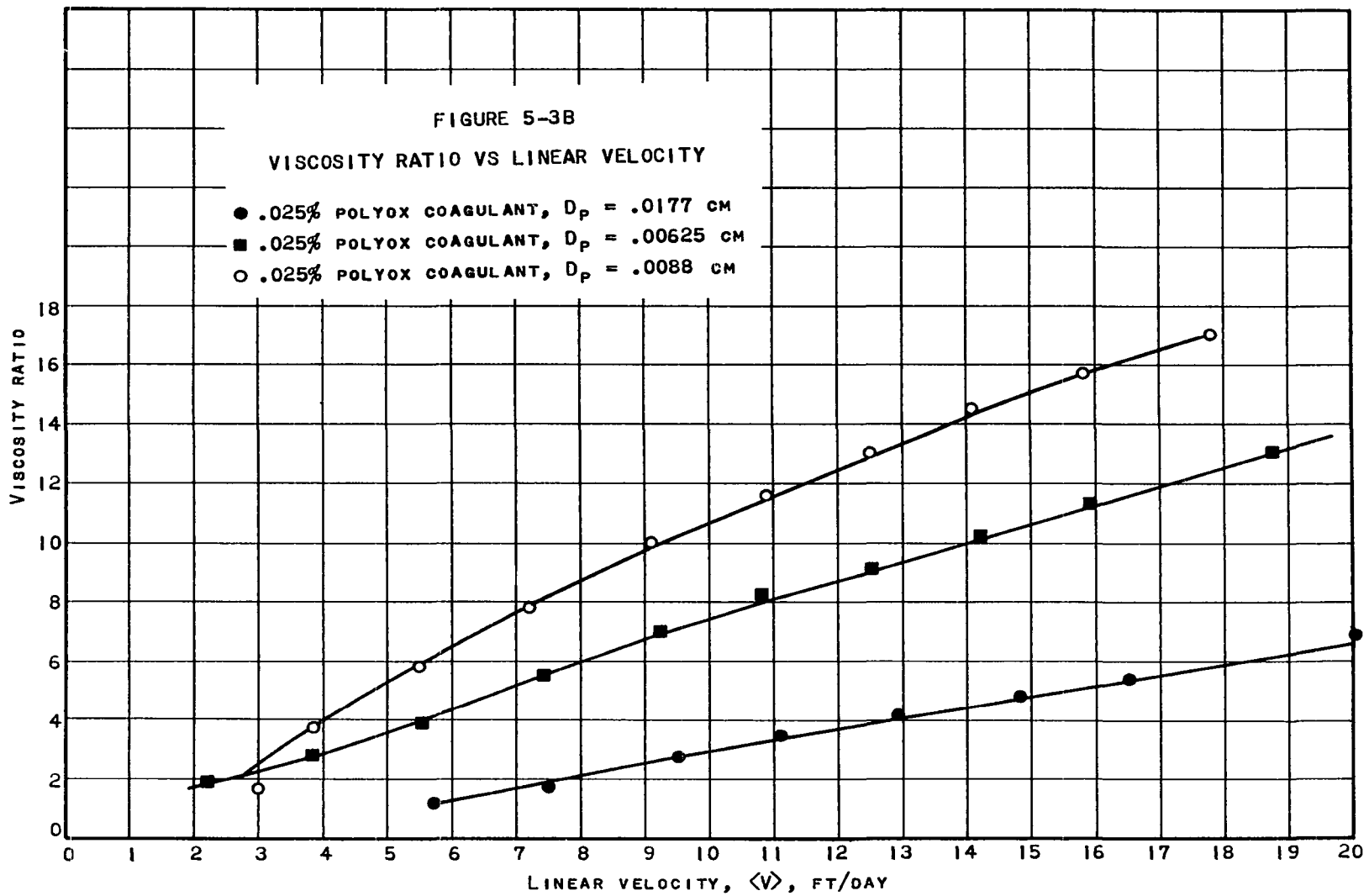
Run No.	U.S. Standard Sieve Mesh#	Porosity (percent)	Permeability (darcies)	Polymer and Concentration (weight percent)
1	70-100	36.4	16.03	0.199 WSR-301
2	50-70	34.7	18.00	0.199 WSR-301
3	70-100	36.7	16.00	0.100 WSR-301
4	200-270	38.9	2.43	0.050 WSR-301
5	70-100	36.5	16.00	0.585 WSR-35
6	200-270	38.1	2.43	0.585 WSR-35
7	70-100	37.1	16.03	0.025 Coagulent
8	200-270	38.3	2.43	0.025 Coagulent
9	140-200	38.7	3.81	0.025 Coagulent
10	70-100	35.8	16.03	0.296 Coagulent
11	50-70	37.3	18.00	0.075 Coagulent
12	70-100	36.7	16.03	0.075 Coagulent
13	140-200	39.2	3.81	0.075 Coagulent
14	70-100	36.6	16.03	0.149 Coagulent
15	70-100	36.8	16.03	0.394 WSR-205
16	140-200	38.2	3.81	0.394 WSR-205
17	140-200	38.1	3.81	0.149 Coagulent
18	70-100	36.2	16.03	0.486 Coagulent

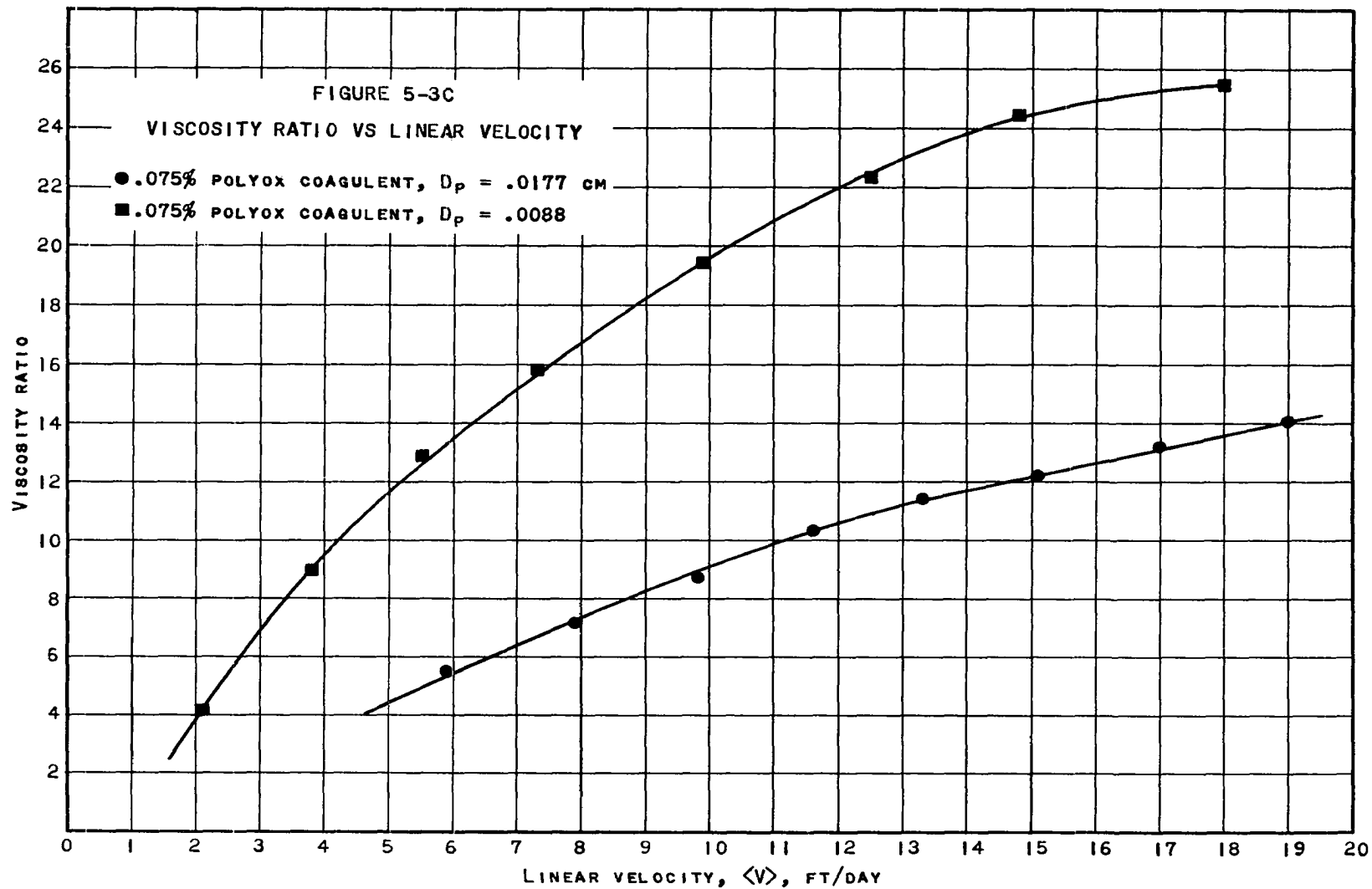
FIGURE 5-3A

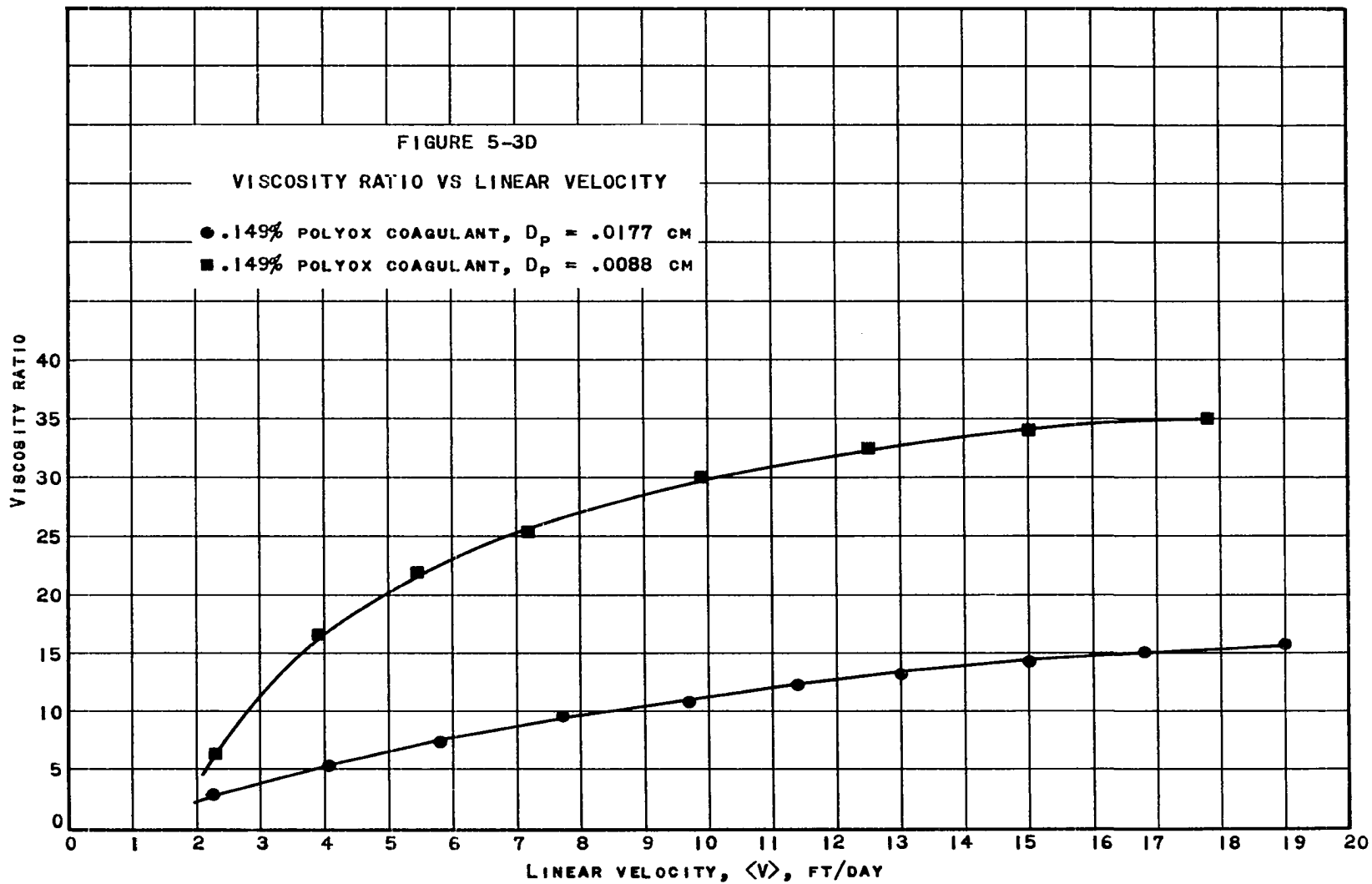
VISCOSITY RATIO VS LINEAR VELOCITY

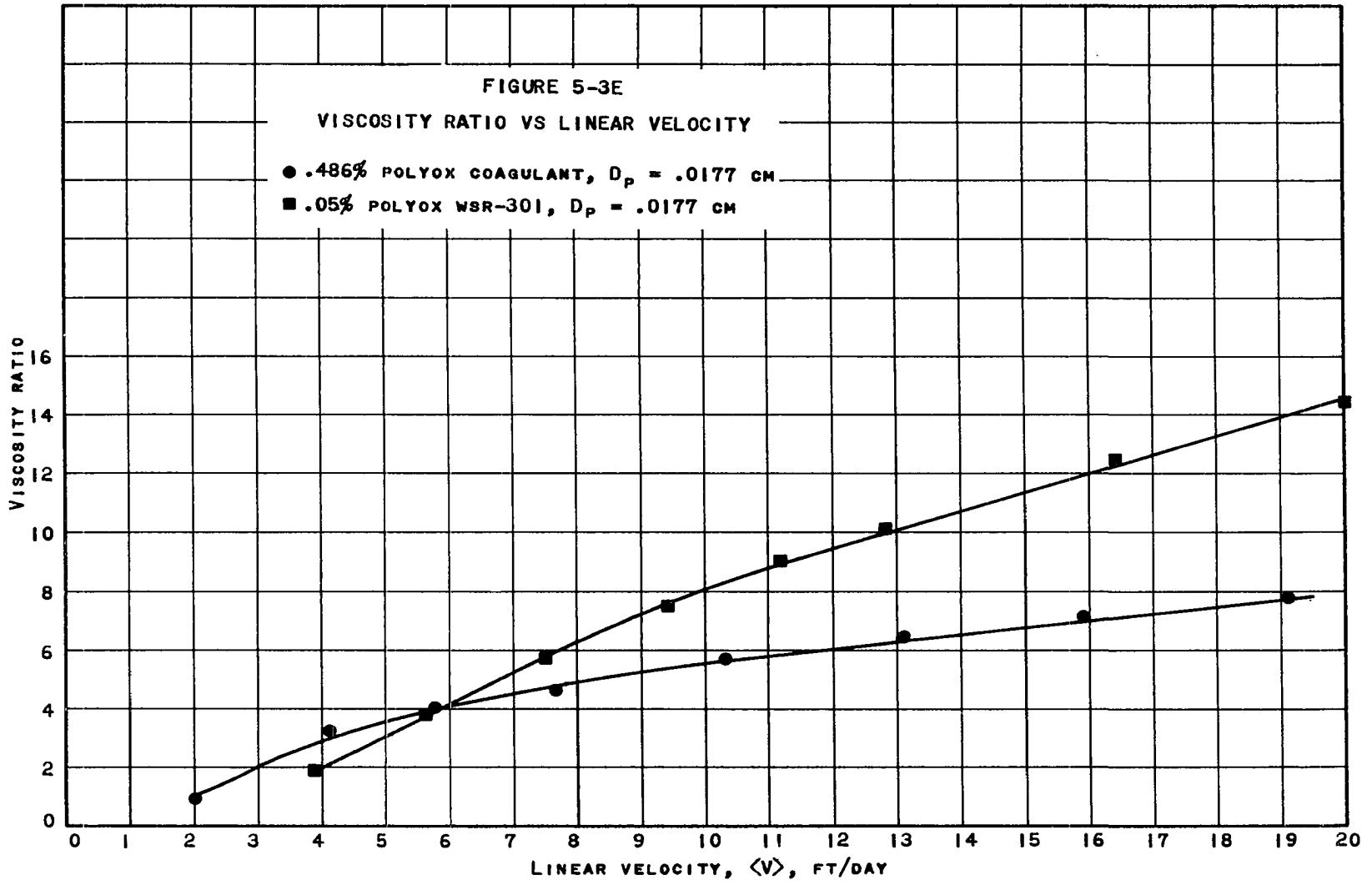
- .199% POLYOX WSR 301, $D_p = .0177$ CM
- .199% POLYOX WSR 301, $D_p = .0250$ CM
- .05% POLYOX WSR 301, $D_p = .00625$ CM

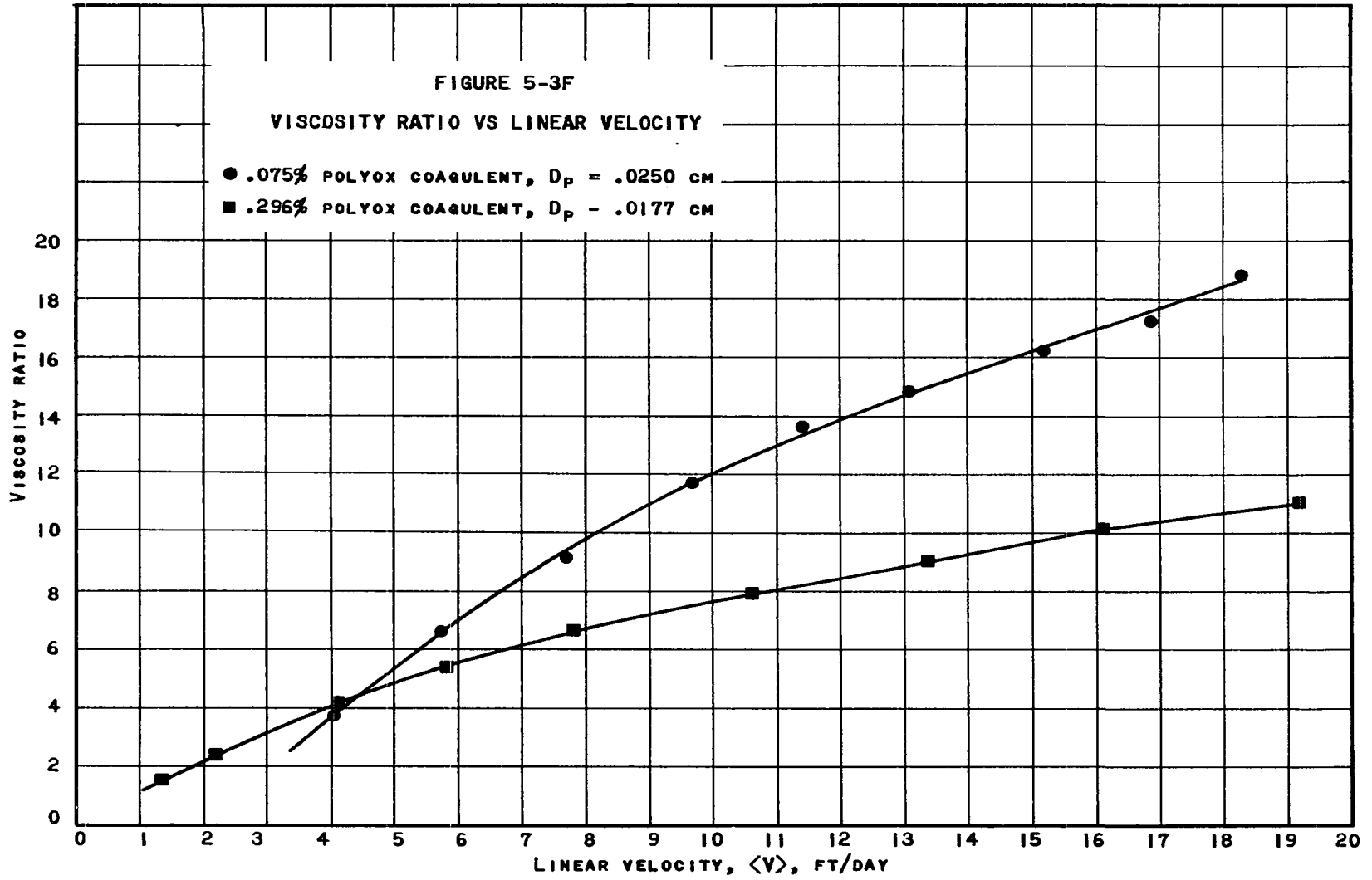












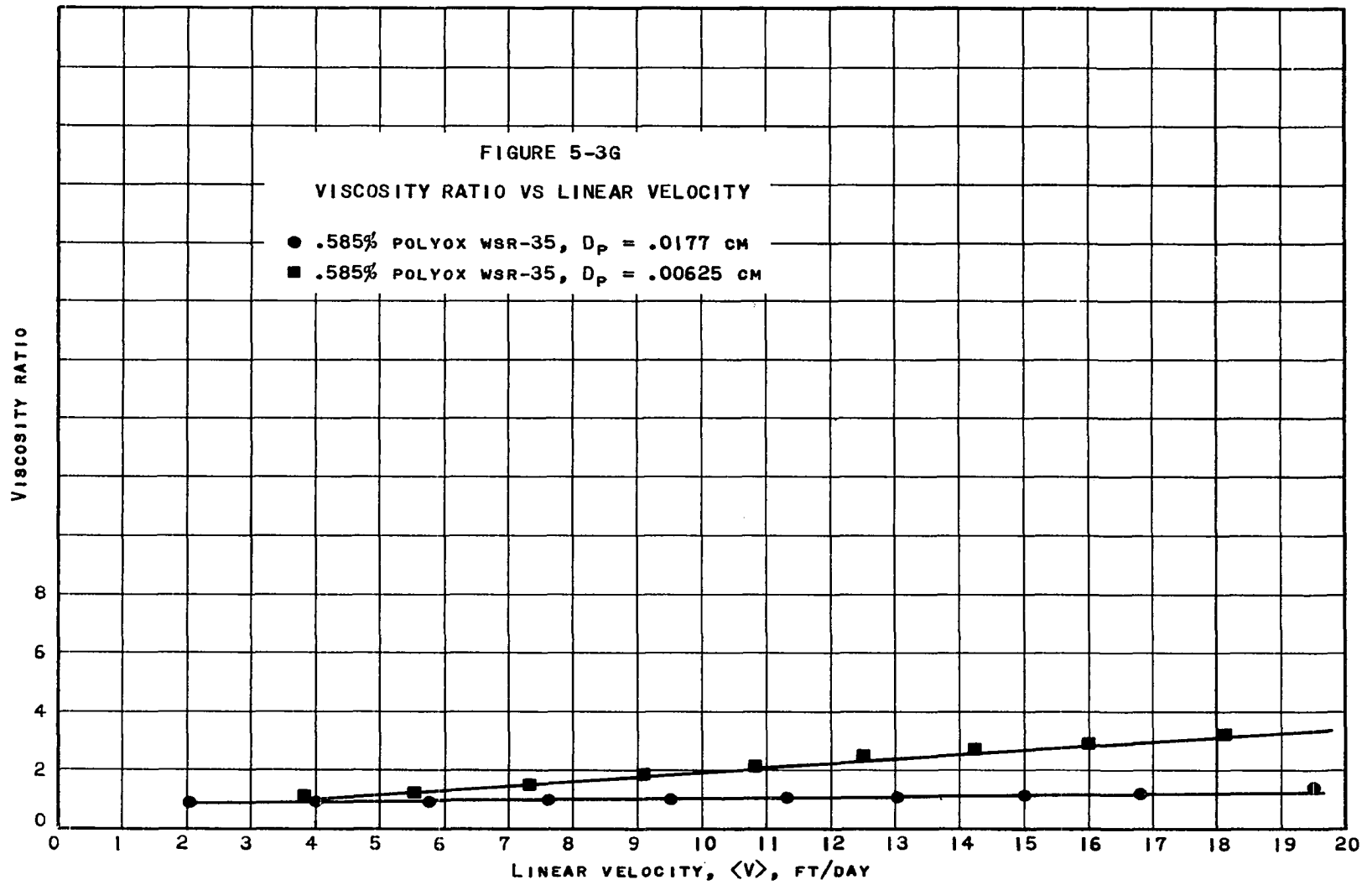
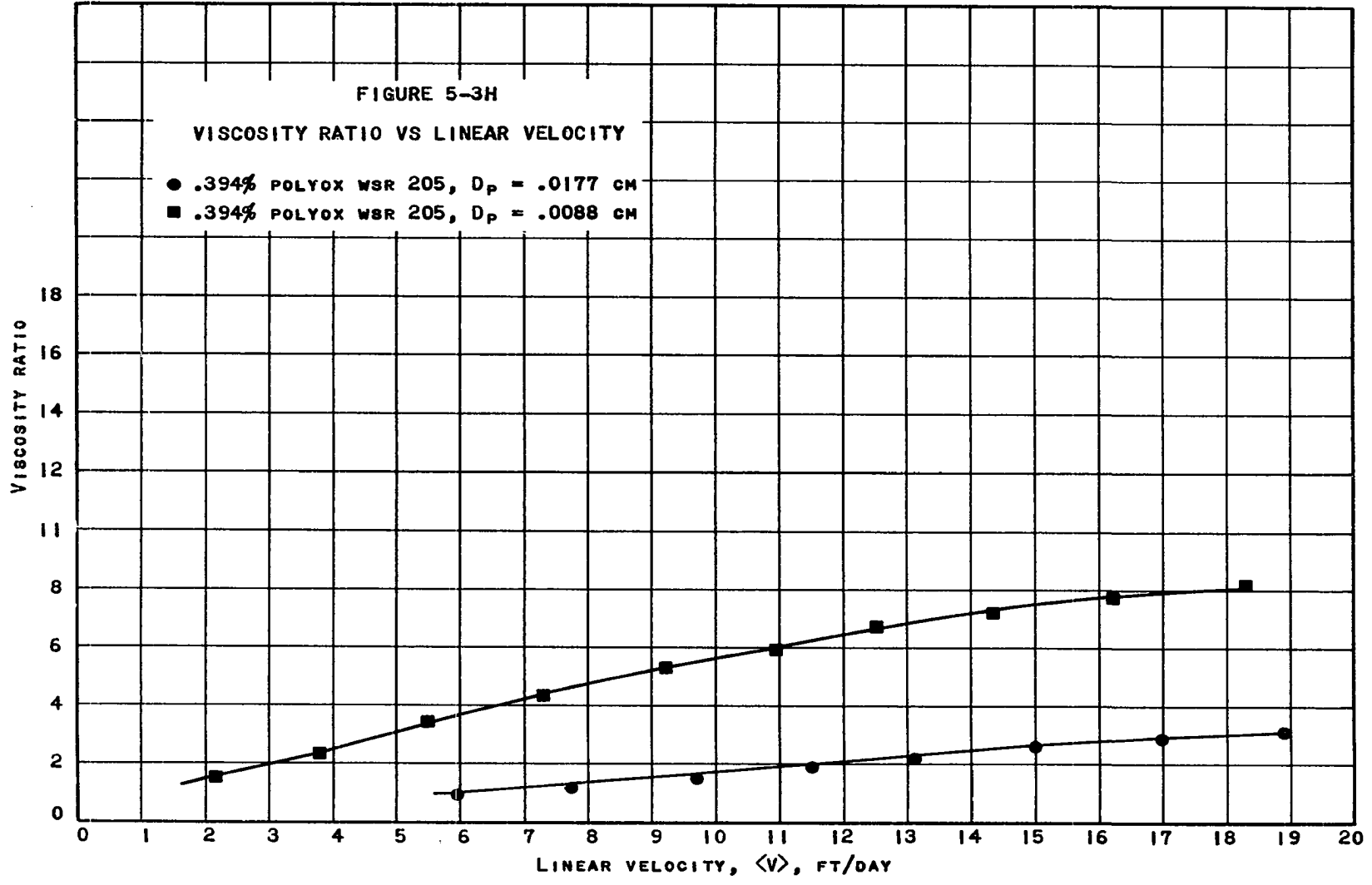


FIGURE 5-3H

VISCOSITY RATIO VS LINEAR VELOCITY

- .394% POLYOX WSR 205, $D_p = .0177$ CM
- .394% POLYOX WSR 205, $D_p = .0088$ CM



$$R = \frac{\text{apparent viscosity in porous media as calculated from Darcy's equation}}{\text{viscosity determined from a steady state experiment}} \quad (5-4)$$

The numerator in Equation (5-4) will be referred to as "insitu viscosity" and the denominator by "steady state viscosity." Thus the insitu viscosity is calculated by

$$\eta = \frac{K\Delta P}{VL} \quad (5-5)$$

where the permeability was determined by flowing a Newtonian fluid through the porous media. The steady state viscosity was determined by a capillary experiment, previously described. The steady state viscosity is a function of the shear rate, and thus one must arrive at some average shear rate in the porous media in order to estimate the viscosity.

To predict a shear rate requires two quantities: a velocity (or volumetric flow rate) and the radius through which the fluid moves. The average velocity will be assumed to be the pore velocity, defined by Equation (3-3). Of course, this velocity cannot be assumed to be entirely accurate, as the fluid travels in a tortuous path, and undergoes considerable acceleration and deceleration. The radius of the flow channels can be estimated by use of the hydraulic radius theory for porous media. Fair and Hatch⁹ define the hydraulic radius for porous media as

$$\text{Radius} = 2R_h$$

$$\begin{aligned} R_h &= \frac{\text{volume available for flow}}{\text{total wetted perimeter}} \\ &= \frac{\text{volume of spheres}}{\text{surface area of spheres}} \frac{\phi}{(1-\phi)} \\ &= \frac{D_p \phi}{6(1-\phi)} \end{aligned} \quad (5-6)$$

R_h is the hydraulic radius, D_p the diameter of the spheres, and ϕ the porosity. The shear rate can be estimated by

$$\gamma_w = \frac{4V}{R} \quad (5-7)$$

By substitution of Equation (5-6) into (5-7) the following expression results:

$$\gamma_{pm} = \frac{24\langle V \rangle(1-\phi)}{D_p \phi} \quad (5-8)$$

The term γ_{pm} is designated as the shear rate in porous media. As is customary a tortuosity factor will be included to account for the fluid traveling in a tortuous path. This factor is quite arbitrary, but the $\sqrt{2}$ is often used. Equation (5-9) thus becomes

$$\gamma_{pm} = \frac{24 \sqrt{2} \langle V \rangle (1-\phi)}{D_p \phi} \quad (5-9)$$

For the range of flow rates encountered in this study, the range of shear rates is very small. For most of the solutions

the steady state viscosity changes very little with shear rate, and any inaccuracies in Equation (5-9) do not cause serious error.

As is evident from Figures 5-3 A, B, C, etc. the insitu viscosity increases as the flow rate increases. This is an unexpected result, as a pseudoplastic fluid has a decreasing viscosity with increasing flow rate. The results of this research are in apparent contradiction to Sadowski and Christopher, as their results showed a decreasing viscosity with increasing flow rates. This research, however, confirms some of the results encountered by Pye. Several reasons will be advanced to explain the difference in results of this research with those of other investigators.

Adsorption Phenomena

In calculating the insitu viscosity from Equation (5-5) the assumption was made that the permeability, K , was the same for polymer flow as it is for distilled water. Some experimental evidence,^{6,14} has indicated a reduction in the permeability as a result of flowing polymer solutions through porous media. Under such conditions an additional pressure drop is required for the same volumetric flow rate. Thus, by using Equation (5-5) an anomalously high viscosity is indistinguishable from a reduction in permeability. The experimental evidence in this research indicates that any reduction of permeability is negligible. Three reasons are

cited:

1) The insitu viscosity and the steady state viscosity converge to the same value at some low flow rate, usually between 0.5 ft/day to 1.5 ft/day. If significant reduction in permeability has occurred the calculated insitu viscosity would be higher than the steady state viscosity at these low rates.

2) In flowing polymer solutions through the packed cell the system would come to equilibrium condition and remain at that condition for an indefinite time; i.e., at any given flow rate, the pressure drop across the flow cell remained constant. This reason alone does not indicate the absence of a plugging action. It does indicate, however, that if some plugging does occur that it does not continuously reduce the permeability.

3) On several runs, distilled water was pumped back through the flow cell, displacing polymer from the cell. The permeability was checked when the concentration of polymer in the effluent appeared to be zero, as determined by the efflux time in an Ostwald viscometer. The permeability at this point appeared to be somewhat less than the original permeability. With continued water injection and time, however, the permeability was restored to near its original value.

Based upon these observations it appears that any plugging action was nominal in this research. This does not

suggest in general that plugging is a negligible factor, for it is quite conceivable that in some cases the problem is severe. Plugging would be expected to be more pronounced in actual formation rock because of its low permeability. The type of polymer and the degree of affinity of the polymer for the solvent are also important considerations. The theory advanced by Sadowski regarding adsorption (See Chapter II) appears plausible, but it is clear that additional experiments are needed to define the problem more clearly.

Factors Affecting Flow Behavior

The single most important observation made in this research is that the insitu viscosity in many cases is significantly greater than the steady state viscosity. In one case the insitu viscosity was 35 times that of the steady state viscosity at 18 ft/day. In other cases the insitu viscosity was very nearly the same as the steady state viscosity. This anomalously high flow resistance is not due to entrance effects. When the polymer solution displaced the distilled water from the bead pack a gradual increase in pressure occurred. A rapid climb in pressure would indicate "face" plugging, or a high entrance pressure loss. The behavior of these polymer solutions appear to be functions of several variables, some of which are suggested in Chapter III. These variables will now be discussed.

The relationship of pressure drop and flow rate is

non-linear. The Darcy equation predicts that a linear relationship exists between flow rate and pressure drop. In most of the runs the pressure drop-flow rate curve has the configuration as shown in Figure 5-4. In most cases the data plotted as a straight line on log paper, suggesting the relationship,

$$\frac{\Delta P}{L} = bV^m . \quad (5-10)$$

A quantitative prediction of these constants will be made in a later section.

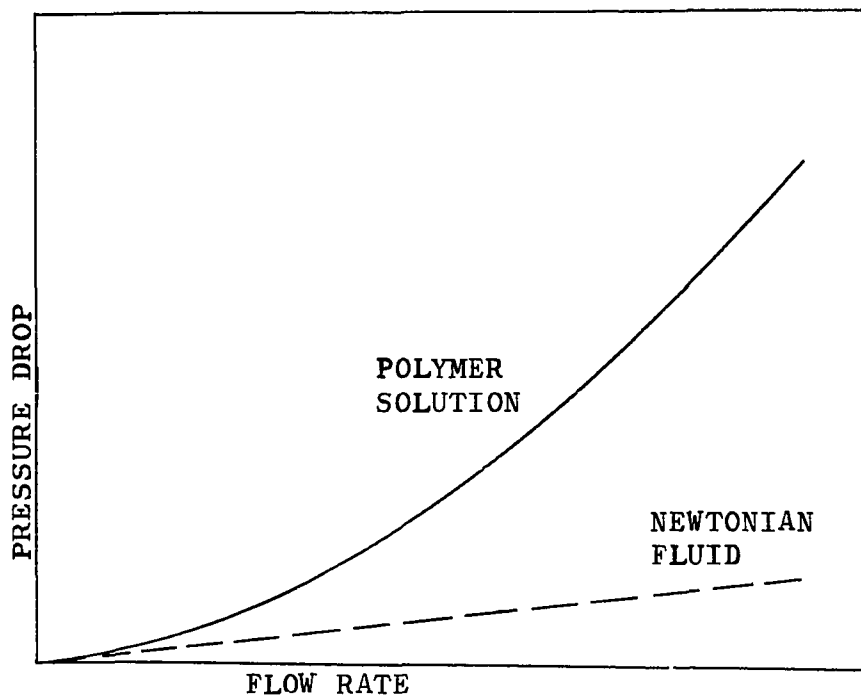


FIGURE 5-4. TYPICAL SHAPE OF A PRESSURE DROP - FLOW RATE CURVE

The molecular weight of the polymer is a very important factor. The size of the molecule is related to its molecular weight. At the present time there is not a method of determining in absolute terms the size of a macromolecule in solution. The problem is complicated by the fact that the molecules are constantly changing in size and shape. The most reliable measure of the size of the polymer molecule, unless physical measurements are made, can be obtained by assuming the random coil configuration, and the use of Equation (2-2). The size calculated from this equation represents a minimum size, as the constant in Equation (2-3) usually varies between 1 and 10. In the case where entanglements occur the effective size of the accumulated molecule may be many times that of a single macromolecule. The root mean square length of a 6 million molecular weight polyethylene oxide molecule was calculated to be 0.0664 microns. The extended length was calculated to be 48.9 microns. When one considers that entanglements and associations occur the effective size of the molecule may be many times greater than calculated. The size of a macromolecule in solution is also a function of the degree of polymer-solvent affinity. If the solvent has a high degree of affinity for the polymer, the effective size of the molecule will be larger.

Of particular importance is the relative size of the flow channel to the size of the macromolecule. Merrill²⁰ indicates that in a capillary when the diameter is less than

20 times greater than the diameter of the largest particle, particle-wall interactions can occur, resulting in an increased pressure drop (or an apparent increase in viscosity). This effect will be termed "wall effect." It is conceivable that in the case of a tortuous path, such as in porous media, the critical diameter may be considerably greater than 20. Graton and Fraser¹⁵ and Fraser¹¹ have made a comprehensive study of the systematic packing of spheres and their relationship to porosity and permeability. There are six stable packings possible with spheres of the same size. The loosest packing (cubic packing) has a porosity of 47.64% and the tightest packing (rhombohedral) has a porosity of 25.95%. The four other forms of packing have porosities which lie between these two extremes. The porosity of the porous media in this research was about half way between the two extremes. If a large number of spheres of each diameter is arranged in any strictly systematic packing, there is a certain diameter ratio for a smaller sphere which can just pass through the throats between the larger spheres into the interstices. For the rhombohedral packing the critical diameter is $0.154 D_p$, and for the cubic packing the critical diameter is $0.414 D_p$. In this research, because the porosity lies somewhere between the two extremes, a critical diameter half way between appears to be a reasonable estimate. Using this estimation the critical diameter is $0.282 D_p$. The smallest beads used in this research has an average diameter of 62.5

microns. The critical diameter then is 17.6 microns. If the macromolecule can be assumed to be analogous to spheres, the ratio of the critical diameter to the diameter of the macromolecule is

$$\text{Ratio} = \frac{17.6}{0.0664} = 265 .$$

It becomes evident that particle-wall interaction is possible, particularly when one considers that the effective size of the molecule, due to entanglements and associations, may be considerably larger than the predicted value of 0.0664 microns, and that fluid travels in a tortuous path.

The experimental evidence shows that the relationship between pore size and molecular weight is a direct one. In all cases but one as the diameter of the beads is decreased the viscosity ratio becomes higher. The most conclusive evidence of this phenomena is shown in Figure 5-3 g. Here a 0.585% solution of WSR-35 was pumped through the porous media. The solution was Newtonian by steady state viscosity measurements, and had a viscosity of 4.2 cp. Using beads of a diameter of 177 microns, very little effect of added flow resistance was noted. Using the smaller beads, 62.5 microns in diameter, the viscosity ratio was several fold at the higher velocities.

The wall effect is believed to be a significant reason for the high flow resistance of these polymer solutions. It is believed that the macromolecules strike the sides of the

flow channel, particularly when the fluid is undergoing a change of direction, and rebounds back into the main flow stream. As a result considerable energy is dissipated. Based upon this theory, the effect would be more pronounced at higher flow rates, as the macromolecule strike the walls with greater frequency and at a higher velocity. The macromolecules are easily deformed, and can pass through some narrow openings, although an additional pressure drop would be required to do so. It appears very likely that a stiff molecule could not very easily flow through porous media. It would either be broken down or plug off some of the pores.

Another effect which is believed to be significant in this research is the normal stress effect. Consider the following figure.

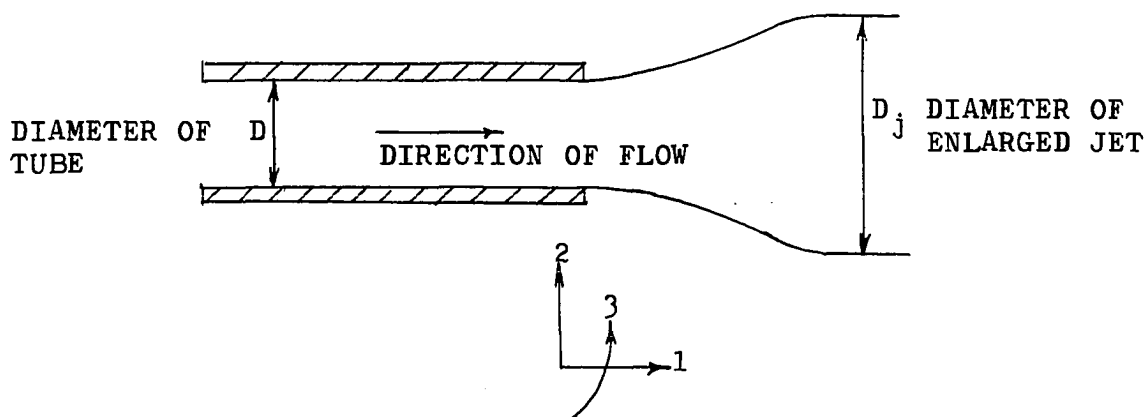


FIGURE 5-5. FLOW OF A VISCOELASTIC FLUID
OUT OF A CAPILLARY

As a viscoelastic fluid flows out of a capillary, the fluid swells as it exits from the tube. As the fluid flows through the capillary stresses normal to the direction of

flow are generated. Thus a force must be applied to keep the capillary from flying apart. The same notation is used as was indicated in Chapter III. The direction of flow is denoted 1, the radial direction is 2, and the angular direction is 3. Metzner, et. al.²² perfected a method for determining the normal stress difference ($P_{11} - P_{22}$) by knowledge of the flow rate, diameter of capillary d , and diameter of jet D_j . The distance at which the jet becomes fully enlarged is a function of the velocity and the relaxation time.

The equation of motion in the radial direction reduces to

$$0 = - \frac{\partial P}{\partial r} + \frac{\partial P_{22}}{\partial r} + \left[(P_{22} - P_{33})/r \right]. \quad (5-11)$$

Integration of this equation from $r = 0$ to any r and using the assumption that $P_{22} = P_{33}$ leads to

$$P(r, z) = P(0, z) + P_{22}. \quad (5-12)$$

Now consider the case of a viscoelastic fluid flowing through a pore, represented pictorially by Figure 5-6. As the fluid passes through a small flow channel normal stresses are generated, and as the fluid enters into a larger opening it expands in a manner similar to the swell at the end of a capillary. Because of this expansion the fluid loses some of its potential energy by an amount proportional to P_{22} . Consider as an approximation that Figure 5-7 represents the condition in porous media where the fluid moves from a small flow channel into a large opening.

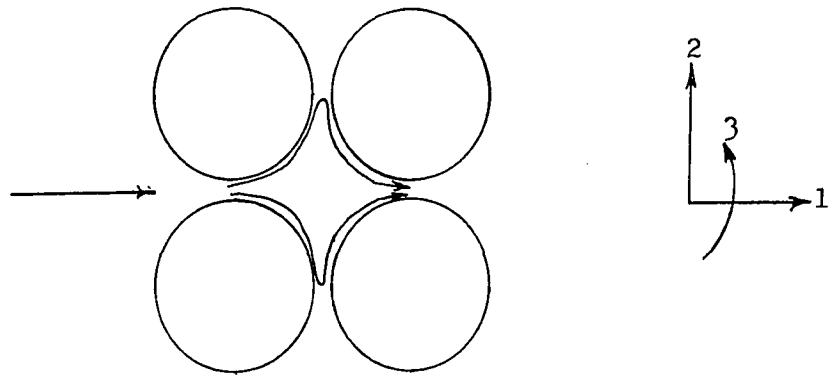


FIGURE 5-6. FLOW OF A VISCOELASTIC FLUID THROUGH A PORE

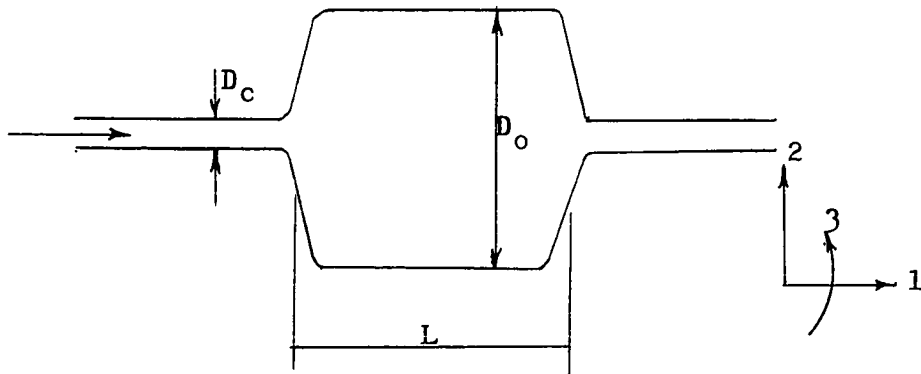


FIGURE 5-7. ENTRY OF A VISCOELASTIC FLUID INTO A LARGE OPENING

As an example, assume the following conditions, in conjunction with Figure 5-7.

0.486% solution of Polyox Coagulent
 $D_c = 20$ microns
 $D_o = 50$ microns
 $L = 50$ microns
 $\langle V \rangle_c = 10$ ft/day

The flow rate in the large opening, by the continuity equation, is 1.6 ft/day. The shear rate at the wall is

$$\gamma_w = \frac{8\langle V \rangle_c}{D_c} = 3.5 \text{ sec}^{-1} \quad \text{small channel}$$

$$\gamma_w = \frac{8\langle V \rangle_o}{D_o} = 0.225 \text{ sec}^{-1} \quad \text{large channel}$$

From Equation (5-1) and Table 5-2,

$$\begin{aligned} P_{11} - P_{22} &= - 1.563(3.5)^{1.236} \quad \text{small channel} \\ &= - 7.34 \text{ dynes/cm}^2 \end{aligned}$$

$$\begin{aligned} P_{11} - P_{22} &= - 1.563(.225)^{1.236} \quad \text{large channel} \\ &= - 0.249 \text{ dynes/cm}^2 \end{aligned}$$

From Equation (3-7) and the Weissenberg assumption that

$$P_{22} = P_{33},$$

$$P_{11} + P_{22} + P_{33} = 0$$

$$P_{11} = - 2P_{22} .$$

Thus, $P_{22} = 2.44 \text{ dynes/cm}^2$ in the small channel, and $P_{22} = 0.0830 \text{ dynes/cm}^2$ in the large channel. The pressure drop due to expansion into the large opening as obtained from Equation (5-12) is

$$\Delta P = P(r,z)_c - P(r,z)_o = (P_{22})_c - (P_{22})_o$$

$$\Delta P = 2.36 \text{ dynes/cm}^2 \quad .$$

As the fluid flows back into the small opening the elastic energy is again restored to the fluid. In porous media this process of expansion and contraction could account for the large pressure drops which occur during the flow of viscoelastic fluids through porous media.

Metzner and White ²³ recently published their results on the flow behavior of viscoelastic fluids in the inlet region of a channel. Their results showed that in the development of velocity profiles in viscoelastic fluids three regions exist: a region of elastic solid-like behavior, followed by a region of boundary layer development and finally a region of fully developed flow. The region of solid-like behavior is characterized frequently by high pressure losses. Their results furnish further evidence that behavior of the viscoelastic fluid in the inlet and exit regions of a pore account for some of the high flow resistance.

Another factor enters into this idealized case, however. This is the time constant, the relaxation time, which is the time required for the fluid to relax after it has been taken out of a stressed position. It is conceivable that if the relaxation time is long enough, or the fluid velocity is great enough, that the fluid can pass through the large opening and back into a small opening before the fluid has had time to relax. Under such a condition the fluid would behave more as a viscous fluid and less like a

viscoelastic fluid. Again, using the above example, the relaxation time and the fluid transit time will be calculated. From Equation (5-3) and Table 5-3 the relaxation time becomes

$$t_c = \frac{1.563}{2.602} (3.5)^{1.236-.604-1}$$

$$= .378 \text{ sec .}$$

The fluid transit time becomes

$$t = \frac{.0050}{1.6} \frac{86,400}{30.4} = 8.9 \text{ sec .}$$

Thus it takes 8.9 sec for the fluid to pass through the large opening and 0.378 sec for the fluid to relax. For a 0.296% solution of Polyox coagulent the relaxation time is 0.0815 sec, and for a 1% solution of WSR-301 the relaxation time is 0.43 sec. In this example problem the fluid has ample time to relax, and should correspondingly experience a loss of potential energy as it moves from the small flow channel into the larger opening.

If the theory regarding the normal stress effect is correct, one can explain the vast differences in results of this research and the investigations of Sadowski and Christopher. As was previously indicated, the basic difference in results is that in this research the insitu viscosity increased with increasing flow rate, whereas, the opposite effect was found by Sadowski and Christopher. Some important differences will be cited: 1) In this research

the bead size ranged from an average diameter of 62.5 microns to 250 microns. Beads used by Sadowski ranged from 1124 to 2807 microns in diameter, and those used by Christopher had an average diameter of 775 microns. 2) The flow rates in this research were generally much slower. 3) Less viscous solutions were used. 4) Much higher molecular weight polymers were used. In addition, polyethylene oxide is much more elastic than the polymers used by Sadowski and Christopher.

Two main reasons are cited to explain the difference in results of this research from the other investigators. First, the polymer solutions, for a given concentration, are more elastic. This is due primarily to the nature of the polyethylene oxide molecule, and the high molecular weight. Generally, the elastic properties become more pronounced as the molecular weight increases. For this reason, elastic effects were noticeable even when the concentration is very low. To achieve the same degree of elasticity in lower molecular weight polymers, such as those used by the other investigators, requires a greater concentration. In general, the relaxation time increases as the viscosity increases. Thus, by the combination of higher flow rates and slower relaxation times the resistance effect, based upon the theory previously advanced, will not be appreciable. Second, the wall effect, believed to be significant when extremely high molecular weight polymer solutions flow through small channels, was not evident in the research of the other

investigators. The size of the flow channels were much larger and the molecular weight of the polymer were much less. This research, in general, substantiates the results of Pye.

It is interesting to note that Sadowski did obtain different results with his highest molecular weight polymer. At a certain flow rate he encountered increased resistance to flow. This polymer appeared to be the only polymer which exhibited elastic effects, and he concluded that this effect was related to its elastic properties. To account for this behavior he introduced the following dimensionless parameter:

$$\frac{\eta_0 / \tau_{\frac{1}{2}}}{D_p / V_0} .$$

In this expression η_0 is the zero shear viscosity, $\tau_{\frac{1}{2}}$ the shear stress at $\eta = \frac{1}{2} \eta_0$, D_p the diameter of a particle, and V_0 the velocity of the fluid. The fluid relaxation time was taken to be the numerator of the expression. The relaxation time defined in such manner is subject to criticism because any pseudoplastic fluid, whether or not it has elastic effects, is predicted to have time dependent effects. Nevertheless, Sadowski recognized that some characteristic time of the fluid and some characteristic time of the flowing fluid together influence the flow behavior.

In this research, it can be observed the greatest resistance effect occurred when the concentration is between

0.075% and 0.149% (for Coagulant solutions). The resistance effect is very evident with the 0.025% solution of Coagulant, but not as pronounced as some of the higher concentration solutions. The resistance effect begins to decline when the concentration reaches 0.296% and becomes more pronounced when the concentration reaches 0.486%. This conclusion is in agreement with the results of Pye.

Development of a Correlative Equation

As was previously indicated, the data appeared to fit the relationship

$$\frac{\Delta P}{L} = b \langle V \rangle^m \quad (5-10)$$

where b and m are constants. In order to predict non-Newtonian flow in porous media the constants b and m must be functions of the rheological parameters of the fluid and some property of the porous media, such as permeability. The constant m was found to be predicted with a reasonable degree of accuracy by the following empirical expression:

$$m = a n \quad (5-13)$$

$$a = 2.0 \quad \text{Coagulant solutions}$$

$$a = 2.28 \quad \text{WSR-301 solutions}$$

As can be observed from Figure 5-3, the viscosity ratio approaches the value of one at low flow rates. Thus, if one can estimate the flow rate at which the viscosity ratio becomes one,

TABLE 5-4

FLOW THROUGH POROUS MEDIA - CONSTANTS b AND m

Run No.	b	m
1	0.112	1.722
2	0.060	1.740
3	0.016	1.896
4	0.294	2.330
5	0.00884	1.224
6	0.0425	1.710
7	0.000823	2.270
8	0.0338	1.933
9	0.00263	1.991
10	0.445	1.423
11	0.00235	1.864
12	0.0255	1.746
13	0.275	1.700
14	0.0848	1.618
15	0.0020	2.092
16	0.054	1.842
17	1.500	1.403
18	1.630	1.179

$$\frac{\Delta P}{L} = \frac{\langle V \rangle \phi \eta(\gamma)}{6.33K} = b \langle V \rangle^m . \quad (5-14)$$

This is equivalent to saying that the Darcy equation becomes equal to Equation (5-10) at some low flow rate. The value of $\langle V \rangle$ at which the two expressions in Equation (5-14) are equivalent, was found empirically to be

$$\langle V_c \rangle = cnK^{0.20} \quad (5-15)$$

$$c = 0.70 \quad \text{Coagulent Solutions}$$

$$c = 1.15 \quad \text{WSR-301 Solutions}$$

With these assumptions

$$\eta = B \langle V \rangle^{m-1} \quad (5-16)$$

$$B = \frac{\eta(\gamma_c)}{\langle V_c \rangle^{m-1}} .$$

The viscosity $\eta(\gamma_c)$ is the viscosity evaluated at $\langle V_c \rangle$. Thus from Equation (5-9), and some manipulations,

$$\eta(\gamma_c) = c \left[\frac{.006 \langle V_c \rangle^{(1-0)}}{D_p^0} \right]^{n-1} \times 100 . \quad (5-17)$$

In Equations (5-14), (5-15), (5-16), and (5-17), K has the units of Darcy, $\langle V \rangle$ ft/day, D_p in cm, η cp and $\Delta P/L$ psi/ft. In the case where the fluid has nearly Newtonian viscosity or it becomes difficult to estimate the shear rate in the formation, the viscosity may be estimated with reasonable accuracy at any low shear rate. As can be seen in Appendix

F the steady state viscosity varies very little for most of the solutions within the range of shear rates encountered.

Equation (5-16) is the basic equation used to describe non-Newtonian flow in porous media. For any given flow rate the viscosity is predicted. The effects of permeability on the insitu viscosity are included in the equation. Equation (5-16) can be used in conjunction with the Darcy equation,

$$q = \frac{6.33 \text{ KA}\Delta P}{\eta L} \quad (5-18)$$

where η is the non-Newtonian viscosity calculated by Equation (5-16), and is subject to the condition that $\langle V \rangle \gg \langle V_c \rangle$. For the case where $\langle V \rangle \ll \langle V_c \rangle$, η is essentially constant and can be evaluated by Equation (5-17).

The correlation developed here is by no means a complete answer to non-Newtonian flow in porous media. The fact that Sadowski and Christopher obtained quite different results is ample evidence that this correlation is not valid under all flow conditions. This correlation is expected to yield approximate results only when using polyethylene oxide or a similar polymer and under conditions similar to that in this research. The constants a and c appear to be functions of the molecular weight.

Recommendations for Future Research

Additional work can be done to study the behavior of polymer solutions in a stratified reservoir. In the case of

conventional water injection into a reservoir which contains layers of highly different permeability, the water preferentially flows in the zone of highest permeability. In a secondary recovery project where such stratification occurs, water often flows through the more permeable streaks quite rapidly and reaches the producing well. In some cases the well is producing nearly all water before significant oil is recovered from the less permeable zones. By increasing the viscosity of water, the rate of frontal advance in the more permeable zones relative to that in the tighter zone is lowered. Consequently, more oil is recovered.

Laboratory experiments can be performed to study the effect of flow rate on oil recovery. The results of this research indicate that higher oil recovery would be expected at the higher flow rates, due to the higher apparent viscosity of the displacing phase. In practical field operations it is not always possible to increase the injection rate, particularly for viscous water injection, due to the accompanying high pressures.

CHAPTER VI

CONCLUSIONS

The purpose of this research was to understand more clearly the physical parameters involved in flowing long chained polymers through porous media, and to mathematically describe the flow behavior by knowledge of certain rheological parameters and some characteristic of the porous media. Water solutions of polyethylene oxide were used in this research. The primary observation made in this research is that under certain conditions, the polymer solutions offer considerable resistance to flow in porous media. The magnitude of this resistance appeared to be a function of the following variables:

1. Flow Rate. The flow resistance increases as the flow rate is increases. The "insitu viscosity" is a measure of this resistance and was defined as that viscosity which is calculated from the Darcy Equation. The "steady state" viscosity was defined as the viscosity that would be predicted from steady state viscometric measurements. At low flow rates the insitu viscosity and the steady state viscosity were identical. At a critical flow rate, usually

between 0.5 to 1.5 ft/day, the insitu viscosity became greater than the steady state viscosity.

2. Molecular Weight. The resistance effect is most pronounced in the high molecular weight polymers. The molecular weight of polymers ranged from 5,000,000 (Coagulent) to 200,000 (WSR-35). The WSR-35 solutions showed only a small resistance effect.

3. Pore Size. The pore size was varied by using different sizes of glass beads. The pore size is important only in conjunction with the molecular weight. All other conditions equal, for each molecular weight polymer as the pore size is decreased the insitu viscosity increases.

4. Concentration. The viscosity ratio, defined as the ratio of the insitu viscosity and steady state viscosity, increased as the concentration increased up to approximately 0.15%, after which it begins to decrease.

Based upon the experimental data and normal stress measurements it was concluded that the resistance effect is chiefly a function of two causes: 1) Interaction between the macromolecules and the walls of the flow channels, and 2) The behavior of viscoelastic fluids in the inlet and exit regions of a pore. The relative importance of these two variables have not been evaluated.

By knowledge of the power law parameters for a polymer solution and the permeability of the formation, one can

predict the flow behavior by use of Equation (5-16). The use of this equation is subject to the restrictions previously mentioned.

REFERENCES

1. Blick, Edward F. "Capillary-Orifice Model for High-Speed Flow through Porous Media," I&EC Process Design and Development, Vol. V, January, 1966.
2. Blount, Elmo M. Theoretical Investigation of Polymer Flooding. Special Problem. University of Oklahoma, Unpublished, July, 1964.
3. Bueche, F. Physical Properties of Polymers. New York: Interscience Publishers, 1962.
4. Burcik, Emil J. "A Note on the Flow Behavior of Polyacrylamide Solutions in Porous Media," Producers Monthly, June, 1965.
5. Christopher, Robert H., and Middleman, Stanley, "Power-Law Flow through a Packed Tube," Industrial and Engineering Chemistry Fundamentals, IV, No. 4 (November, 1965), pp. 422-26.
6. Clay, Terrell Dane. "The Effect of Polymer Additives on Oil Recovery in Conventional Waterflooding." Unpublished Master's dissertation, Department of Petroleum Engineering, University of Oklahoma, 1965.
7. Collins, Royal Eugene. Flow of Fluids through Porous Materials. New York: Reinhold Publishing Corporation, 1961.
8. Daniels, Farrington. Outlines of Physical Chemistry. New York: John Wiley and Sons, Inc., 1948.
9. Fair, Gordon M., and Hatch, Loranus P. "Fundamental Factors Governing the Streamline Flow of Water through Sand," Journal of the American Water Works Association, XXV (1933), pp. 1551-65.
10. Ferry, John D. Viscoelastic Properties of Polymers. New York: John Wiley and Sons, Inc., 1961.
11. Fraser, H. J. "Experimental Study of the Porosity and Permeability of Plastic Sediments," Journal of Geology, XLIII (1943), pp. 910-1010.

12. Frederickson, A. G. "Viscoelastic Phenomena in Thick Liquids," Modern Chemical Engineering. Edited by Andreas Acrivos. Chapter 5, I, pp. 197-259.
13. Frederickson, Arnold G. Principles and Application of Rheology. Englewood Cliffs, New Jersey: Prentice-Hall, Inc., 1964.
14. Gallus, J. P., Lummus, J. L., and Fox, J. E. Jr. "Use of Chemicals to Maintain Clear Water for Drilling," AIME Transactions (1958), p. 70.
15. Gratton, L. C., and Fraser, H. J. "Systematic Packing of Spheres - With Particular Relation to Porosity and Permeability," Journal of Geology, XLIII (1943), pp. 785-909.
16. Kotaka, Tadao, Kurata, Michio, and Tamura Mikio. "Normal Stress Effect in Polymer Solutions," Journal of Applied Physics, XXX, No. 11 (November, 1959), pp. 1705-1712.
17. Lodge, A. S. Elastic Liquids. New York: Academic Press, 1964.
18. Markovitz, Hershel, and Brown, David R. "Parallel Plate and Cone-Plate Normal Stress Measurements on Polyisobutylene-Cetane Solutions," Transactions, Society of Rheology, VII (1963), pp. 137-54.
19. McKinley, R. M., Jahns, H. O., Harris, W. W., and Greenhorn, R. A. "Non-Newtonian Flow in Porous Media," AIChE Journal, XII, No. 1 (January, 1966), pp. 17-20.
20. Merrill, Edward W. "Non-Newtonianism in Thin Liquids: Molecular and Physical Aspects," Modern Chemical Engineering. Edited by Andreas Acrivos, I. New York: Reinhold Publishing Corp, 1963.
21. Merrington, A. C. "Flow of Visco-Elastic Materials in Capillaries," Nature (December 4, 1943).
22. Metzner, A. B., Houghton, W. T., Sailor, R. A., and White, J. L. "A Method for the Measurement of Normal Stresses in Simple Shearing Flow," Transactions of the Society of Rheology, V. (1961), pp. 133-47.
23. Metzner, A. B., and White, J. L. "Flow Behavior of Viscoelastic Fluids in the Inlet Region of a Channel," AIChE Journal, XI, No. 6 (1965), pp. 989-95.

24. Noll, Walter. "A Mathematical Theory of the Mechanical Behavior of Continuous Media," Archive for Rat. Mech. and Anal., II (1958), pp. 197-226.
25. Patent No. 2,827,964. Secondary Recovery of Petroleum, Burton B. Sandiford, March 25, 1965.
26. Patent No. 3,039,529. Secondary Recovery of Petroleum, Keith M. McKennon, June 19, 1958.
27. Patent No. 3,116,791. Secondary Recovery of Petroleum, Burton B. Sandiford, January 7, 1964.
28. Philippoff, Wladimir, and Gaskins, Frederick H. "The Capillary Experiment in Rheology," Transactions of the Society of Rheology, II (1958).
29. Pye, David, J. "Improved Secondary Recovery by Control of Water Mobility," Journal of Petroleum Technology (August, 1964), pp. 911-16.
30. Reiner, M. Lectures in Theoretical Rheology. North Holland, Amsterdam: 1960.
31. Sadowski, T. J. "Non-Newtonian Flow through Porous Media." Unpublished Ph.D. dissertation, University of Wisconsin, 1963.
32. Sadowski, Thomas J., and Bird, R. Byron. "Non-Newtonian Flow through Porous Media," Transactions of the Society of Rheology, 9:2, I Theoretical, pp. 243-50, II Experimental, pp. 251-71, 1965.
33. Sandiford, B. B. "Laboratory and Field Studies of Water Floods Using Polymer Solutions to Increase Oil Recoveries," Journal of Petroleum Technology (August, 1964), pp. 917-22.
34. Scheidegger, Adrian E. The Physics of Flow through Porous Media. University of Toronto Press, 1960.
35. Schowalter, W. R. "Non-Newtonian Viscosities and the Equation of Motion," Progress in International Research on Thermodynamic and Transport Properties. J. F. Masi and D. H. Tsai, editors. New York: Academic Press, 1962.
36. Severs, Edward T. Rheology of Polymers. New York: Reinhold Publishing Corp., 1962.

37. Snell, Gene W., and Schurz, George F. "Polymer Chemicals Aid in Unique Recovery Process," The Petroleum Engineer (February, 1966), pp. 53-59.
38. Stille, John K. Introduction to Polymer Chemistry. New York: John Wiley and Sons, Inc., 1962.
39. Tamura, Mikio, Kurata, Michio, and Kotaka, Tadao. "Normal Stress Effect in Polymer Solutions," I. Measurements in a Parallel Plate Instrument," Bulletin Chemical Society of Japan, XXXII (1959), p. 471.
40. Union Carbide Corporation Information Bulletin No. F-41101A, How to Dissolve Polyox Water Soluble Resins, December, 1964.
41. Union Carbide Corporation Information Bulletin No. F-40340, Polyox Coagulant--A New Organic Flocculating Agent, June, 1958.
42. Union Carbide Corporation Information Bulletin No. F-40246-C, Polyox Water-Soluble Resins, January, 1964.
43. Van Wazer, J. R., Lyons, J. W., Kim, K. Y., and Colwell, R. E. Viscosity and Flow Measurement. New York: Interscience Publishers, 1963.
44. White, J. L., and Metzner, A. B. "Normal Stresses in Fluids: Methods of Measurement, Their Interpretation and Quantitative Results," Progress in International Research on Thermodynamic and Transport Properties. J. F. Masi and D. H. Tsai, editors. New York: Academic Press, 1962.
45. Williams, Michael, and Bird, R. Byron. "Steady Flow of an Oldroyd Viscoelastic Fluid in Tubes, Slits, and Narrow Annuli," AIChE Journal, VIII, No. 3 (1962), pp. 378-82.
46. Williams, Michael C. "Normal Stress and Viscosity Measurements for Polymer Solutions in Steady Cone-and-Plate Shear," AIChE Journal, XI, No. 3 (1965), pp. 467-73.

APPENDIX A

NOMENCLATURE

APPENDIX A

NOMENCLATURE

a	constant in Equation (5-13)
A	cross sectional area
b	constant in Equation (5-10)
B	value defined by Equation (5-16)
c	constant defined by Equation (5-15)
C	power law constant
D	diameter of capillary
D_p	diameter of particle
f	friction factor
G	mass flow rate ρV
$h(r)$	height of rise in capillary of parallel plate instrument
K	permeability
L	length
m	constant in Equation (5-10)
n	power law constant
P_{11}, P_{22}, P_{33}	normal pressures
ΔP	pressure drop
q, Q	volumetric flow rate
r	radius of capillary

R_e	Reynolds number
R_h	hydraulic radius
S	recoverable shear, defined by Equation (3-20)
t_c	relaxation time
V, V_{avg}	velocity, = q/A
$\langle V \rangle$	pore velocity, = V/o

Greek Symbols

μ	Newtonian viscosity
η	non-Newtonian viscosity
γ	shear rate
τ	shear stress
χ	constant in Equation (2-13)
ϕ	porosity
δ	diameter associated with porous media
Ω	rotation speed
ρ	fluid density

APPENDIX B

DERIVATION OF THE MOONEY-RABINOWITSCH EQUATION

DERIVATION OF THE MOONEY-RABINOWITSCH EQUATION

The Mooney-Rabinowitsch Equation describes the steady flow of viscous fluids through a tube of constant cross section. The equation is a common one and is derived in a number of sources. The derivation here follows that of reference 35.

The Mooney-Rabinowitsch Equation is derived from the equation of motion, presented in Equation (B-1).

The r component is given by

$$\rho \frac{dV_r}{d\theta} + V_r \frac{dV_r}{dr} + \frac{V_\phi}{r} \frac{dV_r}{d\phi} - \frac{V_\phi^2}{r} + V_z \frac{dV_r}{dz} \tag{B-1a}$$

$$= - \frac{dP}{dr} - \left[\frac{1}{r} \frac{d}{dr} (r\tau_{rr}) + \frac{1}{r} \frac{d\tau_{r\phi}}{d\phi} - \frac{\tau_{\phi\phi}}{r} + \frac{d\tau_{rz}}{dz} \right] + \rho g_r$$

the ϕ component by

$$\rho \left(\frac{dV_\phi}{d\theta} + V_r \frac{dV_\phi}{dr} + \frac{V_\phi}{r} \frac{dV_\phi}{d\phi} + \frac{V_r V_\phi}{r} + \frac{V_z dV_\phi}{dz} \right) \tag{B-1b}$$

$$= - \frac{1}{r} \frac{dP}{d\phi} - \left[\frac{1}{r^2} \frac{d}{dr} r^2 \tau_{r\phi} + \frac{1}{r} \frac{d\tau_{\phi\phi}}{d\phi} + \frac{d\tau_{\phi z}}{dz} \right] + \rho g_\phi$$

and the z component by

$$\rho \left(\frac{dV_z}{d\theta} + V_r \frac{dV_z}{dr} + \frac{V_\phi}{r} \frac{dV_z}{d\phi} + V_z \frac{dV_z}{dz} \right) \quad (\text{B-1c})$$

$$= - \frac{dP}{dz} - \left[\frac{1}{r} \frac{d}{dr} (r\tau_{rz}) + \frac{1}{r} \frac{d\tau_{\phi z}}{d\phi} + \frac{d\tau_{zz}}{dz} \right] + \rho g_z .$$

These equations are the "Navier-Stokes" equations. In Equations (B-1) ρ is the fluid density, g the acceleration due to gravity, V the fluid velocity, τ the stress tensor, r the radial coordinate, z the axial coordinate, ϕ the angular coordinate, and θ is time. The first three terms in each of these equation represent the rate of increase of momentum per unit volume and are zero for steady state conditions. The term $\rho V_\phi^2 / r$ describes the centrifugal force and the term on the left in these equation, except for the first terms, represent the rate of momentum loss per unit volume by convection. The first terms on the right cover the pressure per unit volume. The terms in brackets stand for the rate-of-momentum gain by viscous transfer per unit volume. In considering viscous flow, only the shear stress τ_{rz} is considered. This component is defined in Equation (B-2)

$$\tau_{rz} = - \left[\frac{dV_z}{dr} + \frac{dV_r}{dz} \right] . \quad (\text{B-2})$$

The following assumptions are made:

1. Flow must be steady.

2. There are no radial and tangential components of velocity.
3. The axial velocity is a function of the distance from the axis alone.
4. There is no slippage at the wall ($V=0$ at $r = R$).
5. The tube is sufficiently long that end effects are negligible.
6. The fluid is incompressible.
7. There are no external forces.
8. Isothermal conditions exist throughout.
9. Viscosity does not change appreciably with the change in pressure down the tube.

From the assumptions the following equation is derived from Equation (B-1c):

$$\frac{1}{r} \left[\frac{d(r\tau_{rz})}{dr} \right] = \left[\rho g_r - \frac{dP}{dz} \right]. \quad (\text{B-3})$$

By integration,

$$\tau_{rz} = \frac{r}{2} \left[\rho g_c - \frac{dP}{dz} \right] + C_1 \quad (\text{B-4})$$

By Equation (B-2) and the assumptions made,

$$\tau_{rz} = - \frac{dV_z}{dr}.$$

When $r = 0$, $dV_z/dr = 0$, and τ_{rz} must be 0. Thus $C_1 = 0$.

When gravity forces are neglected, and dP/dz is constant, Equation (B-4) becomes

$$\tau_{rz} = \frac{\Delta Pr}{2L} \quad . \quad (B-5)$$

The shear rate equation will now be developed. The volumetric flow rate is given by

$$Q = \int_0^R 2\pi r V(r) dr \quad . \quad (B-6)$$

Integration by parts gives

$$Q = \left[\pi r^2 V \right]_0^R - \pi \int_0^R r^2 \frac{dV}{dr} dr \quad . \quad (B-7)$$

Since $V = 0$ at $r = R$, the first term of the right side of Equation (B-7) is zero. Since $r/R = \tau_r/\tau_R$, transformations of the variables in Equation (B-7) gives

$$\frac{4Q}{\pi R^3} = \frac{4}{\tau_R^3} \int_0^R f(\tau) \tau^2 d\tau \quad . \quad (B-8)$$

Differentiation with respect to τ_R leads to

$$\left(- \frac{dV}{dr} \right)_w = f(\tau_R) = \frac{3}{4} \left(\frac{4Q}{\pi R^3} \right) + \frac{1}{4} \tau_R \left[\frac{d}{d \tau_R} \left(\frac{4Q}{\pi R^3} \right) \right] \quad . \quad (B-9)$$

The second term on the right side of (B-9) may be transformed such that a similar expression results.

$$\left(- \frac{dV}{dr} \right)_w = \frac{3}{4} \left(\frac{4Q}{\pi R^3} \right) \left[\frac{d \log(4Q/\pi R^3)}{d \log \left(\frac{\Delta PR}{2L} \right)} \right] \quad . \quad (B-10)$$

If we let $b = \frac{d \log(4Q/\pi R^3)}{d \log \frac{\Delta PR}{2L}}$ the result is

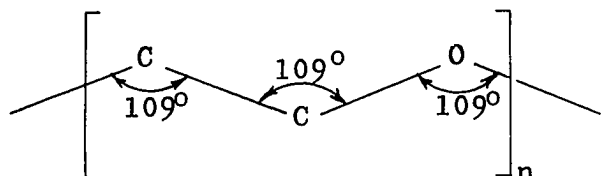
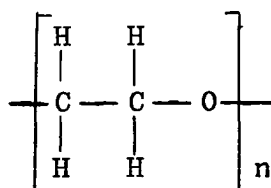
$$\left(- \frac{dV}{dr} \right)_w = \left(\frac{3+b}{4} \right) \left(\frac{4Q}{\pi R^3} \right) \quad . \quad (B-11)$$

APPENDIX C

SIZE CALCULATIONS OF A POLYMER MOLECULE

SIZE CALCULATIONS OF A POLYMER MOLECULE

The configuration of polyethylene oxide is given as



One measure of the size of a random coiling macromolecule in solution is the root mean square, R , defined by Equation (2-2) and shown pictorially in Figure 2-1. This value may be considered to represent some approximation of the diameter of the molecule. The actual size of a macromolecule in solution may be many times greater than calculated here, due to the many entanglements and associations.

Consider as an example a 6 million molecular weight polymer. The molecular weight of the structural unit is 44. For a molecular weight of 6 million, n is 136,300. There are a total of 6 single bonds within the chain portion, 4 carbon and 2 oxygen bonds. Thus, the total number of bonds

is 545,200, and the total number of oxygen bonds is 272,600. The single carbon bond length is 0.77\AA ,⁸ and the single oxygen bond length is 0.66\AA . Using Equation (2-2)

$$\begin{aligned} R^2(\text{angstroms}) &= (545,200)(.77)^2 + (272,600)(0.66)^2 \\ &= 441,600 \end{aligned}$$

$$R = 664 \text{ angstroms} = 664 \times 10^{-8} \text{ cm} = 0.0664 \text{ microns.}$$

The extended length of the structural unit is

$$\begin{aligned} L &= 4(\sin 54.5^\circ)(.77) + 2 \sin (54.5^\circ)(.66) \\ &= 4(.814)(.77) + 2(.814)(.66) \\ &= 3.59 \text{ \AA} \end{aligned}$$

The extended length of a 6 million molecular weight polymer is then

$$\begin{aligned} L &= (136,300)(3.59) \\ &= 489,000 \text{ angstroms} \\ &= 48.9 \text{ microns.} \end{aligned}$$

APPENDIX D
VISCOMETRIC DATA

TABLE D-1

VISCOMETRIC DATA - 0.1% POLYOX WSR-301

Height cm	Time sec	Fluid Recovery cc	Shear Stress dynes/cm ²	Apparent Shear Rate sec ⁻¹	Shear Rate sec ⁻¹
149.8	1920	9.55	16.90	513.8	525.1
144.6	1800	8.60	16.32	493.5	504.3
139.5	1800	8.25	15.74	473.4	483.8
134.4	1800	7.87	15.17	451.6	463.6
129.2	1800	7.53	14.58	432.1	442.6
124.5	1800	7.20	14.04	413.2	422.3
118.5	1800	6.80	13.37	390.2	398.8
113.3	1800	6.40	12.78	367.3	375.4
107.6	1800	6.03	12.14	346.0	353.6
102.0	1800	5.65	11.52	324.2	331.3
97.7	1800	5.40	11.02	309.9	316.7
92.2	2700	7.60	10.41	290.8	297.2
87.0	2700	7.10	9.82	271.7	277.7
81.6	2700	6.7	9.20	256.3	261.9
75.2	2700	6.08	8.49	232.6	237.7
69.4	3600	7.40	7.83	212.4	217.1
63.7	4200	7.80	7.18	191.8	196.0
58.7	3720	6.35	6.62	176.6	180.5
51.5	5400	8.13	5.81	156.0	159.4
45.4	5220	6.75	5.12	133.6	136.5
40.0	5400	6.00	4.52	114.8	117.3
33.7	5800	5.50	3.80	96.6	98.7
28.2	9360	7.20	3.19	79.4	81.1
24.8	11640	7.88	2.80	69.9	71.4
19.3	7800	3.98	2.18	52.7	53.9
14.5	23880	8.90	1.64	38.5	39.3
10.7	11100	3.65	1.20	34.0	34.7
7.1	42300	7.40	0.80	18.1	18.5

Radius of Tube 0.0231 cm

Length of Tube 100.0 cm

TABLE D-2

VISCOMETRIC DATA - 0.585% POLYOX WSR-35

Height cm	Time sec	Fluid Recovery cc	Shear Stress dynes/cm ²	Apparent Shear Rate sec ⁻¹	Shear Rate sec ⁻¹
151.3	2200	9.0	17.07	418.7	418.7
145.6	2460	9.6	16.42	403.0	403.0
139.6	2400	8.98	15.75	386.5	386.5
129.0	2400	8.25	14.55	355.0	355.0
119.4	3000	9.39	13.48	323.3	323.3
111.7	3000	8.92	12.60	307.1	307.1
104.5	3000	8.33	11.79	286.8	286.8
97.5	3840	9.90	11.01	266.3	266.3
89.3	4200	9.68	10.07	238.1	238.1
82.3	4380	9.50	9.29	224.0	224.0
76.0	4200	8.35	8.57	205.3	205.3
69.7	4560	8.32	7.87	188.5	188.5
63.2	4620	7.50	7.13	167.6	167.6
56.2	2700	3.73	6.34	142.6	142.6
48.3	5400	6.7	5.45	128.2	128.2
40.4	7740	8.05	4.56	107.4	107.4
32.8	3180	2.75	3.70	89.3	89.3
21.2	9000	5.00	2.39	57.3	57.3
14.5	15000	5.7	1.64	39.2	39.2

Radius of Tube 0.0231 cm

Length of Tube 100.0 cm

TABLE D-3

VISCOMETRIC DATA - 0.025% POLYOX COAGULENT

Height cm	Time sec	Fluid Recovery cc	Shear Stress dynes/cm ²	Apparent Shear Rate sec ⁻¹	Shear Rate sec ⁻¹
148.6	780	9.07	16.77	1201.3	1201.3
141.5	780	8.65	15.96	1145.5	1145.5
134.1	900	9.40	15.13	1078.3	1078.3
125.4	900	8.80	14.15	1010.2	1010.2
118.4	1020	9.37	13.36	949.2	949.2
111.2	1020	8.80	12.54	891.4	891.4
103.4	1080	8.63	11.66	825.3	825.3
93.1	1260	9.0	10.51	737.5	737.5
83.9	1260	8.13	9.47	666.2	666.2
75.5	1500	8.75	8.51	602.2	602.2
65.3	1920	9.65	7.37	519.5	519.5
58.4	2220	9.95	6.59	462.7	462.7
52.6	2100	8.45	5.94	415.2	415.2
45.0	2220	7.67	5.08	356.3	356.3
36.9	2220	6.30	4.17	293.3	293.3
30.7	4080	9.28	3.46	234.5	234.5
25.1	3900	7.20	2.83	191.1	191.1
18.7	3630	4.6	2.11	131.2	131.2
15.8	7200	7.6	1.78	109.5	109.5
12.3	8280	6.75	1.39	84.7	84.7
9.8	8280	5.35	1.11	67.1	67.1
5.7	11400	4.40	0.65	40.3	40.3

Radius of Tube 0.0231 cm
Length of Tube 100.0 cm

TABLE D-4

VISCOMETRIC DATA - 0.296% POLYOX COAGULENT

Height cm	Time sec	Fluid Recovery cc	Shear Stress dynes/cm ²	Apparent Shear Rate sec ⁻¹	Shear Rate sec ⁻¹
100.2	360	9.82	39.98	281.2	313.8
94.8	360	9.00	37.83	257.7	287.6
88.9	420	9.73	35.47	238.8	266.5
83.4	480	9.98	33.28	214.3	239.1
78.3	480	9.08	31.25	195.0	217.6
72.8	540	9.20	29.05	175.6	196.0
67.3	600	9.10	26.86	156.4	174.5
62.6	600	8.10	24.98	139.2	155.3
57.1	780	9.19	22.79	121.4	135.5
51.4	900	9.10	20.51	104.2	116.3
45.4	960	7.92	18.12	85.0	94.9
40.7	1200	8.85	16.24	76.0	84.8
35.4	1380	8.33	14.13	62.3	69.5
30.6	1800	8.88	12.21	50.8	56.7
25.1	2520	9.22	10.01	37.7	42.1
20.1	3300	8.78	8.02	27.4	30.6
15.7	4320	8.07	6.27	19.3	21.5
11.0	9100	9.40	4.39	10.6	11.8

Radius of Tube 0.0498 cm

Length of Tube 60.96 cm

TABLE D-5

VISCOMETRIC DATA - 0.075% POLYOX COAGULENT

Height cm	Time sec	Fluid Recovery cc	Shear Stress dynes/cm ²	Apparent Shear Rate sec ⁻¹	Shear Rate sec ⁻¹
112.1	2400	9.1	12.65	391.7	401.5
105.1	2820	9.98	11.86	365.5	374.6
100.2	2640	8.80	11.31	344.3	352.9
93.1	2580	7.80	10.51	312.2	320.0
85.8	3120	8.72	9.68	288.7	294.9
79.0	3420	8.78	8.92	265.1	271.7
74.0	4200	9.80	8.35	241.0	247.0
67.2	3600	7.57	7.59	217.2	222.6
60.4	4560	8.55	6.81	193.7	198.5
53.6	3900	6.4	6.05	169.5	173.7
46.8	4620	6.55	5.28	146.5	150.2
40.4	4800	5.80	4.56	124.8	127.9
35.2	6600	6.85	3.97	107.2	109.9
30.0	8700	7.50	3.38	89.0	91.2
25.1	12660	9.0	2.83	73.4	75.2
21.5	8400	5.05	2.42	62.1	63.7
18.0	14580	7.33	2.03	52.0	53.3
13.9	14400	5.4	1.57	38.7	39.7
9.7	21600	5.55	1.10	26.5	27.2

Radius of Tube 0.0231 cm

Length of Tube 100.0 cm

TABLE D-6

VISCOMETRIC DATA - 0.199% POLYOX WSR-301

Height cm	Time sec	Fluid Recovery cc	Shear Stress ₂ dynes/cm ²	Apparent Shear Rate sec ⁻¹	Shear Rate sec ⁻¹
159.7	2040	9.58	37.88	546.6	590.3
153.5	2100	9.30	36.42	515.4	556.6
148.0	2280	9.58	35.11	489.1	528.2
142.9	2400	9.18	33.89	445.2	480.8
136.9	2760	10.00	32.49	421.7	455.4
130.3	2400	8.10	30.91	392.8	424.2
124.7	2700	8.60	29.57	370.7	400.3
118.7	3000	8.94	28.16	346.9	374.6
112.9	3420	9.50	26.78	323.4	349.3
108.2	3300	8.70	25.66	306.8	331.3
102.2	3900	9.57	24.23	285.6	308.4
97.7	2760	6.38	23.16	269.0	290.5
92.5	3600	7.8	21.95	252.2	272.4
86.3	3900	7.75	20.47	231.3	249.8
80.1	4800	8.6	19.01	208.6	225.3
75.5	4500	7.2	17.92	186.2	201.1
68.4	7020	9.9	16.22	164.1	177.2
62.0	7200	8.85	14.71	143.0	154.4
56.0	5220	5.60	13.28	124.9	134.9
49.0	7200	6.45	11.63	104.3	112.6
43.0	5400	4.03	10.20	86.8	93.7
35.3	8520	4.98	8.38	68.0	73.4
28.7	7200	3.2	6.80	51.7	55.8
23.0	16800	5.62	5.46	38.9	42.0
16.3	21600	4.72	3.86	25.5	27.5
9.6	29400	3.38	2.28	13.4	14.5

Radius of Tube 0.0222 cm

Length of Tube 45.7 cm

TABLE D-7

VISCOMETRIC DATA - 0.149% POLYOX COAGULENT

Height cm	Time sec	Fluid Recovery cc	Shear Stress dynes/cm ²	Apparent Shear Rate sec ⁻¹	Shear Rate sec ⁻¹
112.7	1860	9.6	26.74	600.7	628.3
106.6	1800	8.55	25.29	552.9	578.3
100.1	2290	10.0	23.76	508.3	531.7
93.1	960	3.87	22.15	469.2	490.8
86.0	1980	7.18	20.40	422.1	441.5
79.4	2460	8.02	18.85	379.5	397.0
74.5	3060	9.2	17.68	350.0	366.1
67.3	3120	8.2	15.98	305.9	320.0
61.2	3720	8.75	14.52	273.8	286.4
54.1	4260	8.55	12.85	233.6	244.3
47.4	4560	7.8	11.25	199.2	208.0
41.6	5880	8.68	9.86	171.8	179.7
35.3	7980	9.6	8.38	140.0	146.4
28.5	7620	7.0	6.75	107.0	111.9
22.5	8760	6.14	5.34	81.6	85.3
17.0	10440	5.22	4.03	58.2	60.9
11.3	9000	2.8	2.67	36.2	37.9
7.0	10020	1.8	1.65	20.9	21.9

Radius of Tube 0.0222 cm

Length of Tube 45.7 cm

TABLE D-8

VISCOMETRIC DATA - 0.05% POLYOX WSR-301

Height cm	Time sec	Fluid Recovery cc	Shear Stress dynes/cm ²	Apparent Shear Rate sec ⁻¹	Shear Rate sec ⁻¹
126.5	1355	10.0	14.27	762.3	762.3
121.2	1435	10.2	13.67	734.2	734.2
116.3	1440	9.8	13.12	703.0	703.0
110.7	1440	9.32	12.49	668.5	668.5
103.0	1620	9.65	11.62	615.3	615.3
95.5	1800	9.93	10.78	569.9	569.9
90.1	1800	9.40	10.16	539.4	539.4
85.1	1800	8.80	9.60	505.0	505.0
80.5	1800	8.30	9.08	476.3	476.3
75.5	1800	7.75	8.52	444.8	444.8
68.2	1800	6.78	7.69	389.1	389.1
62.1	2220	7.80	7.01	363.0	363.0
55.6	2820	8.80	6.27	322.3	322.3
46.4	4000	9.90	5.23	255.6	255.6
41.2	3600	7.93	4.64	227.5	227.5
36.9	3600	7.03	4.16	201.7	201.7
32.1	3600	6.15	3.63	176.4	176.4
27.5	3600	5.2	3.11	149.1	149.1
23.7	7200	9.0	2.68	129.1	129.1
19.8	7200	7.53	2.23	108.0	108.0
14.0	7560	5.50	1.58	75.2	75.2
8.5	18360	8.07	0.96	44.0	45.4
5.4	36000	9.0	0.61	25.8	25.8
1.7	43200	4.4	0.20	10.2	10.5

Radius of Tube 0.0231 cm

Length of Tube 100 cm

TABLE D-9

VISCOMETRIC DATA - 0.486% POLYOX COAGULENT

Height cm	Time sec	Fluid Recovery cc	Shear Stress dynes/cm ²	Apparent Shear Rate sec ⁻¹	Shear Rate sec ⁻¹
128.6	630	9.8	59.23	160.3	187.6
122.3	690	9.9	56.37	147.9	173.0
114.9	720	9.0	52.91	128.9	150.8
109.4	780	8.95	50.41	118.2	138.3
103.0	900	9.2	47.44	105.3	123.2
96.8	960	8.85	44.61	95.0	111.1
88.9	1260	10.0	40.93	81.9	95.8
83.6	1380	9.95	38.53	74.3	86.9
76.3	1620	9.95	35.13	63.3	74.1
71.0	1800	9.60	32.73	54.9	64.2
65.3	1800	8.4	30.09	48.1	56.3
58.8	2100	8.3	27.07	40.7	47.6
46.4	3240	8.8	21.36	28.0	32.8
39.5	3600	7.6	18.20	21.8	25.5
32.0	6000	8.95	14.76	15.4	18.0
24.8	7260	6.9	11.41	9.8	11.5
17.6	8100	4.4	8.11	5.6	6.55
12.3	8520	2.6	5.66	3.1	3.63

Radius of Tube 0.0498 cm

Length of Tube 51.7 cm

TABLE D-10

VISCOMETRIC DATA - 1.0% POLYOX WSR-301

Height cm	Time sec	Fluid Recovery cc	Shear Stress dynes/cm ²	Apparent Shear Rate sec ⁻¹	Shear Rate sec ⁻¹
196.1	1860	9.58	172.2	53.1	67.9
186.0	1980	8.8	163.3	45.8	58.7
178.6	1920	7.78	156.9	41.8	53.4
168.0	2340	7.70	147.5	33.9	43.3
157.8	2760	7.9	138.6	29.5	37.7
151.5	3300	8.75	133.0	27.3	34.9
144.8	3600	8.75	127.2	25.1	32.1
137.9	4560	9.85	121.1	22.3	28.5
131.5	4200	8.13	115.5	20.0	25.6
123.4	4800	8.05	108.4	17.3	22.1
114.1	4620	6.40	100.2	14.3	18.3
107.6	6660	8.35	94.5	12.9	16.5
100.3	5100	5.53	88.1	11.2	14.3
93.5	6900	6.55	82.1	9.8	12.5
85.7	4200	3.33	75.2	8.2	10.5
77.8	7833	5.2	68.3	6.8	8.7
70.8	6191	3.4	62.2	5.7	7.3
63.3	11533	4.95	55.5	4.42	5.65
56.4	9105	3.05	49.5	3.45	4.41
48.9	13938	3.4	43.0	2.51	3.21
41.4	22832	3.95	36.3	1.78	2.28
34.8	48600	5.55	30.6	1.18	1.51

Radius of Tube 0.0498 cm

Length of Tube 27.7 cm

TABLE D-11

VISCOMETRIC DATA - 0.394% POLYOX WSR-205

Height cm	Time sec	Fluid Recovery cc	Shear Stress dynes/cm ²	Apparent Shear Rate sec ⁻¹	Shear Rate sec ⁻¹
124.1	1380	9.7	29.44	818.2	818.2
115.6	1440	9.3	27.42	751.7	751.7
104.8	1500	8.77	24.87	680.6	680.6
95.0	1560	8.20	22.54	611.8	611.8
84.1	1920	8.88	19.97	538.3	538.3
73.8	2220	8.93	17.51	468.2	468.2
64.0	2520	8.72	15.18	402.7	402.7
55.8	3060	9.00	13.24	342.4	342.4
45.2	3360	7.98	10.74	276.4	276.4
36.4	4800	9.00	8.65	218.2	218.2
29.0	5400	7.95	6.87	171.3	171.3
23.0	7200	8.4	5.46	135.8	135.8
15.9	11280	8.95	3.76	92.3	92.3
9.9	8580	4.15	2.11	56.3	56.3
5.0	33900	8.58	1.18	29.4	29.4

Radius of Tube 0.0222 cm

Length of Tube 45.7 cm

APPENDIX E

PARALLEL PLATE DATA AND CALCULATIONS

TABLE E-1

BASIC PARALLEL PLATE DATA

Tube No.	Radius from Center in	Radius from Center cm	Relative Height cm	Relative Height cm	Relative Height cm	Relative Height cm	Relative Height cm
1	1.576	4.003	1.3310	1.2610	1.2590	2.03	1.6010
2	1.182	3.002	1.5665	1.6000	1.4835	3.17	2.5080
3	0.788	2.002	1.6310	1.8800	1.6780	4.30	3.3288
4	0.394	1.001	1.7240	2.1110	1.8470	5.25	4.0440
5	0.0	0.0	1.7658	2.2540	1.9557	6.09	4.7170
6	0.394	1.001	1.7310	2.1280	1.8680	5.22	4.0340
7	0.788	2.002	1.6310	1.8630	1.6990	4.30	3.3288
8	1.182	3.002	1.5510	1.6750	1.5590	3.19	2.5165
9	1.576	4.003	1.3350	1.3870	1.3470	2.08	1.6320
Polymer and Concentration			Polyox Coagulant 0.296%	Polyox Coag. 0.486%	Polyox Coag. 0.486%	Polyox WSR-301 1.0%	Polyox WSR-301 1.0%
Spacing between Plates, in			0.0378	0.046	0.046	0.0708	0.0708
Rotational Speed rev/sec			30/22	30/33	30/45	30/30	30/39

TABLE E-2

PARALLEL PLATE CALCULATIONS - 1% POLYOX WSR-301

Radius cm	Shear Rate sec ⁻¹ $\dot{\gamma} = \omega r / l$	$h(0) - h(r)$ cm	$\frac{d(h(0) - h(r))}{d \log_{10} r}$	$dP_{22}/d \ln r$ dynes/cm ²
0.1	3.49	0.075	0.155	65.7
0.2	6.99	0.15	0.440	186.6
0.3	10.48	0.23	0.57	241.8
0.4	13.98	0.31	0.69	292.7
0.5	17.47	0.38	1.04	441.2
0.6	20.97	0.48	1.28	543.0
0.7	24.46	0.57	1.54	653.3
0.8	27.9	0.67	1.76	746.6
0.9	31.4	0.77	2.07	878.1
1.0	34.9	0.87	2.37	1005.0
1.2	41.9	1.05	2.63	1116.0
1.4	48.9	1.24	3.10	1315.0
1.6	55.9	1.41	3.66	1553.0
1.8	62.9	1.60	4.18	1773.0
2.0	69.9	1.82	4.78	2028.0
2.4	83.9	2.25	6.02	2554.0
3.0	104.8	2.92	7.74	3283.0
3.4	118.8	3.37	8.76	3716.0
4.0	139.8	4.05	10.26	4352.0
0.1	2.69	0.075	0.305	129.4
0.2	5.37	0.15	0.260	110.3
0.3	8.06	0.22	0.470	199.4
0.4	10.7	0.28	0.60	254.5
0.5	13.4	0.35	0.71	301.2
0.6	16.1	0.42	0.91	386.0
0.7	18.8	0.49	1.20	509.0
0.8	21.5	0.56	1.32	560.0
0.9	24.2	0.63	1.55	657.0
1.0	26.9	0.70	1.78	755.0
1.4	37.6	0.97	2.29	971.0
1.8	48.4	1.25	2.87	1217.0
2.2	59.1	1.53	3.65	1548.0
2.8	75.2	2.04	5.36	2274.0
3.2	86.0	2.40	6.32	2681.0
3.6	96.7	2.75	7.59	3220.0

Note: For first group of calculations, $\omega = 30$ rev/30 sec,
and the second group, $\omega = 30$ rev/39 sec.

TABLE E-3

PARALLEL PLATE CALCULATIONS - 0.486%
POLYOX COAGULENT

Radius cm	Shear Rate sec^{-1} $\gamma-\dot{w}_r/1$	$h(0)-h(r)$ cm	$\frac{d(h(0)-h(r))}{d \log_{10} r}$	$dP_{22}/d \ln r$ dynes/cm ²
0.1	4.91	0.008	0.027	11.4
0.2	9.77	0.017	0.058	24.6
0.3	14.68	0.028	0.092	39.0
0.4	19.53	0.040	0.127	53.9
0.5	24.45	0.053	0.166	70.4
0.6	29.36	0.070	0.212	89.9
0.7	34.21	0.085	0.258	109.4
0.8	39.13	0.104	0.342	145.1
0.9	43.98	0.122	0.396	168.0
1.0	48.89	0.142	0.468	198.5
1.2	58.66	0.184	0.563	238.8
1.4	68.49	0.228	0.720	305.4
1.6	78.25	0.278	0.860	364.8
1.8	88.02	0.328	1.015	430.6
2.0	97.79	0.375	1.108	470.0
0.1	3.60	0.005	0.030	12.7
0.2	7.16	0.014	0.042	17.8
0.3	10.8	0.023	0.042	17.8
0.4	14.3	0.032	0.097	41.1
0.5	17.9	0.040	0.113	47.9
0.6	21.5	0.050	0.136	57.7
0.7	25.1	0.060	0.195	82.7
0.8	28.7	0.071	0.226	95.9
0.9	32.2	0.082	0.267	113.0
1.0	35.8	0.095	0.305	129.0
1.2	43.0	0.125	0.402	170.0
1.4	50.2	0.156	0.468	198.0
1.6	57.4	0.190	0.620	263.0
1.8	64.5	0.226	0.738	313.0
2.0	71.7	0.262	0.825	350.0

Note: For first group of calculations, $\omega = 30 \text{ rev}/33 \text{ sec}$,
and for the second group, $\omega = 30 \text{ rev}/45 \text{ sec}$.

TABLE E-4

PARALLEL PLATE CALCULATIONS - 0.296%
POLYOX COAGULENT

Radius cm	Shear Rate sec ⁻¹ $\gamma = \omega r / l$	$h(0) - h(r)$ cm	$\frac{d(h(0) - h(r))}{d \log_{10} r}$	$dP_{22} / d \ln r$ dynes/cm ²
0.2	17.76	0.008	0.016	6.78
0.3	26.64	0.011	0.016	6.78
0.4	35.52	0.014	0.037	15.69
0.5	44.40	0.018	0.046	19.51
0.6	53.29	0.022	0.066	28.00
0.70	62.17	0.027	0.090	38.18
0.8	71.04	0.032	0.105	44.50
0.9	79.92	0.038	0.130	55.10
1.0	88.80	0.044	0.147	62.4
1.2	106.57	0.058	0.185	78.5
1.4	124.30	0.072	0.226	95.9
1.6	142.09	0.088	0.282	119.6
1.8	159.85	0.103	0.338	143.4
2.0	177.61	0.118	0.377	160.0
2.5	222.01	0.158	0.512	217.2
3.0	266.42	0.207	0.797	338.1

APPENDIX F

POROUS MEDIA DATA AND CALCULATIONS

TABLE F-1

POROUS MEDIA DATA AND CALCULATIONS - RUN 1

Pressure Drop cm Hg	Time sec	Fluid Recovery cc	Velocity ft/day	Insitu Viscosity cp	Steady State Viscosity cp	Shear Rate sec ⁻¹	Predicted Viscosity cp
75.66	274	10.0	18.16	208.97	18.12	10.7	197.5
66.86	304	10.0	16.37	204.89	18.59	9.67	183.5
52.89	366	10.0	13.59	195.13	19.48	8.04	160.8
40.06	448	10.0	11.10	180.91	20.49	6.56	139.3
31.51	530	10.0	9.39	168.34	21.37	5.55	123.7
22.06	668	10.0	7.45	148.54	22.64	4.40	104.9
14.11	880	10.0	5.65	125.16	24.25	3.34	86.3
10.51	1052	10.0	4.73	111.45	25.36	2.80	76.0
7.23	1283	10.0	3.87	93.50	26.65	2.29	66.0
4.36	1020	6.12	2.98	73.25	28.45	1.76	54.8
2.29	900	3.80	2.10	54.67	31.07	1.24	42.7
0.81	1200	3.00	1.24	32.66	35.42	0.74	29.4

TABLE F-2

POROUS MEDIA DATA AND CALCULATIONS - RUN 2

Pressure Drop cm Hg	Time sec	Fluid Recovery cc	Velocity ft/day	Insitu Viscosity cp	Steady State Viscosity cp	Shear Rate sec ⁻¹	Predicted Viscosity cp
53.45	272	10.0	19.19	164.56	19.12	8.65	215.0
41.83	320	10.0	16.31	151.51	19.91	7.35	191.6
31.40	389	10.0	13.42	138.26	20.91	6.05	166.8
25.30	444	10.0	11.75	127.15	21.61	5.30	151.8
18.70	530	10.0	9.85	112.18	22.59	4.44	133.9
13.15	656	10.0	7.95	97.64	23.83	3.59	115.1
7.22	894	10.0	5.83	73.06	25.75	2.63	92.4
3.55	960	7.6	4.13	47.89	28.07	1.86	72.3
2.60	1020	6.3	3.22	47.64	29.87	1.45	60.6
1.43	1020	4.3	2.20	38.39	32.86	0.99	46.2
0.52	900	2.2	1.27	24.07	37.66	0.58	31.4

TABLE F-3

POROUS MEDIA DATA AND CALCULATIONS - RUN 3

Pressure Drop cm Hg	Time sec	Fluid Recovery cc	Velocity ft/day	Insitu Viscosity cp	Steady State Viscosity cp	Shear Rate sec ⁻¹	Predicted Viscosity cp
40.58	183	10.0	26.97	74.85	4.41	15.74	103.5
33.0	209	10.0	23.61	69.52	4.45	13.77	89.5
26.15	247	10.0	19.98	65.11	4.51	11.65	74.5
18.84	300	10.0	16.45	56.97	4.58	9.60	60.2
12.18	386	10.0	12.78	47.39	4.68	7.46	45.6
9.58	442	10.0	11.16	42.68	4.73	6.52	39.3
6.78	517	10.0	9.36	36.01	4.80	5.46	32.4
4.20	659	10.0	7.49	27.90	4.88	4.37	25.4
2.13	880	10.0	5.60	18.89	5.00	3.27	18.5
0.75	1271	10.0	3.88	9.60	5.15	2.26	12.3

TABLE F-4

POROUS MEDIA DATA AND CALCULATIONS - RUN 4

Pressure Drop cm Hg	Time sec	Fluid Recovery cc	Velocity ft/day	Insitu Viscosity cp	Steady State Viscosity cp	Shear Rate sec ⁻¹	Predicted Viscosity cp
88.92	290	10.0	16.05	39.40	2.06	24.17	46.1
70.62	337	10.0	13.81	36.36	2.07	20.79	38.3
48.52	412	10.0	11.30	30.54	2.07	17.01	29.9
28.77	530	10.0	8.78	23.30	2.08	13.22	21.9
16.82	665	10.0	7.00	17.09	2.09	10.54	16.5
8.35	881	10.0	5.28	11.24	2.11	7.95	11.7
2.95	1305	10.0	3.56	5.88	2.12	5.37	7.2
0.75	900	3.7	1.91	2.78	2.15	2.88	3.3

TABLE F-5

POROUS MEDIA DATA AND CALCULATIONS - RUN 5

Pressure Drop cm Hg	Time sec	Fluid Recovery cc	Velocity ft/day	Insitu Viscosity cp	Steady State Viscosity cp	Shear Rate sec ⁻¹
2.25	255	10.0	19.47	5.78	4.19	11.45
1.67	296	10.0	16.76	4.98	4.19	9.86
1.37	330	10.0	15.04	4.55	4.19	8.85
1.12	382	10.0	12.99	4.31	4.19	7.64
0.96	440	10.0	11.28	4.25	4.19	6.64
0.76	522	10.0	9.50	3.99	4.19	5.59
0.58	656	10.0	7.56	3.83	4.19	4.45
0.42	862	10.0	5.75	3.64	4.19	3.38
0.28	1245	10.0	3.98	3.51	4.19	2.34

TABLE F-6

POROUS MEDIA DATA AND CALCULATIONS - RUN 6

Pressure Drop cm Hg	Time sec	Fluid Recovery cc	Velocity ft/day	Insitu Viscosity cp	Steady State Viscosity cp	Shear Rate sec ⁻¹
33.10	264	10.0	18.01	13.35	4.19	28.03
27.0	297	10.0	16.00	12.25	4.19	24.91
22.3	333	10.0	14.27	11.34	4.19	22.22
17.55	381	10.0	12.47	10.21	4.19	19.42
13.45	440	10.0	10.80	9.04	4.19	16.82
9.62	552	10.0	9.10	7.67	4.19	14.18
6.30	650	10.0	7.31	6.25	4.19	11.38
3.90	857	10.0	5.54	5.10	4.19	8.63
2.28	1244	10.0	3.82	4.33	4.19	5.94
1.05	1200	5.15	2.04	3.73	4.19	3.17

TABLE F-7

POROUS MEDIA DATA AND CALCULATIONS - RUN 7

Pressure Drop cm Hg	Time sec	Fluid Recovery cc	Velocity ft/day	Insitu Viscosity cp	Steady State Viscosity cp	Shear Rate sec ⁻¹	Predicted Viscosity cp
7.23	177.0	10.0	27.58	12.90	1.59	15.82	36.0
5.53	205.0	10.0	23.81	11.42	1.59	13.66	31.1
4.25	242.0	10.0	20.17	10.36	1.59	11.57	26.3
2.87	296.0	10.0	16.49	8.56	1.59	9.46	21.5
2.31	330.0	10.0	14.79	7.68	1.59	8.48	19.3
1.73	379.0	10.0	12.88	6.60	1.59	7.39	16.8
1.27	439.0	10.0	11.12	5.62	1.59	6.38	14.5
0.85	515.0	10.0	9.48	4.41	1.59	5.44	12.4
0.42	653.0	10.0	7.47	2.76	1.59	4.29	9.8
0.21	862.0	10.0	5.66	1.82	1.59	3.25	7.4

TABLE F-8

POROUS MEDIA DATA AND CALCULATIONS - RUN 8

Pressure Drop cm Hg	Time sec	Fluid Recovery cc	Velocity ft/day	Insitu Viscosity cp	Steady State Viscosity cp	Shear Rate sec ⁻¹	Predicted Viscosity cp
53.89	252	10.0	18.76	20.75	1.59	28.96	35.8
39.51	298	10.0	15.87	17.99	1.59	24.50	30.2
31.72	334	10.0	14.16	16.18	1.59	21.85	26.9
25.02	378	10.0	12.51	14.45	1.59	19.31	23.8
19.47	439	10.0	10.77	13.06	1.59	16.63	20.5
14.17	517	10.0	9.14	11.19	1.59	14.12	17.4
8.97	641	10.0	7.39	8.78	1.59	11.39	14.0
4.74	861	10.0	5.49	6.23	1.59	8.48	10.4
2.34	1240	10.0	3.81	4.43	1.59	5.87	7.3
0.90	900	4.18	2.19	2.96	1.59	3.39	4.2

TABLE F-9

POROUS MEDIA DATA AND CALCULATIONS - RUN 9

Pressure Drop cm Hg	Time sec	Fluid Recovery cc	Velocity ft/day	Insitu Viscosity cp	Steady State Viscosity cp	Shear Rate sec ⁻¹	Predicted Viscosity cp
43.0	263	10.0	17.19	27.09	1.59	19.18	30.9
35.28	296	10.0	15.81	25.02	1.59	17.04	27.5
29.0	331	10.0	14.14	22.99	1.59	15.24	24.6
22.93	375	10.0	12.48	20.60	1.59	13.45	21.7
17.82	431	10.0	10.86	18.40	1.59	11.70	18.9
13.00	513	10.0	9.12	15.97	1.59	9.83	15.9
8.0	651	10.0	7.19	12.47	1.59	7.75	12.5
4.53	853	10.0	5.48	9.25	1.59	5.91	9.55
2.08	1215	10.0	3.85	6.05	1.59	4.15	6.7
0.70	1560	10.0	3.00	2.61	1.59	3.23	5.2

TABLE F-10

POROUS MEDIA DATA AND CALCULATIONS - RUN 10

Pressure Drop cm Hg	Time sec	Fluid Recovery cc	Velocity ft/day	Insitu Viscosity cp	Steady State Viscosity cp	Shear Rate sec ⁻¹	Predicted Viscosity cp
150.2	263	10.0	19.24	398.0	36.25	11.67	307.8
122.7	315	10.0	16.06	389.61	38.39	9.74	288.2
96.38	379	10.0	13.35	368.22	40.72	8.10	269.4
72.20	478	10.0	10.58	347.89	43.84	6.42	247.6
49.20	645	10.0	7.84	319.82	48.22	4.76	220.1
33.0	866	10.0	5.84	288.08	52.96	3.54	199.4
19.85	1232	10.0	4.10	205.8	59.24	2.49	175.4
7.55	1500	6.55	2.20	174.29	72.15	1.34	140.0
3.48	900	2.4	1.34	131.55	84.80	0.82	117.0

TABLE F-11

POROUS MEDIA DATA AND CALCULATIONS - RUN 11

Pressure Drop cm Hg	Time sec	Fluid Recovery cc	Velocity ft/day	Insitu Viscosity cp	Steady State Viscosity cp	Shear Rate sec ⁻¹	Predicted Viscosity cp
28.21	265	10.0	18.32	84.61	4.50	7.38	57.3
23.91	288	10.0	16.86	77.91	4.53	6.79	53.4
20.43	320	10.0	15.17	74.00	4.57	6.11	48.9
16.41	370	10.0	13.12	68.72	4.63	5.28	43.3
13.21	424	10.0	11.45	63.40	4.68	4.61	38.7
9.79	502	10.0	9.67	55.62	4.74	3.89	33.6
6.19	633	10.0	7.67	44.35	4.83	3.09	27.6
3.41	844	10.0	5.75	32.57	4.95	2.32	21.7
1.41	1208	10.0	4.02	19.28	5.09	1.62	16.1

TABLE F-12

POROUS MEDIA DATA AND CALCULATIONS - RUN 12

Pressure Drop cm Hg	Time sec	Fluid Recovery cc	Velocity ft/day	Insitu Viscosity cp	Steady State Viscosity cp	Shear Rate sec ⁻¹	Predicted Viscosity cp
23.40	260	10.0	18.98	61.32	4.36	11.08	58.5
19.80	290	10.0	17.02	58.02	4.40	9.93	53.4
16.60	325	10.0	15.18	54.38	4.44	8.86	48.5
13.60	372	10.0	13.26	50.99	4.49	7.74	43.3
10.87	425	10.0	11.61	46.56	4.53	6.78	38.7
7.90	502	10.0	9.83	39.97	4.60	5.74	33.7
5.30	627	10.0	7.87	33.49	4.68	4.59	27.9
3.12	841	10.0	5.86	26.45	4.79	3.42	21.9

TABLE F-13

POROUS MEDIA DATA AND CALCULATIONS - RUN 13

Pressure Drop cm Hg	Time sec	Fluid Recovery cc	Velocity ft/day	Insitu Viscosity cp	Steady State Viscosity cp	Shear Rate sec ⁻¹	Predicted Viscosity cp
171.90	258	10.0	17.91	106.26	4.17	18.90	69.2
138.50	312	10.0	14.81	103.53	4.24	15.63	59.0
108.30	370	10.0	12.49	96.00	4.30	13.18	51.1
76.20	465	10.0	9.93	84.89	4.38	10.49	42.2
47.27	631	10.0	7.32	71.46	4.49	7.73	32.7
29.53	836	10.0	5.52	59.14	4.59	5.83	25.8
14.70	1209	10.0	3.82	42.58	4.73	4.03	18.9
3.97	900	4.1	2.10	20.87	4.96	2.22	11.5

TABLE F-14

POROUS MEDIA DATA AND CALCULATIONS - RUN 14

Pressure Drop cm Hg	Time sec	Fluid Recovery cc	Velocity ft/day	Insitu Viscosity cp	Steady State Viscosity cp	Shear Rate sec ⁻¹	Predicted Viscosity cp
50.0	260	10.0	19.03	131.04	8.40	11.15	99.2
43.20	295	10.0	16.77	128.46	8.56	9.83	90.8
37.10	330	10.0	14.99	123.41	8.71	8.79	84.0
30.75	378	10.0	13.09	117.17	8.89	7.67	76.4
25.5	432	10.0	11.45	111.04	9.07	6.71	69.6
19.50	510	10.0	9.70	100.25	9.30	9.30	62.0
14.15	640	10.0	7.73	91.28	9.63	4.53	52.9
8.55	853	10.0	5.80	73.51	10.05	3.40	43.3
4.49	1222	10.0	4.05	55.30	10.61	2.37	33.7
1.50	900	4.07	2.23	33.43	11.61	1.31	22.3

TABLE F-15

POROUS MEDIA DATA AND CALCULATIONS - RUN 15

Pressure Drop cm Hg	Time sec	Fluid Recovery cc	Velocity ft/day	Insitu Viscosity cp	Steady State Viscosity cp	Shear Rate sec ⁻¹
4.96	260	10.0	18.93	12.99	4.20	10.99
4.23	290	10.0	16.97	12.36	4.22	9.86
3.36	328	10.0	15.00	11.10	4.23	8.71
2.47	375	10.0	13.12	9.33	4.25	7.62
1.86	429	10.0	11.47	8.04	4.26	6.66
1.26	509	10.0	9.67	6.46	4.28	5.62
0.74	635	10.0	7.75	4.73	4.31	4.50
0.46	838	10.0	5.87	3.88	4.34	3.41

TABLE F-16

POROUS MEDIA DATA AND CALCULATIONS - RUN 16

Pressure Drop cm Hg	Time sec	Fluid Recovery cc	Velocity ft/day	Insitu Viscosity cp	Steady State Viscosity cp	Shear Rate sec ⁻¹
54.40	259	10.0	18.31	33.75	4.13	20.15
45.38	293	10.0	16.18	31.85	4.15	17.81
37.47	332	10.0	14.28	29.80	4.16	15.72
30.83	378	10.0	12.54	27.92	4.18	13.81
23.82	434	10.0	10.92	24.76	4.19	12.03
18.17	515	10.0	9.20	22.42	4.21	10.13
11.85	647	10.0	7.32	18.36	4.24	8.07
6.95	862	10.0	5.50	14.35	4.27	6.06
3.42	1260	10.0	3.76	10.32	4.32	4.14
1.25	960	4.4	2.17	6.53	4.39	2.39

TABLE F-17

POROUS MEDIA DATA AND CALCULATIONS - RUN 17

Pressure Drop cm Hg	Time sec	Fluid Recovery cc	Velocity ft/day	Insitu Viscosity cp	Steady State Viscosity cp	Shear Rate sec ⁻¹	Predicted Viscosity cp
421.84	267	10.0	17.80	269.85	7.71	19.68	109.8
353.50	316	10.0	15.04	267.63	7.91	16.63	97.6
289.63	380	10.0	12.51	263.69	8.13	13.83	85.8
216.80	482	10.0	9.86	250.36	8.43	10.90	72.7
142.85	654	10.0	7.27	223.83	8.83	8.04	58.7
96.91	858	10.0	5.54	199.21	9.20	6.12	48.6
54.90	1222	10.0	3.89	160.73	9.70	4.30	38.0
13.44	900	4.4	2.32	65.86	10.49	2.57	26.5

TABLE F-18

POROUS MEDIA DATA AND CALCULATIONS - RUN 18

Pressure Drop cm Hg	Time sec	Fluid Recovery cc	Velocity ft/day	Insitu Viscosity cp	Steady State Viscosity cp	Shear Rate sec ⁻¹	Predicted Viscosity cp
291.31	262	10.0	19.10	769.37	99.30	11.39	707.1
239.21	314	10.0	15.93	757.16	106.68	9.50	681.0
193.27	382	10.0	13.10	744.23	115.29	7.80	653.8
148.45	485	10.0	10.31	725.77	126.73	6.15	622.1
100.84	654	10.0	7.65	664.80	142.65	4.56	584.6
73.49	869	10.0	5.75	647.71	159.65	3.43	551.0
47.62	1218	10.0	4.10	584.68	182.49	2.45	513.7
14.57	900	10.0	2.25	132.18	161.88	1.37	547.1